ARE TM (UJS) 87104
ACCN No 75410
JUNE 1987
COPY No 31

ARE TM (UJS) 87104

THE EFFECT OF REVERBERATION ON ACTIVE SONAR PERFORMANCE

by
MS CRAIG

ACCN No 75410

ADMIRALTY RESEARCH ESTABLISHMENT
Procurement Executive, Ministry of Defence,
Southwell, Portland, Dorset.

AMENDMENTS

NUMBER	1	2	3	4	5	6	7	8	9	10
DATE										

DOCUMENT CONTROL SHEET

Overall security classification of sheet ..... UNCLASSIFIED .....

As far as possible this sheet should contain only unclassified information. If it is necessary to enter classified information, the box concerned must be marked to indicate the classification eg (R), (C) or (S).

1. DRIC Reference (if known)	2. Originator's Reference	3. Agency Reference	4. Report Security Classification
	ARE TM (UJS) 87104 Accn No 75410		UNCLASSIFIED/ UNLIMITED
5. Originator's Code (if known)	6. Originator (Corporate Author) Name and Location		
	Admiralty Research Establishment Portland, Dorset, UK		
5a. Sponsoring Agency's Code (if known)	6a. Sponsoring Agency (Contract Authority) Name and Location		

7. Title

The Effect of Reverberation on Active Sonar Performance.

7a. Title in Foreign Language (in the case of translations)

7b. Presented at (for conference papers). Title, place and date of conference

8. Author 1 Surname, initials	9a. Author 2	9b. Authors 3, 4	10. Date	pp.	ref.
Craig M S			6/87	111	4
11. Contract Number	12. Period	13. Project	14. Other References		

15. Distribution statement

15. Descriptors (or keywords)

SONAR • ACTIVE SONAR • PERFORMANCE • REVERBERATION • NOISE • SIGNAL PROCESSING •

Abstract This report investigates the performance of an active sonar, which is limited by reverberation, although noise and limitations due to both noise and reverberation are also discussed. If the transmitted pulse is narrowband, the difference between the frequencies scattered by the target and the reverberation due to their (hopefully) different motion relative to the sonar is used to reduce the effect of reverberation. If the transmitted pulse is broadband, the ability of the processor to decrease the response to reverberation emanating from scatterers whose radial distance to the sonar is different from the radial distance to the target is used to reduce the effect of the reverberation. In either case, the improvement in performance against reverberation due to the processing is calculated using various assumptions on the nature of the reverberation and the processing. The effect on the results of varying many of these assumptions is also being investigated. The results may be used to investigate under what circumstances a sonar is limited by noise only, by reverberation only or by both. In any case, the performance of the sonar given the average signal power, average reverberation power and noise spectrum level and other quantities related to the assumptions made may be estimated.

ARE TM (UJS) 87104
Accession No 75410
June 1987

THE EFFECT OF REVERBERATION ON ACTIVE SONAR PERFORMANCE

by

M S Craig

Abstract

This report investigates the performance of an active sonar, which is limited by reverberation, although noise and limitations due to both noise and reverberation are also discussed. If the transmitted pulse is narrowband, the difference between the frequencies scattered by the target and the reverberation due to their (hopefully) different motion relative to the sonar is used to reduce the effect of reverberation. If the transmitted pulse is broadband, the ability of the processor to decrease the response to reverberation emanating from scatterers whose radial distance to the sonar is different from the radial distance to the target is used to reduce the effect of the reverberation. In either case, the improvement in performance against reverberation due to the processing is calculated using various assumptions on the nature of the reverberation and the processing. The effect on the results of varying many of these assumptions is also investigated. The results may be used to investigate under what circumstances a sonar is limited by noise only, by reverberation only or by both. In any case, the performance of the sonar given the average signal power, average reverberation power and noise spectrum level and other quantities related to the assumptions made may be estimated.

Table of Contents

List of Figures and Tables

1. Introduction

An active sonar system aims to detect the reflected sound from a target against a background of interference. In estimating the performance of the active sonar, it is desirable to be able to calculate the improvement in signal to interference ratio, which is brought about by the processing of the output from the beamformer. This report is concerned with this calculation when the interference consists of white noise (ie with a flat spectrum) or reverberation (ie sound scattered from all scatterers but the target) when using either of two types of processing which are described in the next two paragraphs. Some of the results in this report are available elsewhere, but not, to the author's knowledge, in a form which provides sonar modellers with both the necessary basic results and the mechanism to assess the effect of changes to some important parameters.

One processing option, called doppler processing here, exploits the fact that the reverberation return and the target return may be at different frequencies since differences in the motion of the scatterers and the motion of the target relative to the sonar may induce different doppler shifts in the returns. The output of the beamformer for a time interval of length T (the analysis time) is divided into frequency bins by convolving the output with a (possibly shaded) CW pulse of the desired frequency. If the doppler shift induced by the target is sufficiently different from any shift induced by most of the scatterers, there will be little or no reverberation in the bin(s) containing the target signal and detection of the target will be limited by noise alone. This report will consider how the performance of the sonar depends on the difference in the doppler shifts. The crossover from reverberation limited to noise limited performance of the sonar may then be deduced. Several assumptions regarding the details of this processing option and several different models of reverberation will be considered.

The above approach to reducing the effect of reverberation relies on using a narrowband (eg CW) transmitted pulse. An alternative approach to reduce the effects of reverberation is to use a wide band transmitted pulse, such as a chirp pulse where the frequency increases at a constant rate for the duration of the pulse. By convolving the signal from the beamformer with a pulse with the same frequency behaviour as the transmitted pulse, the contribution from all scatterers outside an annulus at a particular range and of width about c/2B, where c is the speed of sound and B the bandwidth of the pulse, is reduced significantly. When this

particular range coincides with the distance to the target, the signal to reverberation power ratio is increased due to the reduced effective scattering area.

In section 2, standard expressions for probability of detection and false alarm are given. It is noted that under certain assumptions, for a given probability of false alarm, the probability of detection depends only on a single quantity (which is half the output signal to interference ratio and is denoted P and defined by equation [2.9]) and the relationship is shown in figure 1.

The quantity P is calculated in section 3 when the interference consists of white gaussian noise only in the two cases of a CW pulse and an FM chirp pulse and well known expressions for the detection thresholds are derived in these cases.

Section 4 begins with a discussion of reverberation. A base case is established from which a comparison of processing options may be established. The "gain" when a processing option is used is defined as the ratio of the value of P when the option is used to the value of P in the base case (the latter value of P being simply the average signal to reverberation power ratio). For doppler processing, the "gain" is critically dependent on the assumptions made about the nature of reverberation and various forms of the reverberation amplitude covariance function are considered. Although ideally the reverberation will be concentrated at the pulse frequency, it may be distributed in frequency due to motion of the scatterers or uncompensated motion of the sonar. Graphs are presented in section 4.1 of the relationship between the "gain" and the difference between the doppler shift induced by the target and the central doppler shift induced by the other scatterers (suitably non-dimensionalised). Different assumptions of reverberation frequency spread and different combinstions of functions to shape the transmitted pulse and shade the comparison CW pulsewith with which the return is convolved are considered. For the FM chirp pulse, the "gain" is not dependent on the frequency spread of the reverberation and a graph of "gain" (figure 22) as a function of bandwidth is presented for comparison in section 4.2.

In section 5, the nature of the graphs with large differences in doppler shift (doppler processing) or large bandwidth (FM chirp pulses) are explained by calculating asymptotic series for the gain in each case. These series provide a means of estimating the "gain" (relatively easily) in

situations not covered by the graphs.

Section 6 provides an example illustrating the results of this report and section 7 provides a summary of the results presented in this report.

In annex A, expressions for probability of detection and false alarm are derived under more general conditions than used in the main body of the report and these expressions are shown to reduce to the standard equations under the more restrictive assumptions. These more restrictive assumptions are listed in annex B, where the effect of varying each of the assumptions is also noted. Assumptions made in deriving the results of sections 4 and 5 are listed in annex C and effects of varying each of these assumptions are described.

2. The Probability of Detection and False Alarm

A pulse of the form

$$z(t) = (2J)^{0.5}\, W(t) \cos (M(t) + 2\pi F t) \qquad [2.1]$$

is transmitted for a time K. The function W(t) defines the pulse shape and is zero unless $0 \le t \le K$ and is normalised so that

$$K^{-1} \int_0^K W^2(t)\, dt = 1. \qquad [2.2]$$

F is the centre frequency of the transmitted pulse and M(t) defines the frequency modulation which is small compared with F i.e. $M'(t)/F << 1$. The quantity J is the transmitted pulse average power level (if terms of order $(2\pi FK)^{-1}$ may be neglected). Subsequently, the sound received by an array of hydrophones consists of background noise, reverberation and the sound scatterered from the target (if present). On the basis of this sound received by an array of hydrophones a decision is made as to whether the target is present or not. The sound at the individual hydrophones is first combined into beams, each of which contains sound coming mainly from a particular direction. Each beam output is monitored for a finite time and is often monitored for many possibly overlapping short time intervals. Suppose that one of these intervals begins a time $\tau \ge K$ after the start of the pulse transmission and redefine the origin of time t to be the start of the analysis period which is of length T. Let y(t) be the output of a beam from the receiver hydrophone array for $0 \le t \le T$ and on the basis of y(t) it must be decided whether there is a target present in the beam. It is assumed that this is done by evaluating the quantity r, where

$$r = (B^2+C^2)^{0.5} \qquad [2.3]$$

$$B = \int_0^T y(t)\, H(t) \cos (N(t) + 2\pi f t)\, dt \qquad [2.4]$$

$$C = \int_0^T y(t)\, H(t) \sin (N(t) + 2\pi f t)\, dt. \qquad [2.5]$$

The optimal functions H(t) and N(t) to be used depend on the properties of the pulse and the expected interference. Usually N(t)=M(t) as the contribution to the value of r from the target echo will then be maximised.

The function H(t) is normalised so that

$$T^{-1} \int_0^T H^2(t)\, dt = 1. \qquad [2.6]$$

Values of r may be calculated at more than one value of f near to the transmitter frequency F. A detection will be declared if r exceeds some threshold R.

Suppose that a coherent target echo of the form

$$s(t) = (2\mathbb{P})^{0.5}\, W(t-D) \cos (M(t-D) + 2\pi f_1 t + \theta_1) \qquad 0 \le D \le t \le E \le T \qquad [2.7]$$

is present during part or all of the analysis period, where $\mathbb{P}$ is the average signal power level in the beam (neglecting terms of order $(2\pi f_1 K)^{-1}$), D is the time of the start of the target echo, E = min (T,D+K) is the time of the end of the target echo within the analysis time, f_1 is the centre frequency of the signal (approximately the centre transmission frequency F) and θ_1 is the signal phase. It is shown in Annex A that, provided certain assumptions are valid, the probability of detecting the signal in a single look is

$$p_d = \int_{-\ln(p_{fa})}^{\infty} e^{-(u+P)}\, I_0(2\sqrt{(uP)})\, du \qquad [2.8]$$

where p_{fa} is the probability of a false alarm due to the interference level exceeding the threshold R, I_0 is the modified Bessel function of zero order and P, which is half the signal to interference ratio at the output of the processor, is give by

$$P = \mathbb{P}\, Q_1^2 / (4\, \sigma^2) \qquad [2.9]$$

where

$$Q_1^2 = \left(\int_D^E H(t)\, W(t-D) \cos (M(t-D) - N(t))\, dt \right)^2 + \left(\int_D^E H(t)\, W(t-D) \sin (M(t-D) - N(t))\, dt \right)^2 \qquad [2.10]$$

$$\sigma^2 = \int_0^T \int_v^T E[\, x(t)x(t-v)\,]\, H(t)H(t-v) \cos\,(N(t)-N(t-v)+2\pi fv)\, dt\, dv \qquad [2.11]$$

with x(t) being the component of y(t) due to interference alone and E[·] denoting expected value. The probability of detection as a function of P (in decibels) for various values of probability of false alarm, based on equation [2.8], is presented in figure 1. The assumptions made in deriving equation [2.8] and the effect of relaxing some of these assumptions are described in Annex B.

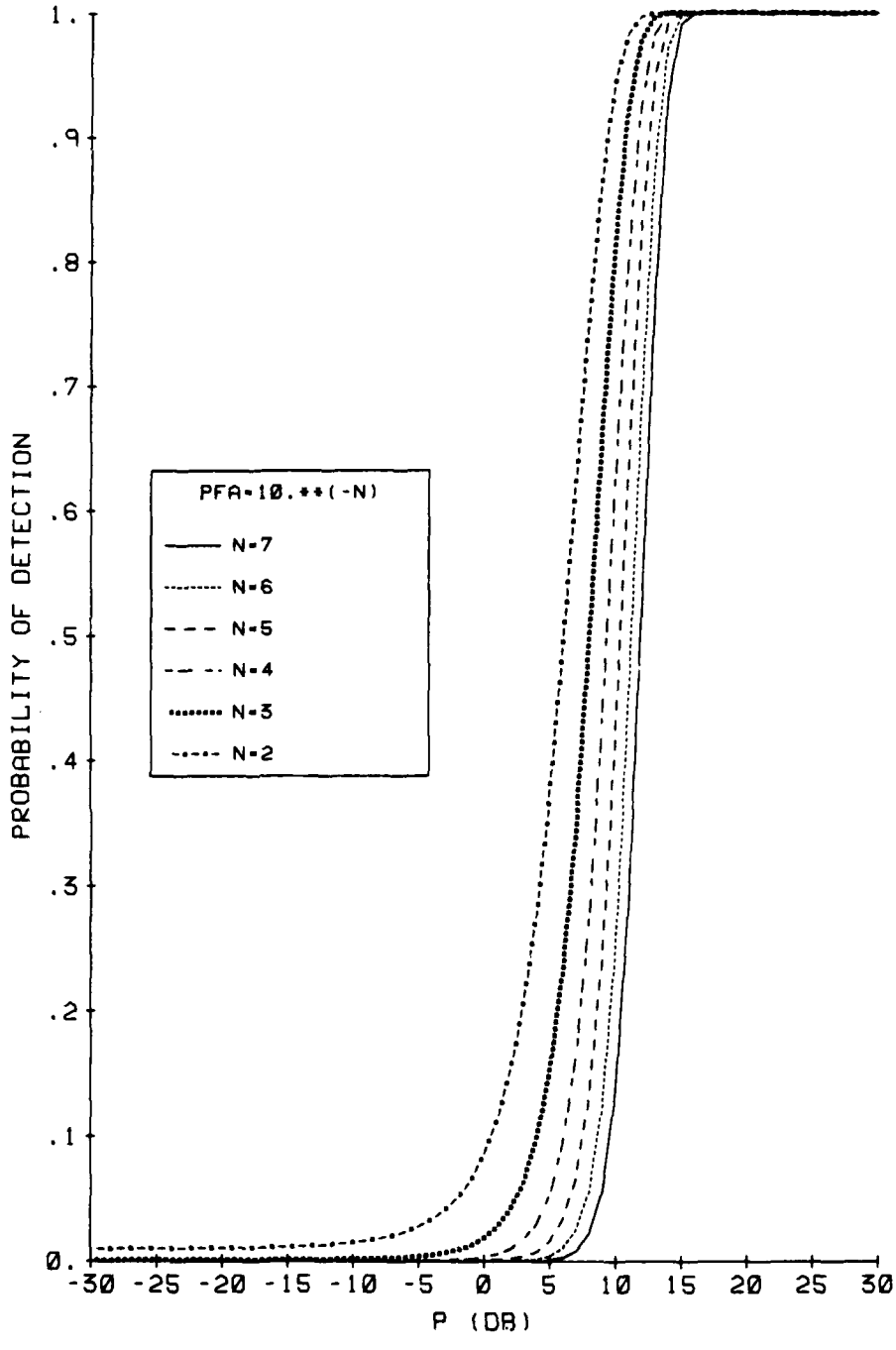

Figure 1(U) Transition Curves

3. Detection in the Presence of White Noise

If the interference consists entirely of white noise with spectrum level N_0, then

$$E[\, x(t)x(u)\,] = N_0\, \delta(t-u) \qquad [3.1]$$

where $\delta()$ is the Dirac delta function.

For a CW pulse where $M(t) = 0$,

$$Q_1^2 = \left(\int_D^E H(t)\, W(t-D) \cos N(t)\, dt\right)^2 + \left(\int_D^E H(t)\, W(t-D) \sin N(t)\, dt\right)^2 \qquad [3.2]$$

$$\sigma^2 = {}^1\!/_2\, N_0 \int_0^T H^2(t)\, dt \qquad [3.3]$$

so that

$$P = \frac{\bar{P}\left\{\left(\int_D^E H(t)\, W(t-D) \cos N(t)\, dt\right)^2 + \left(\int_D^E H(t)\, W(t-D) \sin N(t)\, dt\right)^2\right\}}{2\, N_0 \int_0^T H^2(t)\, dt} \qquad [3.4]$$

which has a maximum value of $\bar{P}T/(2N_0)$ when $H(t)$ equals $W(t)$, $N(t)$ is a constant and the analysis period $[0,T]$ coincides with the signal period $[D,E]$. This is the same as the detection index (apart from a factor of 4), defined ,for example in reference [1], chapter 12, and leads to the same value of detection threshold. In the case where the signal and analysis periods do not coincide, figure 2 shows the relative degradation in P (ie decrease in P expressed in decibels from this optimal value) for values of D/T between 0 and 1, assuming that E=T. The different lines correspond to different combinations of weighting functions W and shading functions H which are considered in the next section and are listed in tables 2 and 3. There is a non-zero degradation when the shading and shaping functions are different even when D=0. If the analysis periods do not overlap, the maximum degradation is obtained when D/T=0.5 as for larger values of D/T, the next analysis interval will contain more of the signal power and will give a degradation corresponding to (1-D/T) with the weighting and shading functions interchanged. This maximum degradation is quite large for some shading and shaping function combinations (eg 20 dB for exp

shading and shaping) but can be reduced by using overlapping analysis intervals although this increases the processing required and may also increase the false alarm rate for a particular probability of false alarm for each analysis period.

For an FM pulse,

$$Q_1^2 = \left(\int_D^E H(t)\, W(t-D) \cos (M(t-D)-N(t))\, dt \right)^2 + \left(\int_D^E H(t)\, W(t-D) \sin (M(t-D)-N(t))\, dt \right)^2 \quad [3.5]$$

$$\sigma^2 = \tfrac{1}{2} N_0 \int_0^T H^2(t)\, dt \quad [3.6]$$

so that

$$P = \frac{P\{\left(\int_D^E H(t)\, W(t-D) \cos (M(t-D)-N(t))\, dt\right)^2 + \left(\int_D^E H(t)\, W(t-D) \sin (M(t-D)-N(t))\, dt\right)^2\}}{2 N_0 \int_0^T H^2(t)\, dt} \quad [3.7]$$

This is maximised when the analysis period [0,T] and the signal period [D,E] coincide, N(t) differs from M(t) by a constant and H(t) equals W(t). The maximum value is the same as in the CW case.

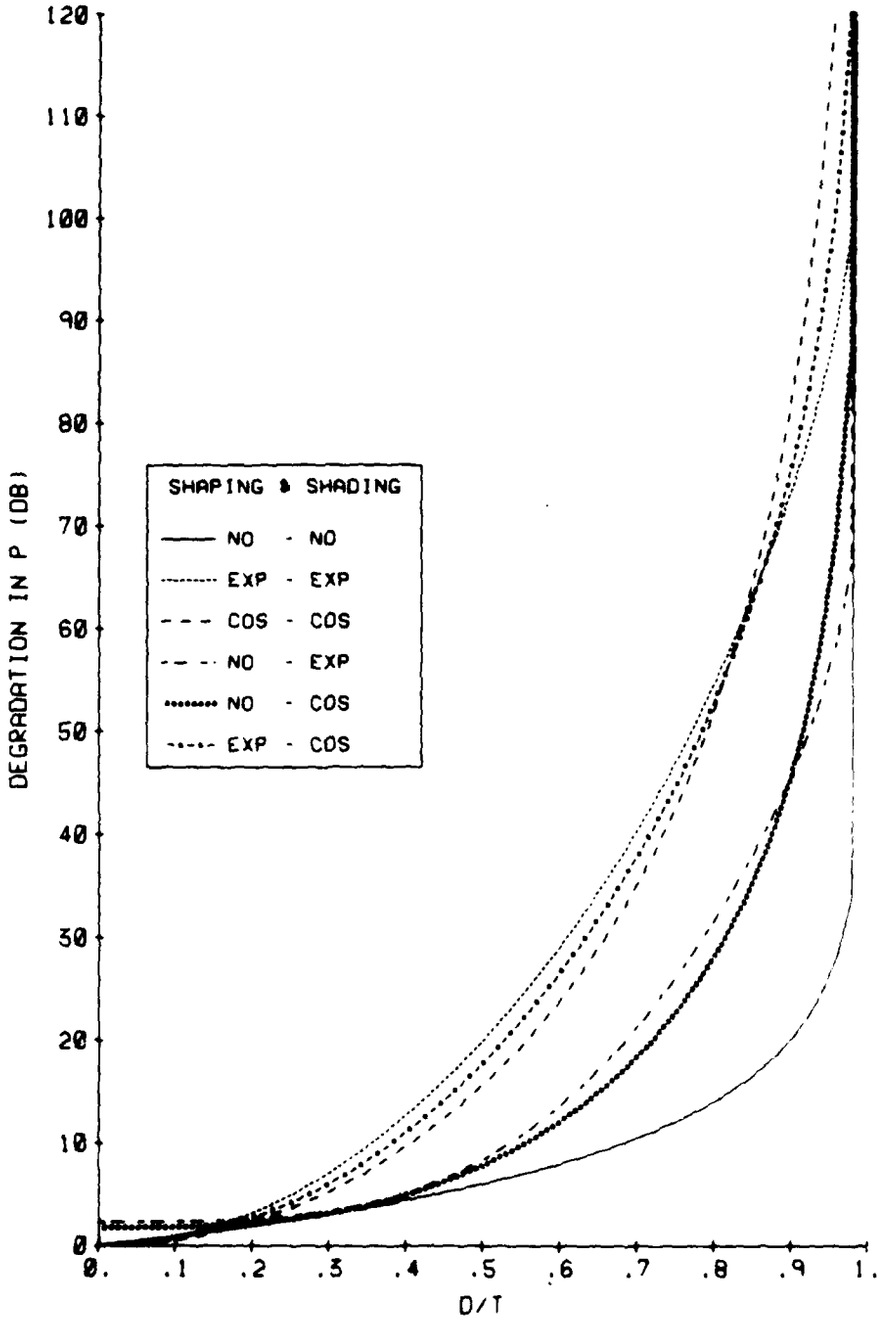

Figure 2(U) Degradation in Gain

4. Detection in the Presence of Reverberation

Let t be a time within the analysis period [0,T]. The reverberation at time t comes from all scatterers where the sum of the travel times from the transmitter to the scatterer and from the scatterer to the receiver lies within the range [t+τ-K,t+τ], where the transmission started at time -τ and the pulse length is K. The component of the reverberation from all scatterers whose total travel time is ζ' + τ and whose centre frequency and phase are f' and θ' respectively, may be written

$$x(t) = g(t,\zeta',f',\theta')\, W(t-\zeta') \cos\left(M(t-\zeta') + 2\pi f' t + \theta' \right) \qquad t-K \le \zeta' \le t \qquad [4.1]$$

where the phase shift θ' ($0 \le \theta' \le \pi$) is due both to scattering and wave travel. The function g which may be positive or negative includes all factors influencing the amplitude such as beam patterns, propagation loss, scatterer reflection coefficients, interference between reverberation from different scatterers and the possibility of a scatterer changing position, velocity or reflection coefficient for the duration of the pulse. The pulse shape function W(t-ζ') is zero unless $t \le \zeta' \le t-K$. The reverberation from all scatterers may then be expressed as

$$x(t) = \int_0^{\pi} \int_{-\infty}^{\infty} \int_{t-K}^{t} g(t,\zeta',f',\theta')\, W(t-\zeta') \cos\left(M(t-\zeta') + 2\pi f' t + \theta' \right) d\zeta'\, df'\, d\theta' \qquad [4.2]$$

In order to use the equations [A.33] and [A.60] for probability of detection and false alarm, it will be assumed that the values of B and C, constructed by using x(t) from equation [4.2] in place of y(t) in equations [2.4] and [2.5], are normally distributed and have zero mean. This assumption is valid if there are a sufficiently large number of independent scatterers contributing to the reverberation. The expected value of x(t)x(u) which is required to calculate the probability of false alarm,

$$E[\, x(t)x(u) \,] = \int_{t-K}^{t} \int_{u-K}^{u} \int_{-\infty}^{\infty} \int_{-\infty}^{\infty} \int_{0}^{\pi} \int_{0}^{\pi} E[\, g(t,\zeta',f',\theta')\, g(u,\zeta'',f'',\theta'') \,] W(t-\zeta')\, W(u-\zeta'') \cdot \cos\left(M(t-\zeta') + 2\pi f' t + \theta' \right) \cos\left(M(u-\zeta'') + 2\pi f'' u + \theta'' \right) d\theta''\, d\theta'\, df''\, df'\, d\zeta''\, d\zeta' \qquad [4.3]$$

Insufficient data are available to estimate with confidence the covariance of g which occurs in this integral. In this report various assumptions are

made about the nature of this covariance function. A specific form of the function is considered in detail in sections 4.1 and 4.2 where the improvements to be made using doppler processing or FM chirp pulses respectively are discussed. A discussion is given in Annex C of the effect of varying some of the assumptions made in these sections. Results are presented of the "gain" obtained when different options are used. This "gain" is defined as the relative improvement in P over its value in the base case which is defined in the next paragraph. This base case value is the ratio of average signal power to average noise power over the analysis period.

The base case arises if the following simple (but not necessarily accurate) model of reverberation is used. Suppose that

$$E[\, g(t,\zeta',f',\theta')\, g(u,\zeta'',f'',\theta'')\,] = (2\mathbb{R}/\pi K^2)\, \delta(f'-\mu)\, \delta(f''-\mu)\, \delta(\theta'-\theta'') \qquad [4.4]$$

so that all the reverberation return is at frequency μ, reverberation at different phases is independent and the reverberation from different scatterers giving contributions at the same phase are totally correlated. In this case for the unshaped CW pulse (i.e. W(t)=1, M(t)=0)

$$E[\, x(t)x(u)\,] = \mathbb{R} \cos 2\pi\mu(t-u) \qquad [4.5]$$

and the scaling factors in equation [4.4] are chosen so that the average reverberation power is $\mathbb{R}$. If no shading or frequency modulation is used (i.e. H(t)=1, N(t)=0),

$$\sigma^2 = \mathbb{R} \int_0^T (T-v) \cos 2\pi f v \cos 2\pi\mu v \, dv \qquad [4.6]$$

$$= \frac{\mathbb{R}}{4} \left(\frac{\sin^2 \pi(f-\mu)T}{\pi^2 (f-\mu)^2} + \frac{\sin^2 \pi(f+\mu)T}{\pi^2 (f+\mu)^2} \right) \qquad [4.7]$$

and

$$Q_1 = E - D. \qquad [4.8]$$

Ignoring terms of order $(2\pi fT)^{-1}$, which is assumed small, and assuming that the reverberation frequency μ equals the analysis frequency f, P has

its maximum value when the analysis period [0,T] coincides with the entire signal period [D,E] so that D=0, T=K and this maximum value is

$$P = P/R \qquad [4.9]$$

which is the average signal power to average reverberation power ratio. This is the base case with which the other options are compared in the remainder of this report in order to assess the "gain" achieved by either doppler processing with a CW pulse or using an FM chirp pulse in a reverberation environment with given characteristics. The average reverberation power R is proportional to the pulse length K (since the width of the scattering region is cK/2, where c is the speed of sound). This must be taken into account in sections 4.1 or 4.2 or Annex C when assessing the effect of a changed pulse length.

In sections 4.1 and 4.2, the following (more realistic) form of the covariance of g is used:

$$E[\, g(t,\zeta',f',\theta')\, g(u,\zeta'',f'',\theta'')\,] = 2R\, L(f')\, \delta(f'-f'')\, \delta(\zeta'-\zeta'')\, \delta(\theta'-\theta'') / (\pi K) \qquad [4.10]$$

where the amplitudes g are independent for different phases, centre frequencies or path lengths and L(f') gives the frequency distribution of the reverberation power and is scaled so that the average reverberation power over the the analysis period is R. Other forms will be considered in Annex C. The expected value of x(t)x(u) may be written for $t \geq u \geq t-K$,

$$E[\, x(t)x(u)\,] = (R/K) \int_{t-K}^{u} \int_{-\infty}^{\infty} L(f')\, W(t-\zeta')\, W(u-\zeta') \cdot \cos(M(t-\zeta')-M(u-\zeta')+2\pi f'(t-u))\, df'\, d\zeta' \qquad [4.11]$$

For $u \geq t \geq u-K$, E[x(t)x(u)] is given by an equivalent expression with u and t interchanged. E[x(t)x(u)] is zero if $|t-u|>K$. In the cases considered in section 4, it is shown in Annex C that

$$E[\, x(t)x(u)\,] = (R/K)\, L(t-u)\, W(t-u) \cos 2\pi\mu(t-u) \qquad [4.12]$$

where the functions L(), W() and the quantity μ are defined by equations [C.24] and [C.18]. In this case,

$$\sigma^2 = (R/K) \int_0^T L(v)\, W(v)\, H(v) \cos 2\pi f v \cos 2\pi \mu v \, dv \qquad [4.13]$$

$$= (R/2K) \int_0^T L(v)\, W(v)\, H(v) \cos 2\pi (f-\mu) v \, dv \qquad [4.14]$$

where H() is defined by [C.40]. The gain G may therefore be written

$$G = \frac{K Q_1^2}{2 \int_0^T L(v)\, W(v)\, H(v) \cos 2\pi (f-\mu) v \, dv} \qquad [4.15]$$

In sections 4.1 and 4.2, attention will be confined to specific functions M, N, L, H and W. The latter three are listed in tables 1 to 3. Of the functions L listed in table 1, the most probable to occur in practice are functions 1 or 4, which would be based on stationary scatterers or scatterers whose radial components of velocity relative to the sonar are normally distributed. For each of the functions 2 to 4, the parameter a is approximately half the 3dB bandwidth of the reverberation power. Each of these functions approach function 1 as $a \rightarrow 0$. The three possible functions W(t) or H(t) are denoted

1) NO for no shading or shaping
2) EXP for exponential (gaussian) shading or shaping
3) COS for cos squared shading or shaping.

Each are normalised by equations [2.2] or [2.6] and each are expressed relative to a time origin set at the start of the pulse (W) or the start of the analysis period (H). The functions W and H in tables 2 and 3 are valid for CW pulses only, where M(t)=N(t)=0.

Table 1

The Functions L(f)

No.	L(f)	L(v)
1	$\delta(f-\mu)$	1
2	$\frac{a}{\pi\left((f-\mu)^2 + a^2\right)}$	$\exp(-2\pi a v)$
3	$\frac{0.72\,a \sin^2\left((f-\mu)/(0.72\,a)\right)}{\pi (f-\mu)^2}$	$(1 - 0.72\pi a v)$ if $\lvert v\rvert < (0.72\pi a)^{-1}$ 0 if $\lvert v\rvert \geq (0.72\pi a)^{-1}$
4	$\frac{(\ln 2)^{0.5} \exp\left(-(f-\mu)^2 (\ln 2)/a^2\right)}{\pi^{0.5}\, a}$	$\exp(-\pi^2 a^2 v^2 /(\ln 2))$

Table 2

The Functions W(t)

No.	W(t)	W(v)
1 (NO)	1	K-v
2 (EXP)	$\frac{6^{0.5} \exp\left(-(18\,(t/K-0.5)^2)\right)}{\pi^{0.25}\,(\mathrm{erf}(3))^{0.5}}$	$\frac{K \exp\left(-(3v/K)^2\right) \mathrm{erf}\left(3(1-v/K)\right)}{\mathrm{erf}(3)}$
3 (COS)	$\frac{8^{0.5} \cos^2\left(\pi\,(t/K-0.5)\right)}{3^{0.5}}$	$(K-v)\,(2 + \cos 2\pi v/K)/3 + \sin(2\pi v/K)/(2\pi)$

Table 3

The Functions H(t)

No.	H(t)	H(v)
1 (NO)	1	T-v
2 (EXP)	$\frac{6^{0.5} \exp(-(18 (t/T-0.5)^2))}{\pi^{0.25} (\mathrm{erf}(3))^{0.5}}$	$\frac{T \exp(-(3v/T)^2) \mathrm{erf}(3(1-v/T))}{\mathrm{erf}(3)}$
3 (COS)	$\frac{8^{0.5} \cos^2 (\pi (t/T-0.5))}{3^{0.5}}$	$(T-v) (2 + \cos 2\pi v/T)/3 + \sin(2\pi v/T)/(2\pi)$

4.1 CW Transmission

If the transmitted pulse is CW,

$$M(t) = 0 \qquad [4.16]$$

so that

$$W(v) = \int_v^K W(w-v)\, W(w)\, dw \qquad [4.17]$$

$$= \int_0^{K-v} W_1(v-w)\, W_1(v+w)\, dw \qquad [4.18]$$

where

$$W_1(x) = W((K-x)/2) \qquad [4.19]$$

Assuming that N(t)=0, which gives the maximum gain against noise, a similar expression may be written for H(v) with H replacing W and T replacing K throughout. The expressions for H(v) and W(v) from tables 2 and 3 may then be used. If D=0 and T=K,

$$Q_1 = \int_0^T H(t)\, W(t)\, dt \qquad [4.20]$$

and the equation [4.15] may be used to evaluate the gain. This gain is presented as a function of a non-dimensional parameter $\omega=2\pi(f-\mu)T$ in figures 3 to 21 for all combinations of the functions L, H and W from tables 1 to 3. Because equation [4.15] is symmetric in H and W in the cases considered here, the same gain is obtained if the shading or shaping functions are interchanged.

The following features may be noted from the figures:

(i) In figure 3, which presents the gain in the case that all the reverberation is confined to one frequency (function 1 from table 1 for L), there is some gain when $\omega=0$ due to the use of a different reverberation model from the one used in the base case. The difference lies in the correlation (or otherwise) of contributions to the reverberation from

scatterers with different path lengths.

(ii) The doppler shift of the signal is given approximately by

$$\Delta f = 2vF/c \qquad [4.21]$$

where v is the radial component of the relative velocity of the target and sonar and c is the speed of sound,

$$\omega = (4\pi FT/c)\, v \qquad [4.22]$$

if the reverberation is centred on the carrier frequency (ie μ=F) and the analysis frequency coincides with the signal (doppler shifted) frequency. Thus ω and hence the gain (which is an increasing function of ω in all figures) will be larger for a sonar with a larger carrier frequency F if the other parameters are unchanged. The value of ω will also be larger for a longer pulse, but the effect of changing T on the gain is more complicated for two reasons. Firstly, increasing T will increase the average reverberation power $\mathbb{R}$, which is proportional to the pulse length unless the pulse is so long that the average reverberation power from equal areas at two ranges cT/2 apart differs significantly from one another. Thus the detection performance will only improve for an increased pulse length if the gain improves faster than linearly with ω. Secondly, when functions 2, 3 or 4 are used for L (figures 4 to 21), the parameter aT is proportional to T, so that increasing T will move from one line to another giving a possibly reduced gain.

(iii) Considerable improvements may be made in the gain for a fixed value of ω by shaping the pulse or using a shading function. The aim of shading or shaping is to reduce the discontinuities in the reverberation due to the sudden turning off or on of contributions from a scatterer when $t=\zeta+K$ or $t=\zeta$ respectively (shaping) and the sudden start and end of the analysis period (shading). These discontinuities widen the reverberation spectrum or the filter spectrum and lead to a reduced gain. The function 1 (no shading or shaping) has large discontinuities at the ends of the interval and will give the worst gains. The function 2 (exp shading or shaping) has very small discontinuities at the endpoints and gives improved gains. The function 3 (cos shading or shaping) is continuous and has a continuous derivative at the endpoints. The discontinuity in the second derivative at the endpoints yields some widening of the spectra, but the effect is much

smaller than in the other cases. Note that H and W should be matched to have the same degree of continuity as there is little to be gained in improving H (say) if W is the dominant cause of the decrease in gain. The possibility that the nature of the propagating medium and the scatterers may limit the reduction in the discontinuities and therefore the gain whatever the functions H and W is discussed briefly in Annex C.

(iv) The effect of broadening the reverberation spectrum by using functions 2, 3 or 4 from table 1 (due to motion of the scatterer or uncompensated motion of the sonar) depends very much on the function selected. The reasons for this are discussed in section 5. If the half bandwidth a is increased, the gain is also increased when ω=0 due to the decrease in maximum reverberation power brought about by the broadening. However the increase in gain with ω is usually slower with the larger values of a, due to the increase in reverberation power in the main analysis frequency band. This slower increase is more marked using function 2 or 3, where the fall of power with frequency away from the centre frequency is slow, than using function 4, where the fall is much faster beyond the 3 dB bandwidth. In fact with function 4 the gain approaches that with a=0 (function 1) for sufficiently large ω, indicating that there is no longer any appreciable reverberation power in the main analysis frequency band.

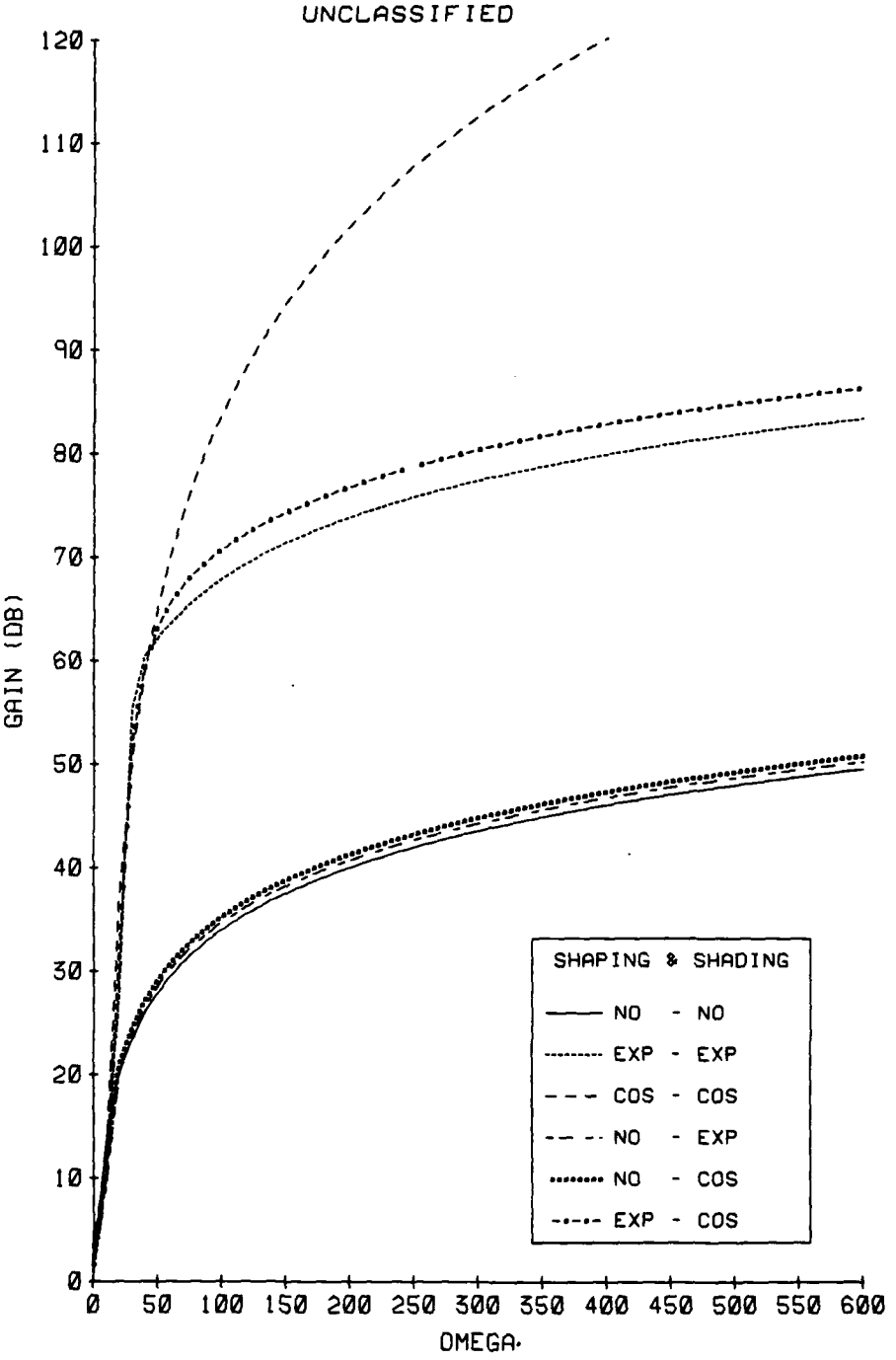

Figure 3(U) Gain using Function 1 for L

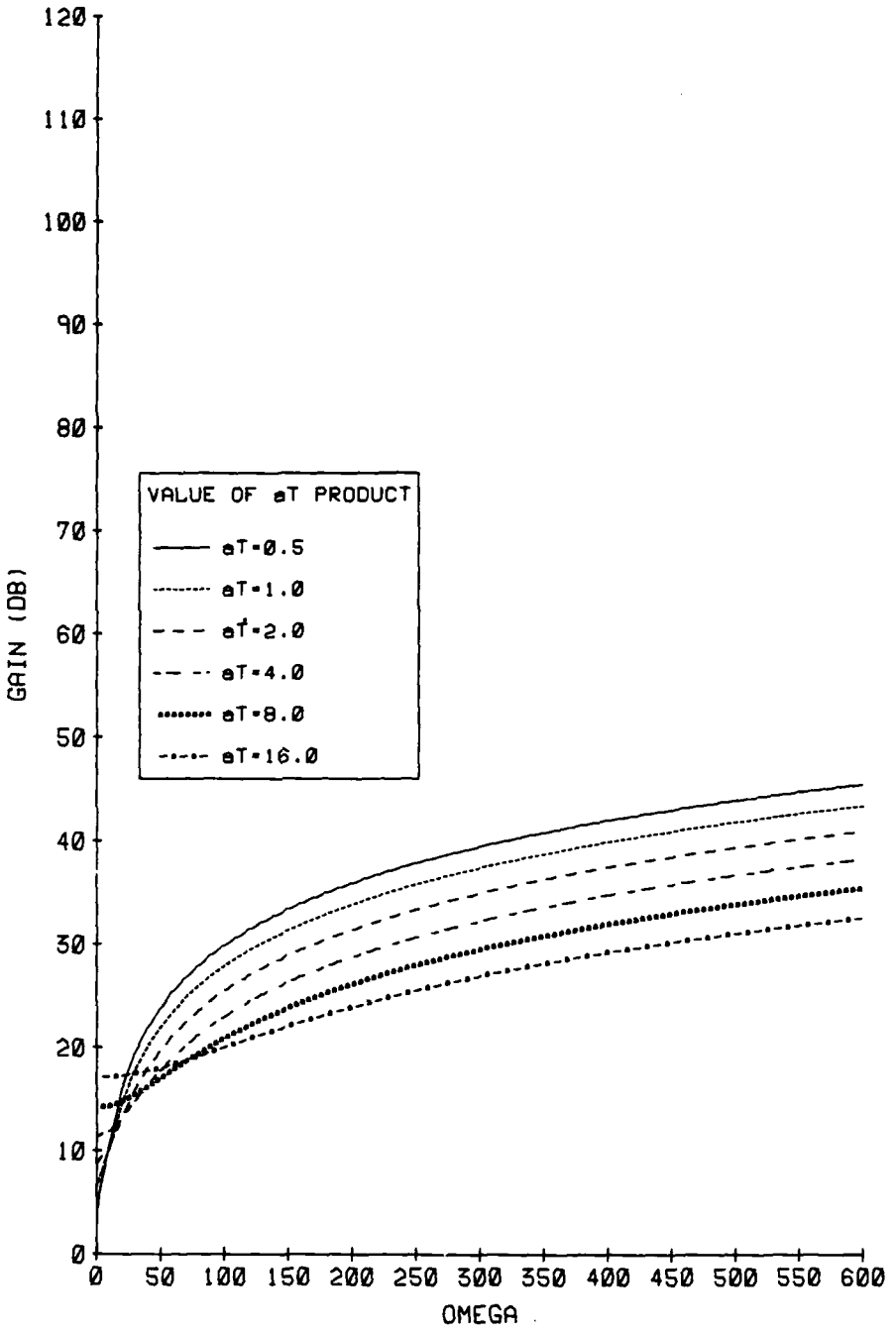

Figure 4(U) Gain using Function 2 for L No Shading and No Shaping

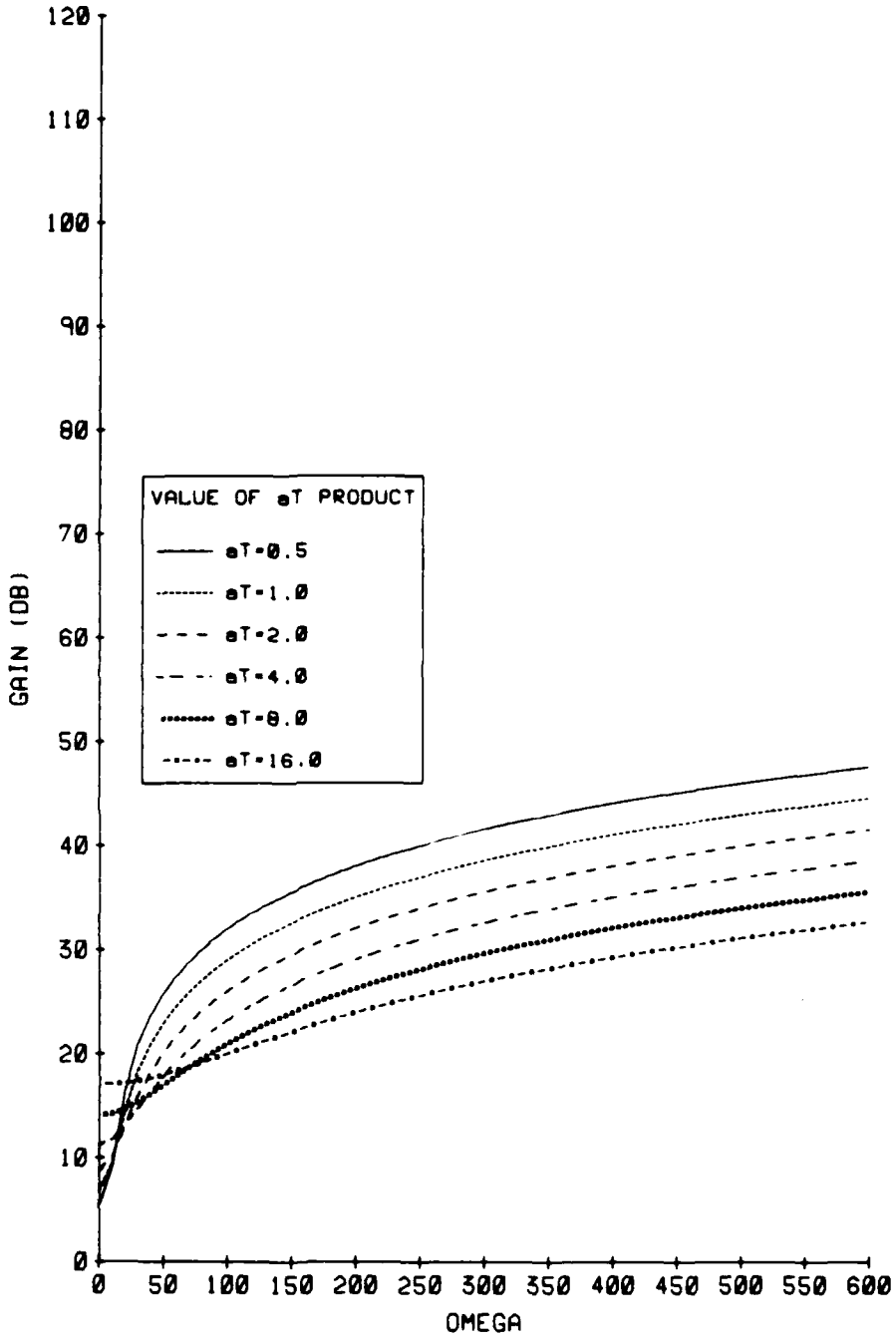

Figure 5(U) Gain using
Function 2 for L
Exp Shading and Exp Shaping

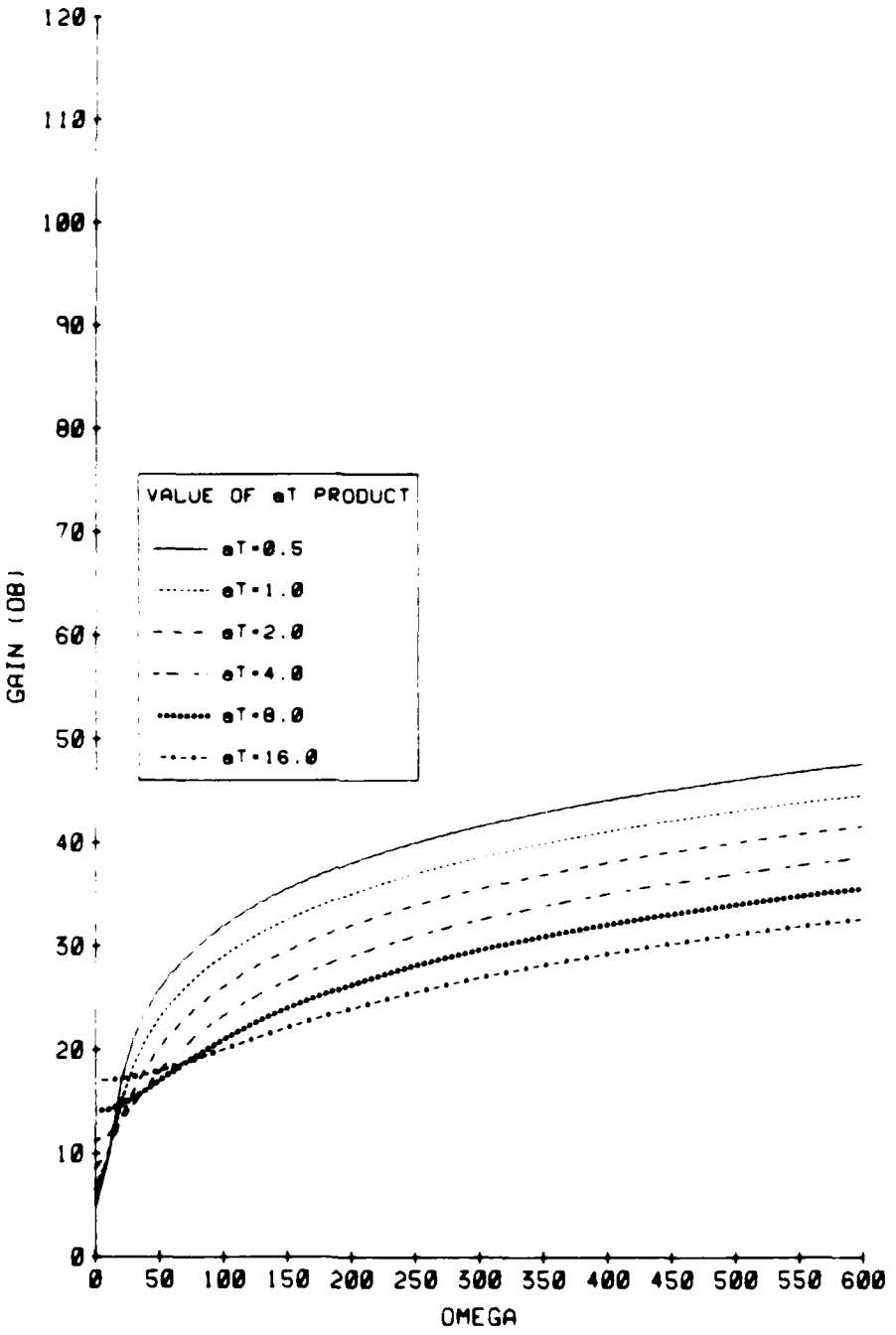

Figure 6(U) Gain using
Function 2 for L
Cos Shading and Cos Shaping

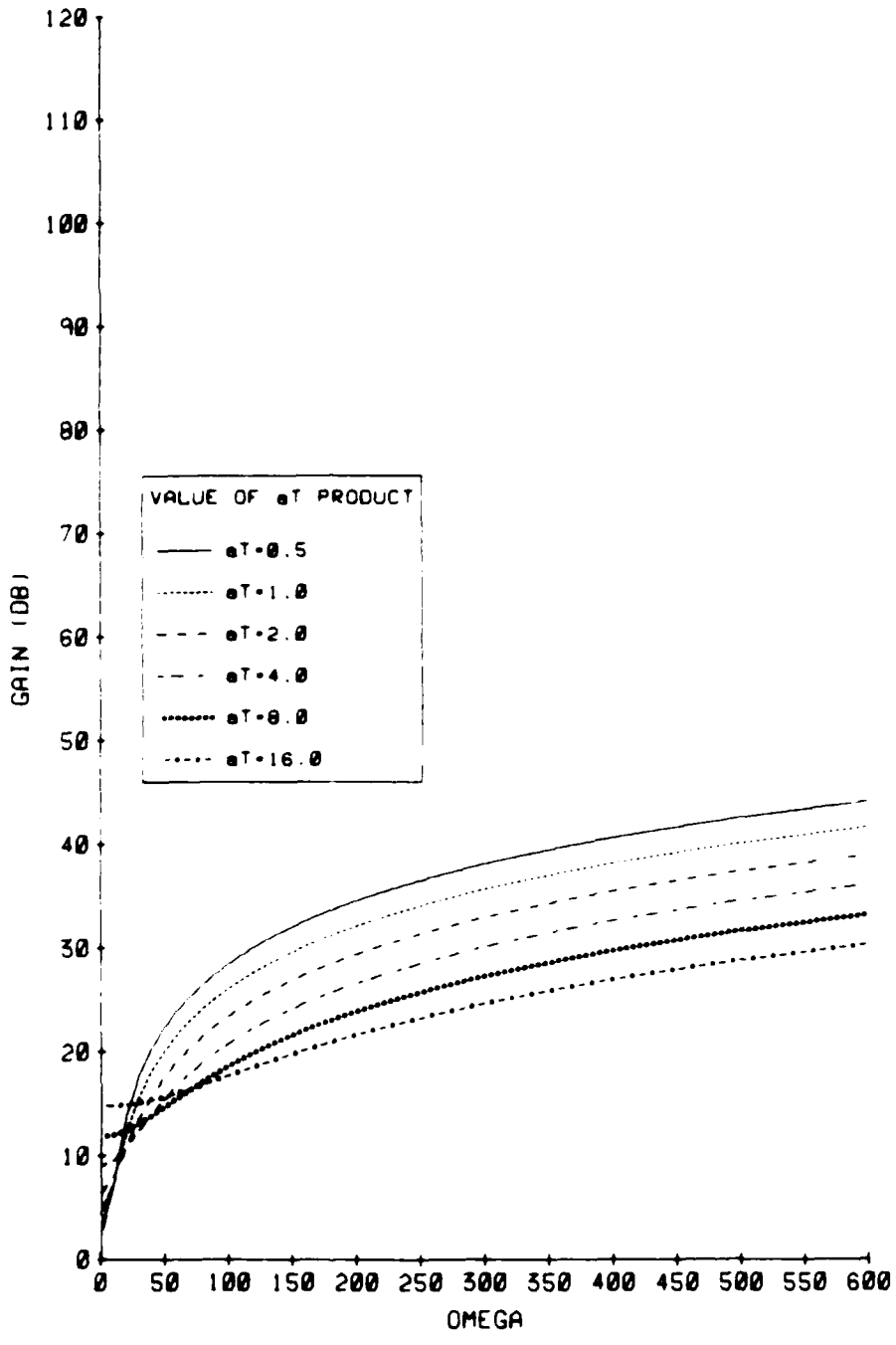

Figure 7(U) Gain using Function 2 for L Exp Shading and No Shaping

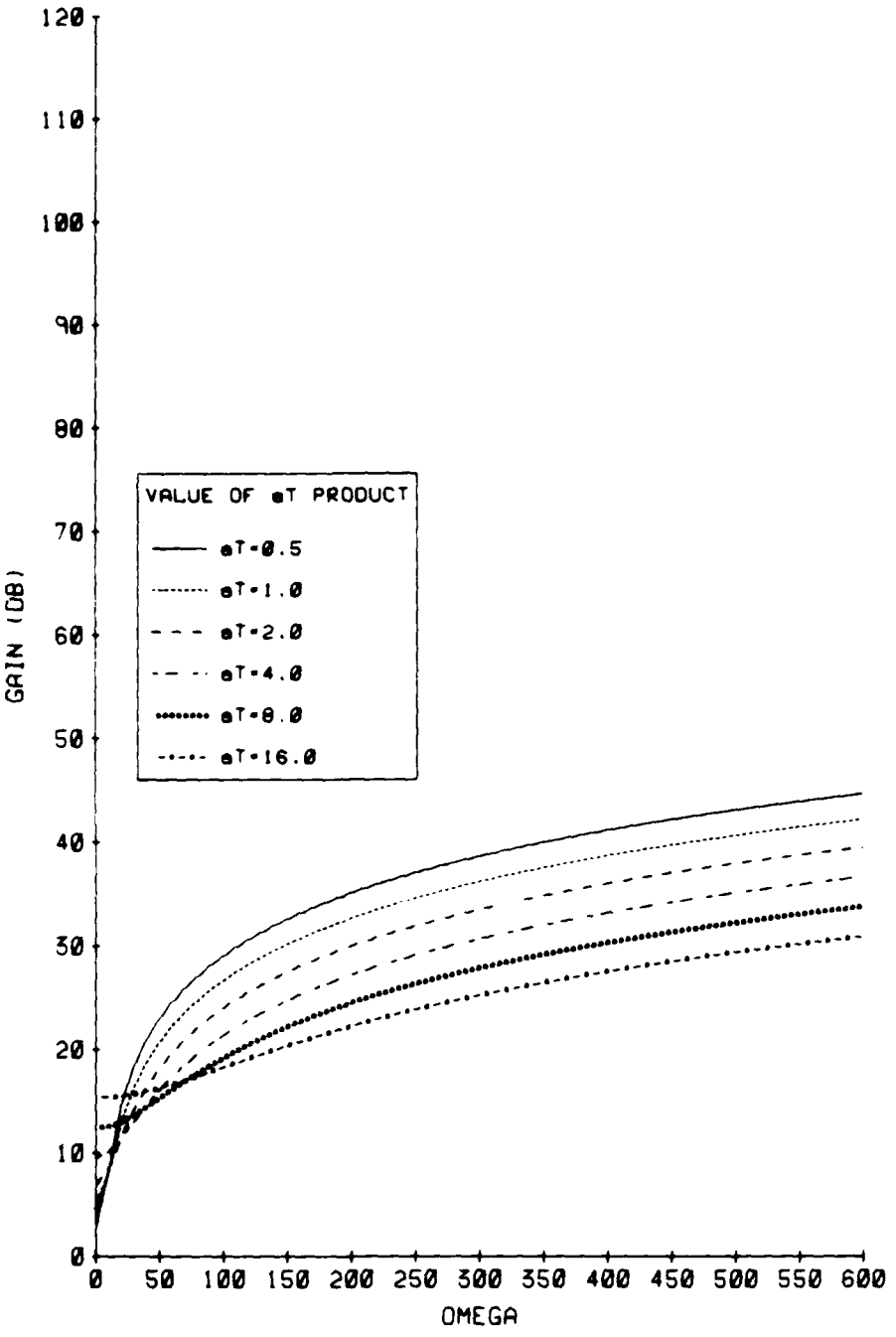

Figure 8(U) Gain using
Function 2 for L
Cos Shading and No Shaping

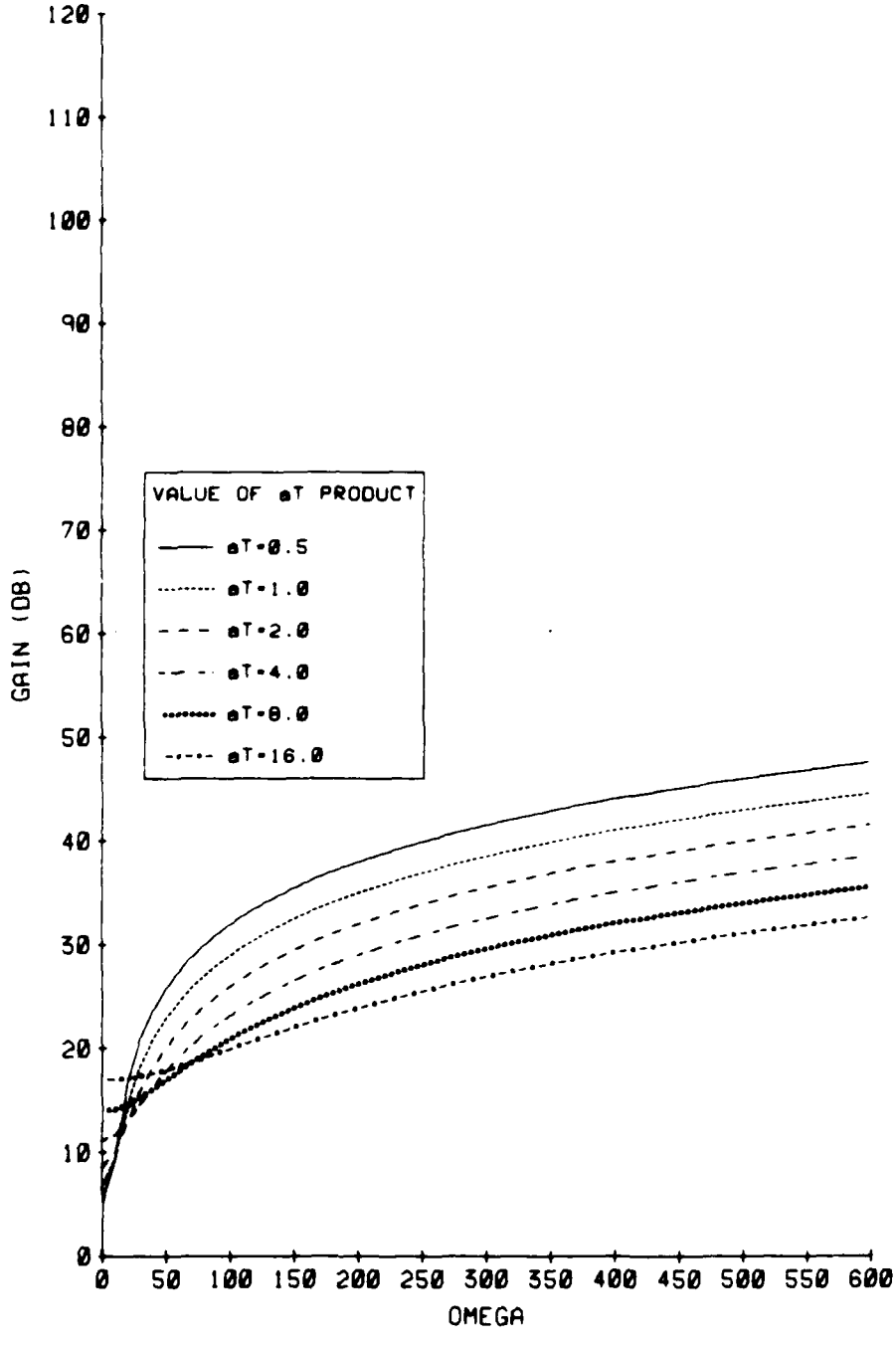

Figure 9(U) Gain using
Function 2 for L
Exp Shading and Cos Shaping

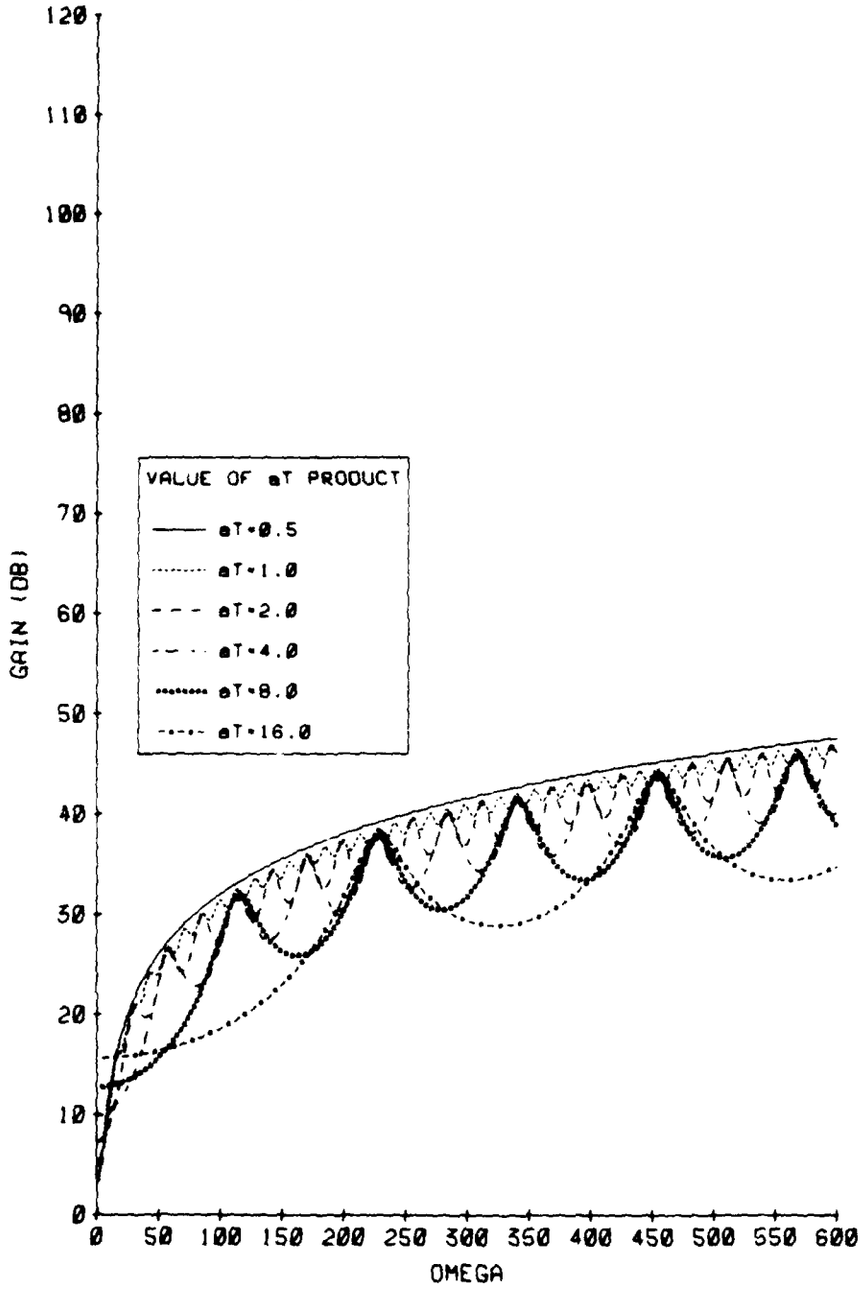

Figure 10(U) Gain using Function 3 for L No Shading and No Shaping

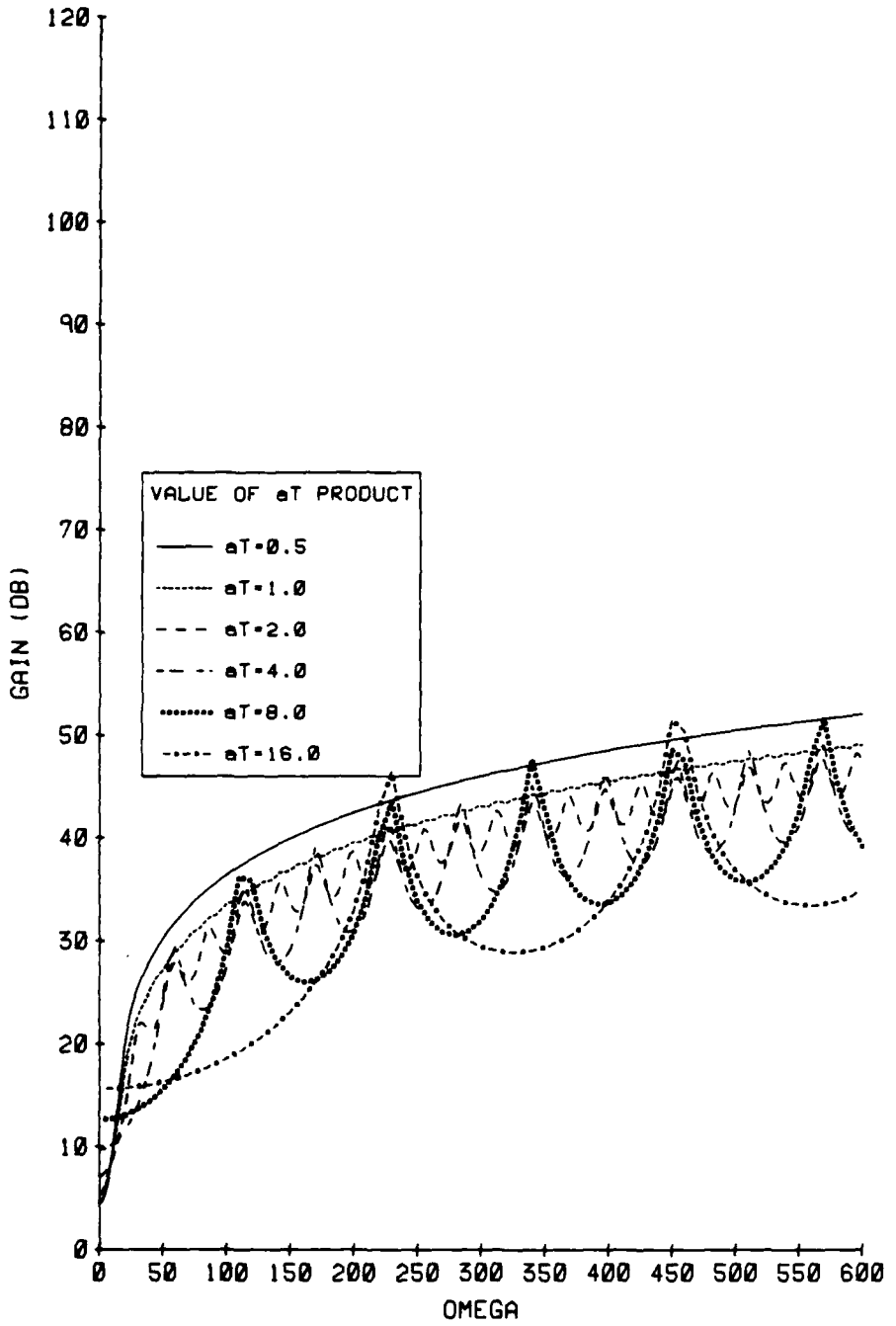

Figure 11(U) Gain using Function 3 for L Exp Shading and Exp Shaping

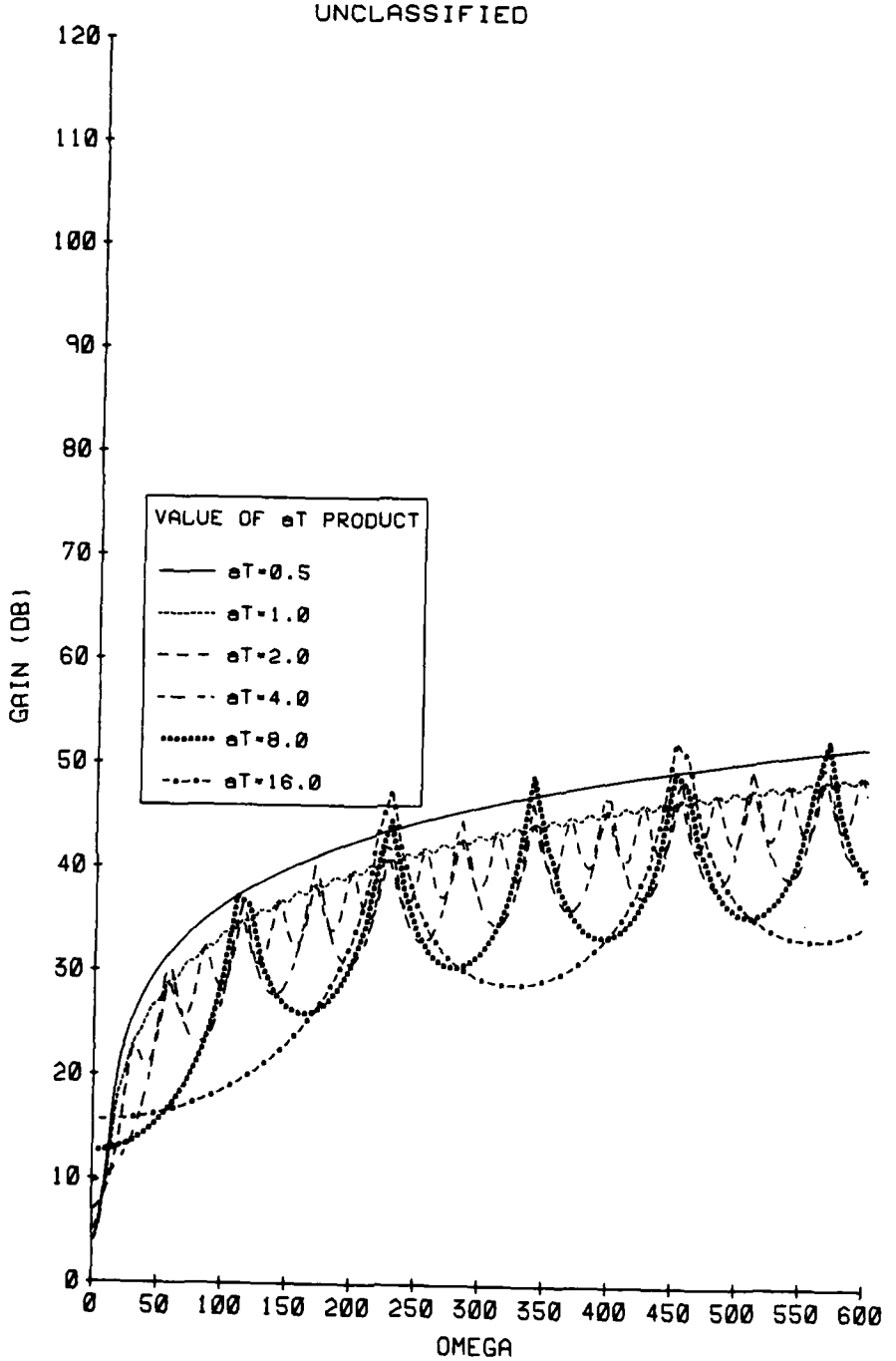

Figure 12(U) Gain using Function 3 for L Cos Shading and Cos Shaping

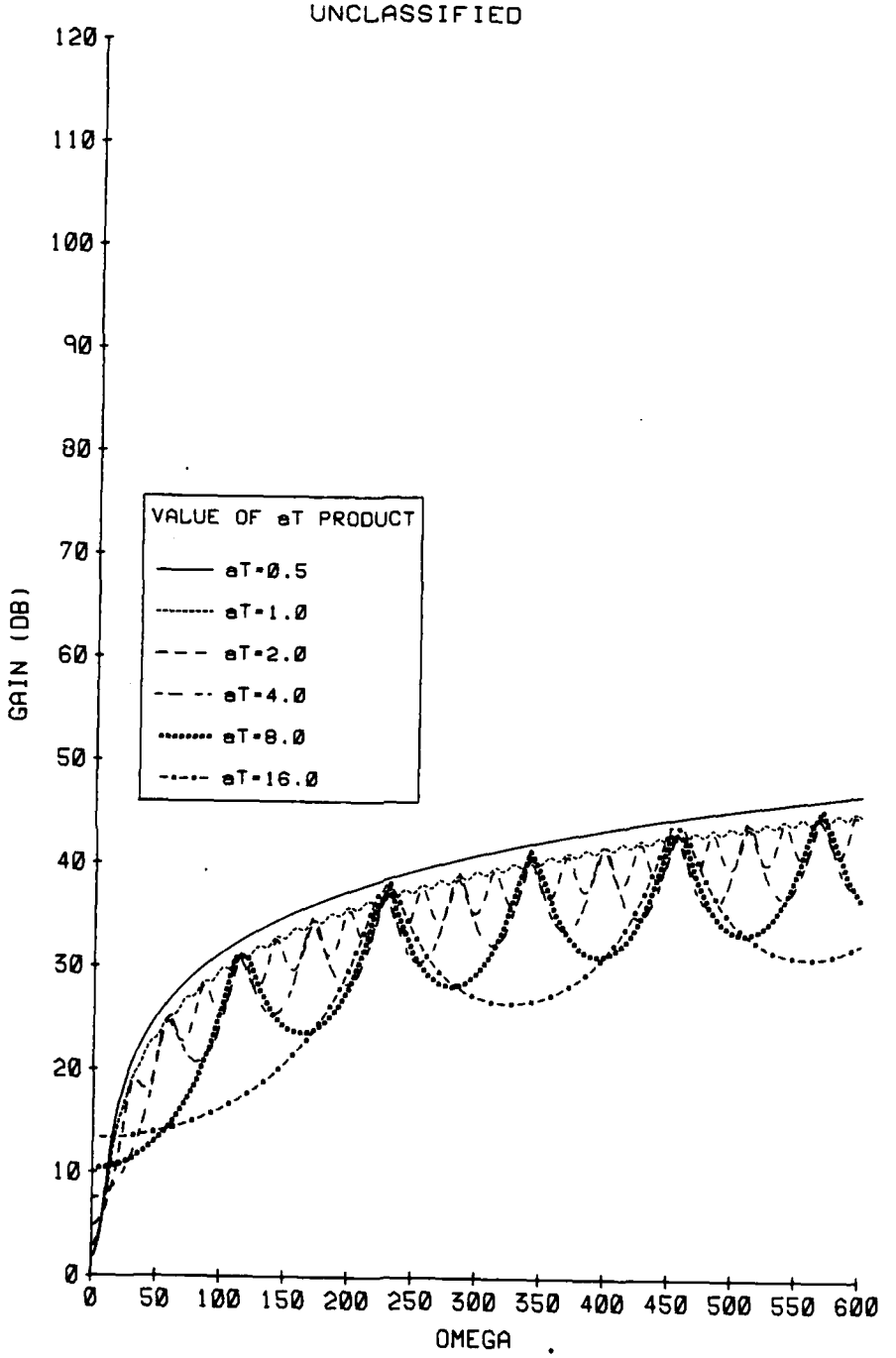

Figure 13(U) Gain using Function 3 for L Exp Shading and No Shaping

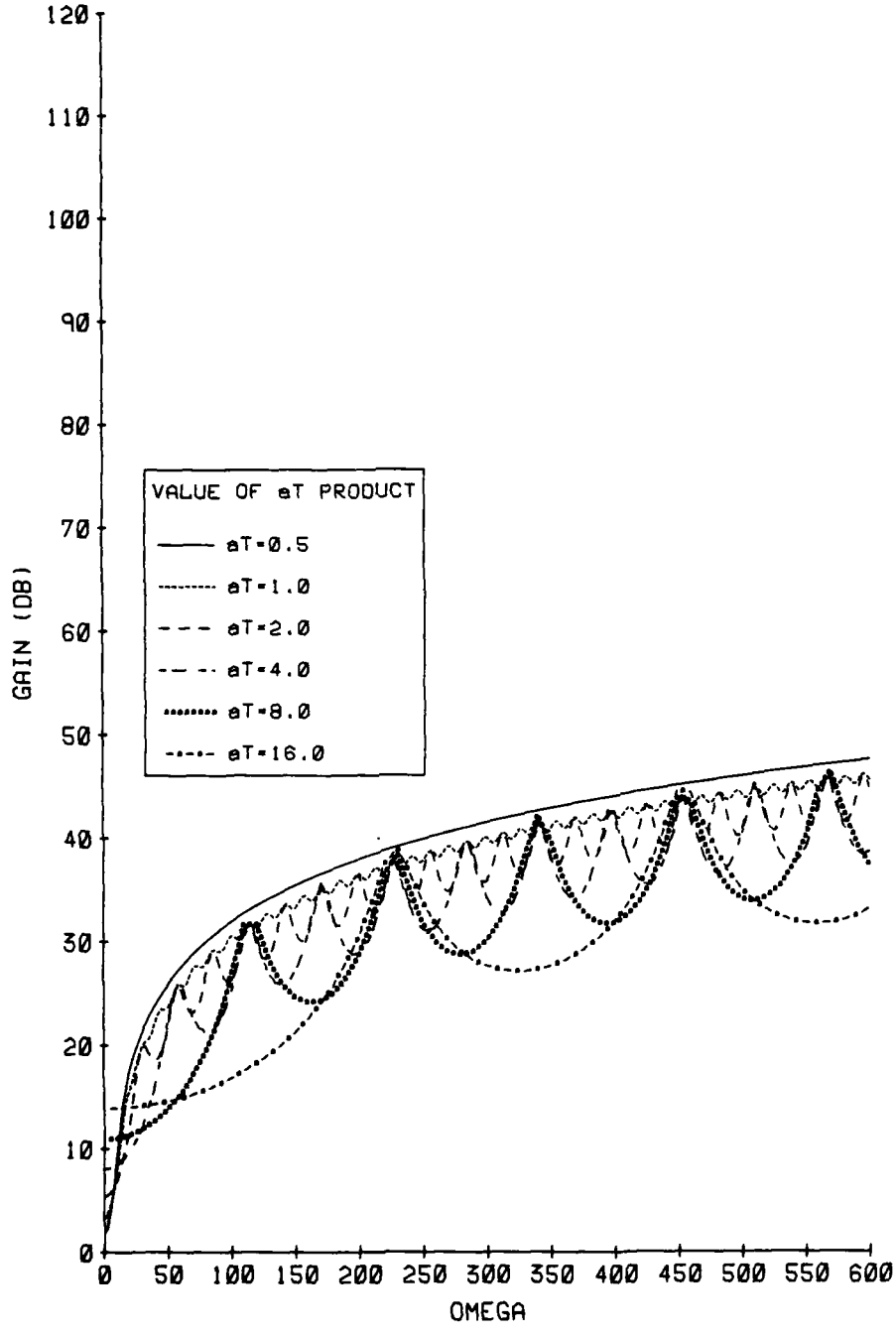

Figure 14(U) Gain using Function 3 for L Cos Shading and No Shaping

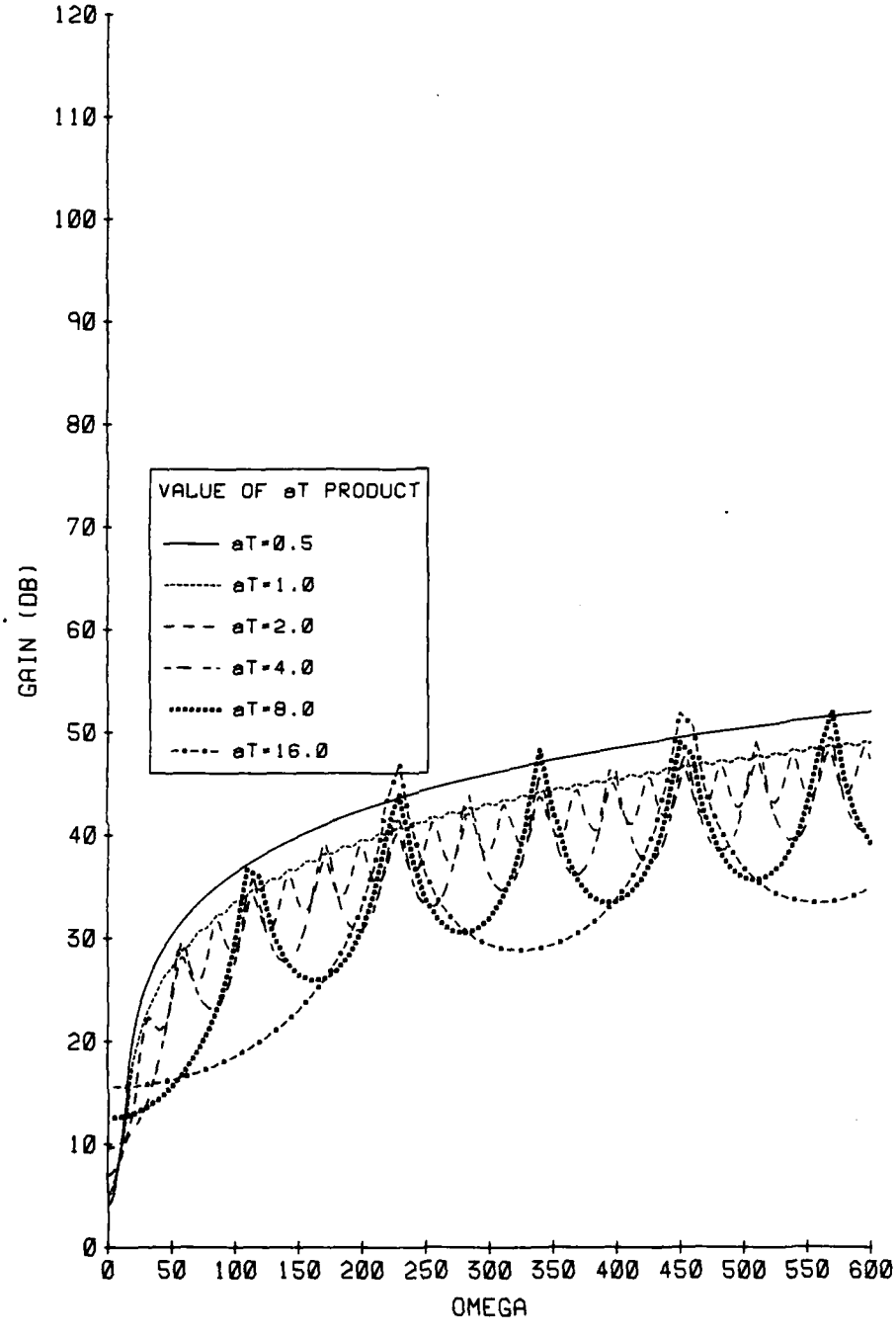

Figure 15(U) Gain using Function 3 for L Exp Shading and Cos Shaping

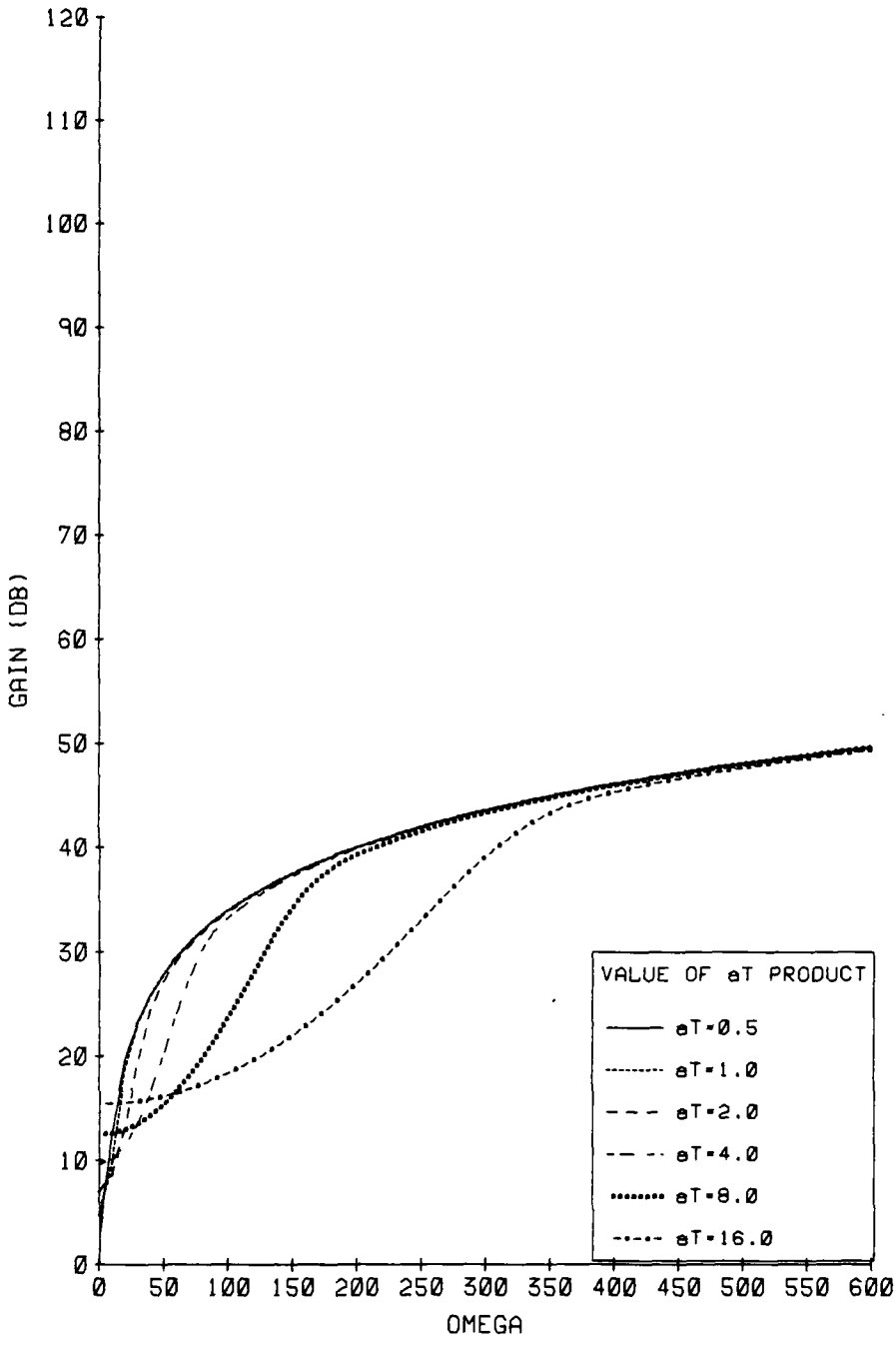

Figure 16(U) Gain using
Function 4 for L
No Shading and No Shaping

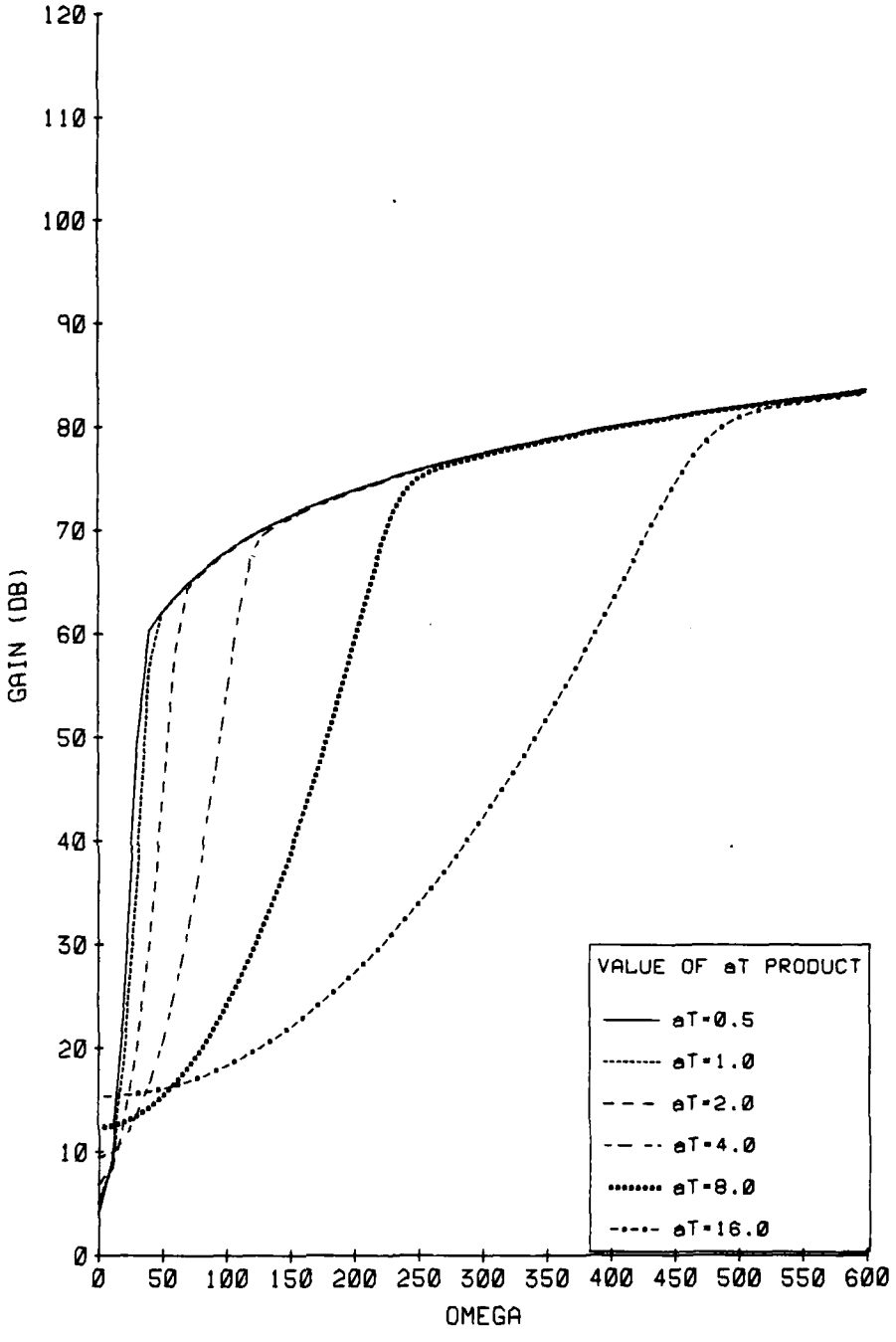

Figure 17(U) Gain using Function 4 for L Exp Shading and Exp Shaping

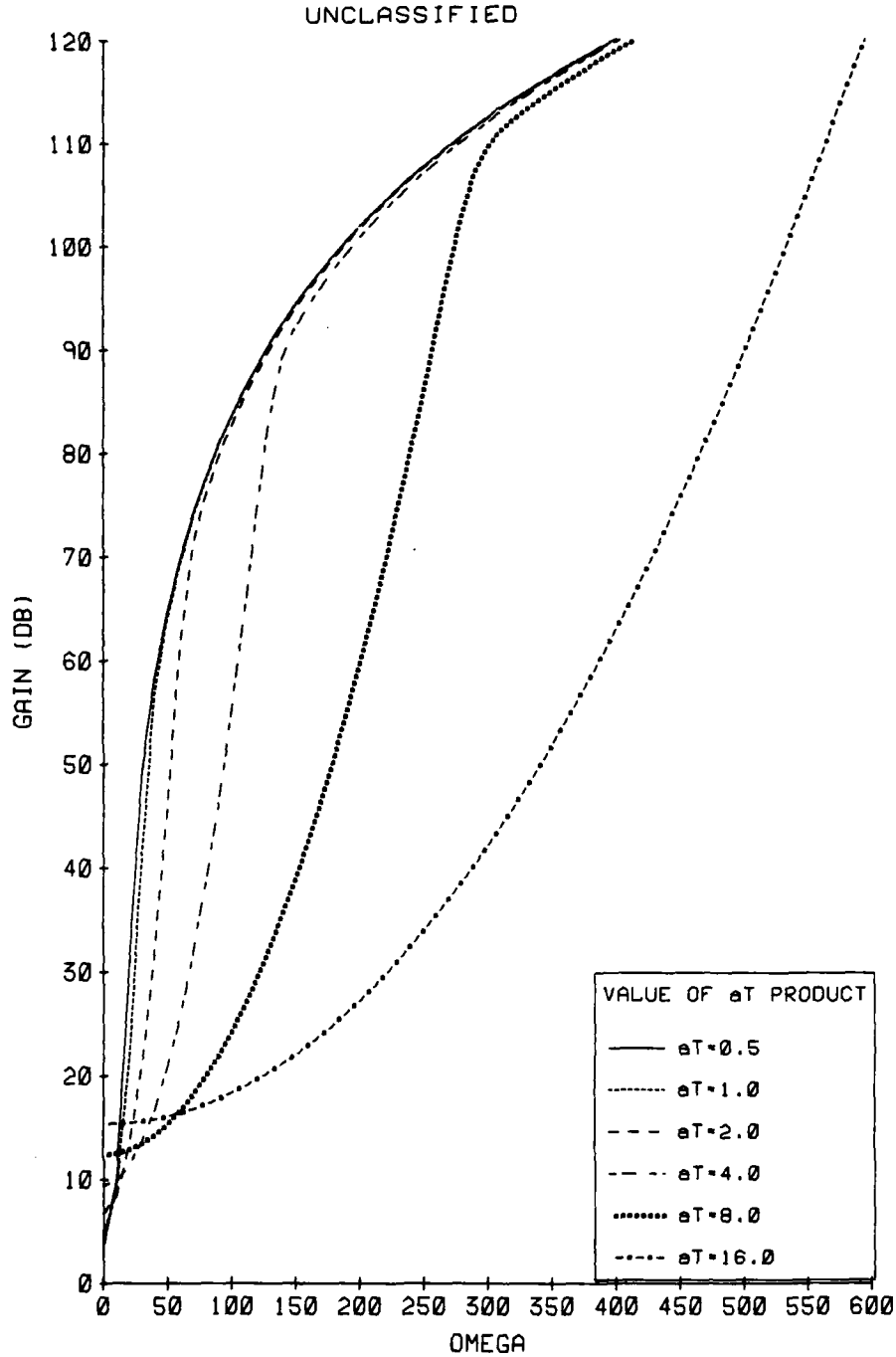

Figure 18(U) Gain using Function 4 for L Cos Shading and Cos Shaping

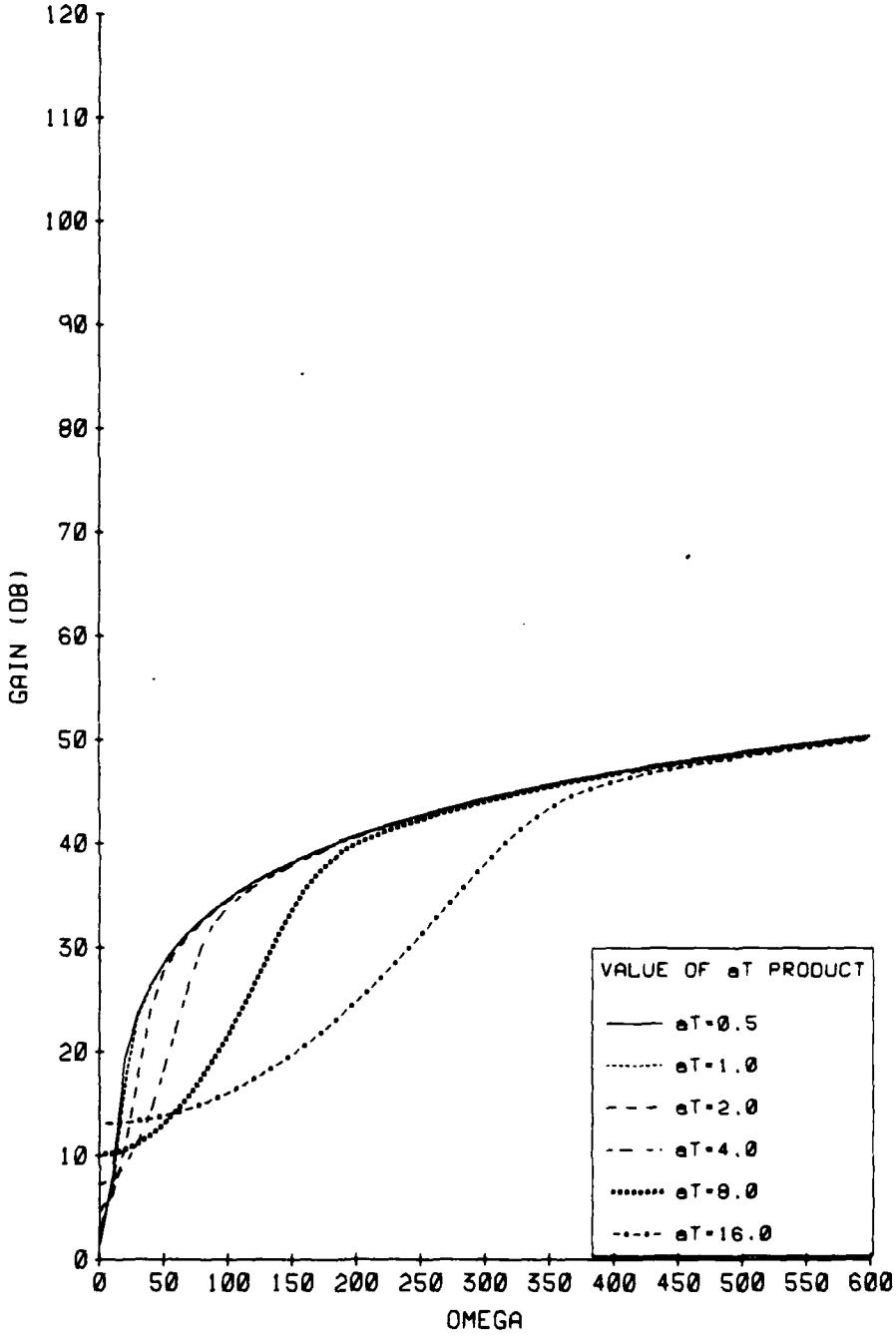

Figure 19(U) Gain using Function 4 for L Exp Shading and No Shaping

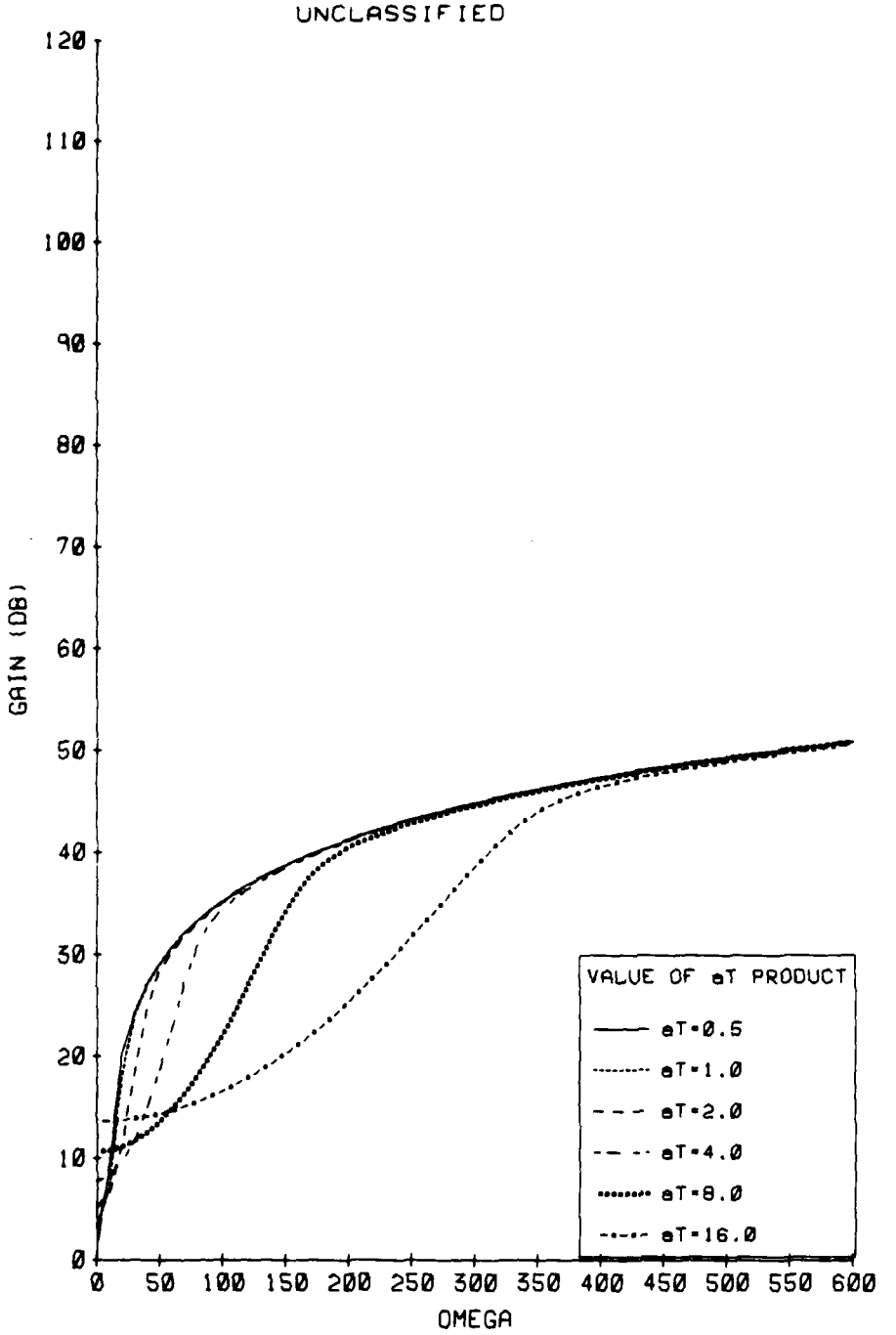

Figure 20(U) Gain using Function 4 for L Cos Shading and No Shaping

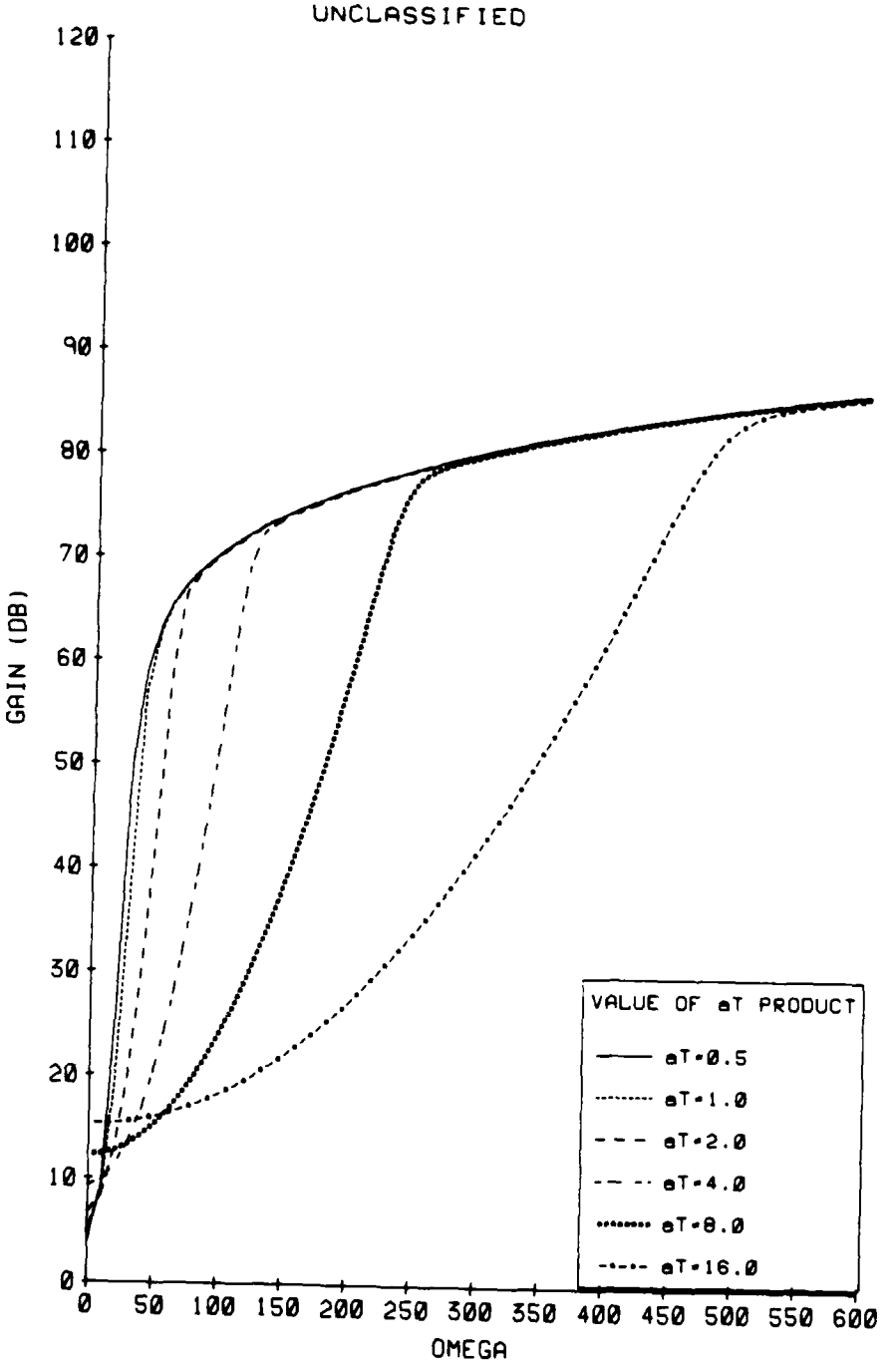

Figure 21(U) Gain using Function 4 for L Exp Shading and Cos Shaping

4.2 Chirp FM Transmission

If the transmitted pulse is a chirp,

$$M(t) = 2\pi\beta(t-K/2)^2 \qquad 0 \le t \le K \qquad [4.23]$$

where $2\beta K$ is the FM bandwidth, so that

$$W(v) = \int_v^K W(w-v)\, W(w) \cos\left(2\pi\beta(2vw - v(v+K)) \right) dw \qquad [4.24]$$

$$= \int_0^{K-v} W_1(v-w)\, W_1(v+w) \cos 2\pi\beta vw \, dw \qquad [4.25]$$

where

$$W_1(x) = W((K+x)/2) = W((K-x)/2) \qquad [4.26]$$

Assuming that $N(t)=\cos 2\pi\beta(t-T/2)^2$, which gives the maximum contribution from the target echo, a similar expression may be written for $H(v)$ with H replacing W and T replacing K throughout. However, the expressions for $H(v)$ and $W(v)$ from tables 2 and 3 are no longer valid. If $D=0$ and $T=K$,

$$Q_1 = \int_0^T H(t)\, W(t)\, dt \qquad [4.27]$$

and the equation [4.15] may be used to evaluate the gain. This gain is presented as a function of $\gamma = 2\pi\beta T^2$ (which is π times the bandwidth-pulse length product) in figure 22 for all combinations of the functions H and W from tables 2 and 3 and function 1 for L from table 1. There is very little difference in the gain for the other functions L except for small values of γ. Again, interchanging the shading and shaping functions has no effect on the gain.

From figure 22, the gain is an increasing function of γ. The gain is proportional to γ at all but very small values of γ as evidenced by the 3 dB increase in gain (in decibels) for each doubling of γ. Thus the gain is proportional to the FM bandwidth and to the pulse length. However, as

noted in section 4.1, the reverberation power will normally be proportional to the pulse length and the detection performance will therefore not be improved by increasing the pulse length.

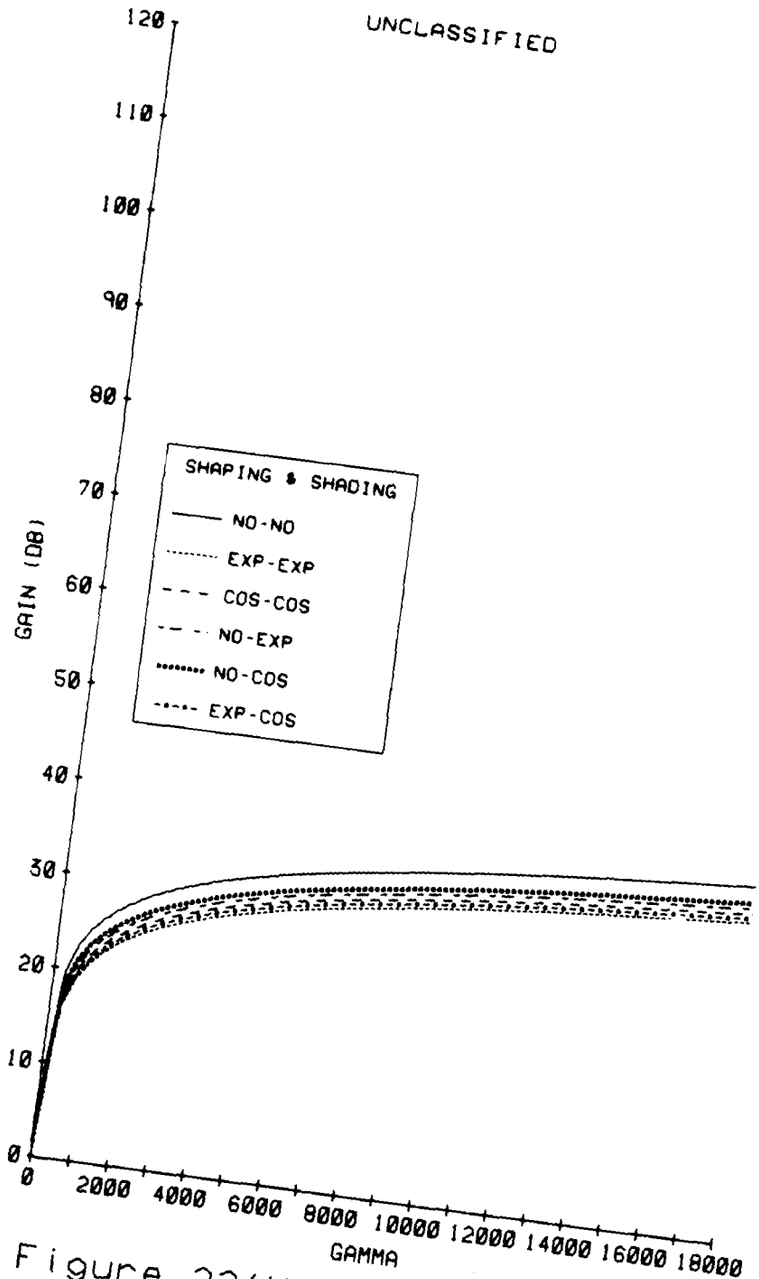

Figure 22(U) Gain Using Chirp Pulses

5. Approximate Expressions for the Gain

5.1 CW Pulses with large ω

In the cases considered in section 4.1, the gain G may be written

$$G = Q_1^2 / 2 \int_0^1 S(v) \cos \omega v \, dv \qquad [5.1]$$

where

$$S(v) = L(vT)\, W(vT)\, H(vT). \qquad [5.2]$$

For ω sufficiently large and assuming that S is infinitely differentiable, the integral in the denominator in equation [5.1] (which will be denoted J) may be expressed, after repeated integration by parts,

$$J = \sum_{n=0}^{\infty} (-1)^n \left(\frac{S^{(2n)}(1) \sin \omega}{\omega^{2n+1}} + \frac{S^{(2n+1)}(1) \cos \omega - S^{(2n+1)}(0)}{\omega^{2n+2}} \right) \qquad [5.3]$$

where $S^{(k)}$ denotes the kth derivative of S. J will be dominated by the first term in the series for which the numerator is non-zero. From equations [C.18] and [C.34], W(T) = H(T) = 0, so that S(1) = S'(1) = 0. If S'(0) ≠ 0 (it must be negative since S(x) is decreasing when x ≥ 0),

$$J = -S'(0)/\omega^2 = -T^2 (T L'(0) + W'(0) + H'(0))/ \omega^2 \qquad [5.4]$$

for large ω. After differentiating equation [C.18] and noting that W and H are symmetric about t = T/2,

$$W'(0) = -W^2(0). \qquad [5.5]$$

Similarly,

$$H'(0) = -H^2(0). \qquad [5.6]$$

Consider now each of the functions L listed in Table 1. If function 1 is used, all the derivatives of L are zero and

$$J = T^2 (W^2(0)+H^2(0))/\omega^2 \qquad [5.7]$$

provided that the term on the right hand side is non-zero. This will be true if there is either no or exp shading or shaping but not if there is both cos shaping and shading. Notice that in figure 3, the gain increases by 6 dB per doubling of ω indicating that G is proportional to ω^2 for large ω except in the cos shading and shaping case. If there is cos shading and shaping,

$$J = T^6 (W''^2(0)+H''^2(0))/\omega^6 \qquad [5.8]$$

and the gain increases by 18 dB per doubling of ω.

If function 4 is used, all odd derivatives of L(u) are zero when u=0 and all derivatives of L(u) are small when u=T. For sufficiently large ω, the gain will approach the value obtained above in the function 1 case; however ω will now have to be larger before this limit is achieved because the even derivatives of L(u) at u=0 can be quite large, especially for large values of a. These large values increase the odd derivatives $S^{(2n+1)}(0)$ for $n \geq 2$ so that a larger value of ω is required before the term $S^{(3)}(0)/\omega^6$ (say) may be neglected. This delay in reaching the limit may be seen in figures 16 to 21. For large a and moderate ω, with no shading or shaping,

$$J = T^2 \int_0^\infty \exp(-pv^2) \cos \omega v \, dv$$
$$= T^2/2 \sqrt{(\pi/p)} \exp(-\omega^2/4p)$$

where $p = \pi^2 a^2 T^2 / (\ln 2)$, which is quite large. Hence the gain is proportional to $\exp(\omega^2/4p)$, which gives the parabolic shape of the gain in decibels for the smaller values of ω in figures 16 to 21. Note that when ω is not too large, the gain is reasonably independent of the shading or shaping functions used.

If function 2 is used,

$$L'(0) = -2\pi a \qquad [5.9]$$

Hence $S'(0) \neq 0$ whatever shading or shaping functions are used and $|S'(0)|$ will be larger and hence the gain less as a increases. The gain will still increase at the rate of 6 dB per doubling of ω. This may be seen in figures

4 to 9.

If function 3 is used, equation [5.3] may not be used as S is not differentiable when 1.18 avT = 1, which occurs within the integration interval in the cases considered in section 4.1. The upper limit for the integral in equation [5.1], 1, must be replaced by $(0.72\ \pi aT)^{-1}$, which will be denoted χ. Thus,

$$J = (S'(\chi) \cos(\omega\chi) - S'(0)) / \omega^2 \qquad [5.10]$$

$$= (L'(\chi)\, H(\chi)\, W(\chi) \cos(\omega\chi) - L'(0) - W'(0) - H'(0)\ ) / \omega^2 \qquad [5.11]$$

This has an oscillating term (with decreasing frequency but increasing amplitude for increasing a) which is non-zero for any of the shading or shaping functions as may be seen in figures 10 to 15. The upper and lower limit of the oscillation grow with ω^2.

5.2 FM Pulses with large γ

If no shading or shaping is used and the reverberation is of the form given by function 1 in table 1 with $f = \mu$ then

$$L(vT) = 1 \qquad [5.12]$$

$$W(vT) = T \sin(\gamma v(1-v)) / (\gamma v) \qquad [5.13]$$

$$H(vT) = T \sin(\gamma v(1-v)) / (\gamma v) \qquad [5.14]$$

and

$$J = T^2 \int_0^1 \sin^2(\gamma v(1-v)) / (\gamma v)^2 \, dv \qquad [5.15]$$

$$= T^2 \gamma^{-1} \int_0^{\gamma} \sin^2(u(1-u/\gamma)) / u^2 \, du \qquad [5.16]$$

on letting $u = \gamma v$. Now the integrand in equation [5.16] is bounded in magnitude by an integrable function (1 for $0 \le u \le 1$ and $1/u^2$ for $u > 1$) and approaches $\sin^2 u / u^2$ as $\gamma \to \infty$. By the Lesbegue dominated convergence theorem (see reference [2], page 53)

$$\lim_{\gamma \to \infty} \int_0^{\gamma} \frac{\sin^2 u(1-u/\gamma)}{u^2} \, du = \int_0^{\infty} \lim_{\gamma \to \infty} \frac{\sin^2 u(1-u/\gamma)}{u^2} \, du \qquad [5.17]$$

$$= \int_0^{\infty} \frac{\sin^2 u}{u^2} \, du \qquad [5.18]$$

$$= \pi/2. \qquad [5.19]$$

Thus

$$J \sim \pi T^2/2\gamma + O(\gamma^{-1.5}) \qquad [5.20]$$

The next term in the asymptotic series is $O(\gamma^{-1.5})$ since on letting $u = \gamma^k v$,

$$\lim_{\gamma\to\infty} \gamma^k \int_0^{\gamma} \frac{\sin^2 u(1-u/\gamma) - \sin^2 u}{u^2}\, du \qquad [5.21]$$

$$= \lim_{\gamma\to\infty} \int_0^{k\sqrt{\gamma}} \frac{\sin^2 (\gamma^k v - \gamma^{2k-1}v^2) - \sin^2 (\gamma^k v)}{u^2} du \qquad [5.22]$$

$$= 0 \text{ if } k < 0.5. \qquad [5.23]$$

This limiting behaviour may be seen in figure 22.

If other functions L are used, the limiting behaviour is the same, since

$$J = \gamma^{-1} \int_0^{\gamma} L(u/\gamma) \sin^2(u(1-u/\gamma)) / u^2\, du \qquad [5.24]$$

where $L(0) = 1$ and $L(v)$ is a decreasing function of v and the integrand is still bounded in magnitude by an integrable function and the limit of the integrand as $\gamma\to\infty$ is still $\pi/2$. Equation [5.20] still applies.

If more general shading or shaping functions are used,

$$J = T^2\gamma^{-1} \int_0^{\gamma} L(vT/\gamma)\, W(vT/\gamma)\, H(vT/\gamma)\, dv \qquad [5.25]$$

so that

$$J \sim \chi\, T^2/\gamma \qquad [5.26]$$

where

$$\chi = \lim_{\gamma\to\infty} T^{-2} \int_0^{\gamma} L(vT/\gamma)\, W(vT/\gamma)\, H(vT/\gamma)\, dv. \qquad [5.27]$$

Now

$$\mathbb{W}(vT/\gamma) = T\int_0^{1-v/\gamma} W_1(Tv/\gamma - Tw)\, W_1(Tv/\gamma + Tw) \cos vw\, dw \qquad [5.28]$$

$$\rightarrow T\int_0^1 W_1^2(Tw) \cos vw\, dw = h_1(v) \text{ (say)} \qquad [5.29]$$

as $\gamma \rightarrow \infty$. Similarly,

$$\mathbb{H}(vT/\gamma) = T\int_0^{1-v/\gamma} H_1(Tv/\gamma - Tw)\, H_1(Tv/\gamma + Tw) \cos vw\, dw \qquad [5.30]$$

$$\rightarrow T\int_0^1 H_1^2(Tw) \cos vw\, dw = h_2(v) \text{ (say)} \qquad [5.31]$$

as $\gamma \rightarrow \infty$. Since $|\mathbb{W}(vT/\gamma)|$ and $|\mathbb{H}(vT/\gamma)|$ are each bounded by a constant times v^{-1} for large v, the product $|\mathbb{W}(vT/\gamma)\, \mathbb{H}(vT/\gamma)|$ is bounded by an integrable function and the Lesbegue dominated convergence theorem implies that

$$\chi = \int_0^\infty h_1(v)\, h_2(v)\, dv. \qquad [5.32]$$

$$= (\pi/2) \int_0^1 H_1^2(Tw)\, W_1^2(Tw)\, dw \qquad [5.33]$$

The equality of the integrals in equations [5.32] and [5.33] is demonstrated in annex C.3, where it is also shown that the gain has its maximum value for a large fixed γ when no shading or shaping are used. The gain is proportional to γ and therefore increases linearly with bandwidth.

6. An Example

To illustrate the use of the results presented in this paper, a simple example of a sonar attempting to detect a target is considered. In this section, the average signal power $\mathbb{P}$, the background noise in a 1Hz band, N_0 and the average reverberation power $\mathbb{R}$ will be expressed in decibels (re 1μpascal) and may be calculated using the usual sonar equations as

$$\mathbb{P} = SL - 2\,PL + TS \quad [6.1]$$

$$N_0 = NL - DI \quad [6.2]$$

$$\mathbb{R} = SL - 2\,PL + S + 10 \log A \quad [6.3]$$

where SL is the source level, PL is the one way propagation loss to the target, TS is the target strength, NL the ambient noise level, DI the directivity index, S the scattering strength and A the reverberating area.

In this example, the sonar transmits 2 second pulses at 4 kHz and the threshold is set to give a false alarm probability of 10^{-5}. Suppose that for the analysis period during which the target signal is maximum,

$$\mathbb{P} = 60 \text{ dB} \quad [6.4]$$

$$N_0 = 48 \text{ dB} \quad [6.5]$$

$$\mathbb{R} = 85 \text{ dB}. \quad [6.6]$$

Consider first the noise limited performance of the sonar ie the performance of the sonar in the presence of noise only. If the conditions of section 3 to give a maximum value of P are met,

$$P = \mathbb{P}T/2N_0 = 12 \text{ dB}. \quad [6.7]$$

Hence, using equation [2.8] or figure 1, the probability of detection is about 0.8. The signal excess, which is defined as the ratio of P to the value of P required for a 50% probability of detection (10 dB here) is about 2 dB.

Next consider the reverberation limited performance of the sonar ie the performance of the sonar in the presence of reverberation alone. If the conditions of the base case of section 4 apply,

$$P = \mathbb{P}/\mathbb{R} = -25 \text{ dB} \quad [6.8]$$

and the probability of detection is 1.04×10^{-5}, only marginally above the false alarm probability. The signal excess is about -35 dB. If doppler processing , as described in section 4, is used, table 4 gives the signal excess and probability of detection for three combinations of shading and shaping functions and several values of the radial component of the velocity of the target relative to the sonar on the assumption of no reverberation frequency spreading. These are derived by first calculating the doppler shift Δf induced in the signal by the radial speed (≈ 2.8 x radial speed (in knots) for 4 kHz sonar) and using this to calculate $\omega = 2\pi\Delta fT$ and hence, using figure 3, the gain in P over its base case value. The signal excess is this improved value (in decibels) less 10 dB as required for the 50% probability of detection. The probability of detection is found from figure 1. Note that even with zero dopploer, there is a slight improvement in signal excess over the base case value due to the different assumptions made about the nature of reverberation.

Against a combined noise and reverberation background, the high values of signal excess and detection probabilities above 0.8 would not be achievable. Instead a value of P given in terms of the value for noise limited performance P_n and the value for reverberation limited performance P_r by

$$P^{-1} = P_n^{-1} + P_r^{-1} \qquad [6.9]$$

should be used to calculate the signal excess and probability of detection. Table 5 gives the signal excesses and the probabilities of detection against the combined background. Note that the signal excess can never be better than the value calculated against noise alone or the value calculated against reverberation alone.

If there is a spread of reverberation frequencies, then figure 3 is not the appropriate one to calculate the gain. If, for example, the spread in the reverberation frequencies had a bandwidth of 4 Hz and a gaussian shape, then function 4 from table 1 with $aT=4$ (a is the half-bandwidth) should be used. The signal excesses and the probabilities of detection in this case, using the $aT=4$ lines in figures 16 to 18 to calculate the gain, are given in table 6. Note that there is no longer any performance with only one or two knots of relative radial speed with exp or cos shaping and shading.

If an FM chirp pulse with bandwidths 200,400 or 800 Hz is used,

instead of the CW pulse with doppler processing, the gain may be calculated from figure 22 with $\gamma = \pi x$bandwidthxpulse length. The signal excesses and probabilities of detection are given in table 7 and these are not sensitive to frequency spreading of the reverberation. Note that this processing option does not give any useful performance in this case.

Table 4

Signal Excesses (dB) and Probabilities of Detection with Reverberation Limitations Only (CW Pulse)

Relative Radial Speed (knots)	No Shading or Shaping		Exp Shading and Shaping		Cos Shading and Shaping	
	SE	pd	SE	pd	SE	pd
0.0	-33	0.00001	-31	0.00001	-32	0.00001
0.5	-16	0.00006	-13	0.0002	-3	0.07
1.0	-10	0.0007	22	1.	19	1.
2.0	-4	0.03	30	1.	39	1.
4.0	2	0.8	36	1.	57	1.

Table 5

Signal Excesses (dB) and Probabilities of Detection with Reverberation and Noise with no Frequency Spreading (CW Pulse)

Relative Radial Speed (knots)	No Shading or Shaping		Exp Shading and Shaping		Cos Shading and Shaping	
	SE	pd	SE	pd	SE	pd
0.0	-33	0.00001	-31	0.00001	-32	0.00001
0.5	-16	0.00006	-13	0.0002	-4	0.07
1.0	-10	0.0007	2	0.8	2	0.8
2.0	-5	0.02	2	0.8	2	0.8
4.0	-1	0.2	2	0.8	2	0.8

Table 6

Signal Excesses (dB) and Probabilities of Detection with Reverberation and Noise and Frequency Spreading (CW Pulse)

Relative Radial Speed (knots)	No Shading or Shaping		Exp Shading and Shaping		Cos Shading and Shaping	
	SE	pd	SE	pd	SE	pd
0.0	-26	0.00001	-26	0.00001	-26	0.00001
0.5	-24	0.00002	-24	0.00002	-24	0.00002
1.0	-20	0.00002	-20	0.00002	-20	0.00002
2.0	-8	0.002	-5	0.02	-5	0.02
4.0	-1	0.2	2	0.8	2	0.8

Table 7

Signal Excesses (dB) and Probabilities of Detection with Reverberation and Noise (FM pulse)

Bandwidth (Hz)	No Shading or Shaping		Exp Shading and Shaping		Cos Shading and Shaping	
	SE	pd	SE	pd	SE	pd
200	-9	0.001	-13	0.0002	-12	0.0003
400	-7	0.004	-10	0.0007	-9	0.001
800	-4	0.03	-8	0.002	-7	0.004

7. Summary

The probability of detection of a reflected signal from a target in the presence of interference depends only on the quantity P, defined by equation [2.9], for a given probability of false alarm provided certain assumptions listed in annex B regarding the nature of the interference are met. This relationship is illustrated in figure 1. Most of the variations in the assumptions that are considered in annex B and illustrated in figures 23 to 28 do not change the value of P required to achieve a particular probabilty of detection by more than a few decibels. The variation with the greatest effect is the rejection of the gaussian assumption.

The quantity P may be estimated if the statistics and other properties of the interference are known. However, P is highly dependent on the following factors

i) the pulse shaping and analysis filter shading functions used
ii) the statistics of the reverberation
iii) the frequency spread of the reverberation and the difference between the main reverberation and the signal centre frequencies if doppler processing is used
iv) the bandwidth if FM pulses are used
v) the alignment of the pulse and analysis periods and the alignment of the pulse and analysis frequencies
vi) the relative values of the pulse length and the length of the analysis period.

In the presence of white gaussian noise, the maximum value of P is given by

$$P = PT/2N_0 \qquad [7.1]$$

where P is the average signal power, T is the pulse length and N_0 is the noise power spectrum level. This leads to the familiar expressions for the detection threshold (eg reference [1] Chapter 12)

Using specific options regarding the factors listed above, a base case for detection in the presence of reverberation may be defined where P is simply the ratio of the average signal power to the average reverberation power. This base case leads to very poor performance in most cases, but this performance may be improved by using other options. The resulting

proportional increase in P is denoted the gain.

Assuming a particular model of the statistics of the reverberation, an expression for the gain is derived (equation [4.15]) as a function of the other factors listed above as i) and iii) to vi).

This expression is used to calculate the gain, assuming no misalignment (see v) above) and equal pulse and analysis periods using three options each of shading and shaping functions. For doppler processing in the case of no reverberation frequency spreading, the gain is presented in figure 3 as a function of $\omega = 2\pi\Delta fT$, where Δf is the difference between the signal frequency and the reverberation frequency and T is the pulse length. Similar results are presented in figures 4 to 21 for various options of reverberation frequency spreading and illustrate the importance of this spreading and the large differences in the results which may be obtained if different assumptions are made about the shape of the spreading function. The spreading could be caused by motion of the scatterer relative to the sonar (eg sea surface reverberation) or if the sonar is moving by the fact that all reverberation entering a beam will not have the same doppler shift. The same effect could be caused if the scatterers change their properties over time periods less than a pulse length. Figure 22 shows the gain using FM chirp pulses as a function of $\gamma = \pi WT$ where W is the bandwidth. This gain is not sensitive to the reverberation frequency spreading considered in the doppler processing case. The gain is greatest when no shading or shaping is used.

Asymptotic expressions for the gain for large values of ω using doppler processing or large values of γ using FM pulses are derived in section 5. It is shown that under most circumstances the gain is proportional to ω^2 for large ω using doppler processing (ie 6 dB improvement in gain for each doubling of ω) and the gain is proportional to γ for large γ using FM pulses. The proportionality constant depends on the shading and shaping functions used and for doppler processing on the function assumed for the frequency spreading of the reverberation.

The combined effect of noise and reverberation is to give a value of P calculated as

$$P^{-1} = P_n^{-1} + P_r^{-1} \qquad [7.2]$$

where P_n is the value of P calculated with interference due to noise only

and P_r is the value of P calculated with interference due to reverberation only.

The mis-alignment of the pulse and analysis periods for doppler processing can give quite large degradations (up to 20 dB using exp shading and shaping as defined in tables 2 and 3) in the gain. This degradation may be reduced by overlapping the analysis periods, which necessitates more processing and may increase the false alarm rate. Misalignment of the pulse and analysis frequencies using doppler processing produces a smaller degradation (at worst 4 dB using no shading or shaping) assuming that the analysis frequencies are separated by T^{-1}.

The misalignment of the pulse and analysis periods for FM pulses is analogous to misalignment of the pulse and analysis frequencies for doppler processing. Providing the analysis periods are overlapped so that their starting times are separated by W^{-1}, the maximum degradation is 4 dB when no shading or shaping is used. The misalignment of the pulse and analysis frequencies for FM pulses is analogous to misalignment of the pulse and analysis periods for doppler processing. Although the selection of a different analysis period may reduce the frequency misalignment, the degradation may be quite large (up to 20 dB for exp shading and shaping as defined in tables 2 and 3).

References

[1] Urick R.J. "Principles of Underwater Sound" McGraw-Hill 1983.

[2] Schwartz L. "Mathematics for the Physical Sciences" Addison-Wesley 1966.

[3] Abramowitz M. and Stegun I.A. "Handbook of Mathematical Functions" Dover 1972.

[4] Lanczos C. "Discourse on Fourier Series" Oliver & Boyd 1966.

ANNEX A

PROBABILITY OF FALSE ALARM AND PROBABILITY OF DETECTION

When a signal is not present, the output y(t) from the beam-former is made up entirely of interference x(t). Assume that, in this case, B and C, as defined in equations [2.4] and [2.5], have a Gaussian distribution with zero mean. The variance of B is then

$$\text{var}(B) = \int_0^T \int_0^T S(t,u) \cos(N(t)+2\pi ft) \cos(N(u)+2\pi fu)\, dt\, du \qquad [A.1]$$

where

$$S(t,u) = E[\, x(t)x(u)\,]\, H(t)\, H(u). \qquad [A.2]$$

On letting v=t-u in equation [A.1],

$$\text{var}(B) = \int_0^T \int_v^T S(t,t-v) \{ \cos(N(t)-N(t-v)+2\pi fv) + \cos(N(t)+N(t-v)+2\pi f(2t-v)) \}\, dt\, dv. \qquad [A.3]$$

Similarly,

$$\text{var}(C) = \int_0^T \int_v^T S(t,t-v) \{ \cos(N(t)-N(t-v)+2\pi fv) - \cos(N(t)+N(t-v)+2\pi f(2t-v)) \}\, dt\, dv \qquad [A.4]$$

$$\text{cov}(B,C) = \int_0^T \int_v^T S(t,t-v) \sin(N(t)+N(t-v)+2\pi f(2t-v))\, dt\, dv. \qquad [A.5]$$

On making the substitution w = T - 2t + v in the second of the inner integrals in equation [A.3] or [A.4],

$$\int_v^T S(t,t-v) \cos(N(t)+N(t-v)+2\pi f(2t-v))\, dt = 0.5 \int_{-T+v}^{T-v} S_1(v-w,v+w) \cos(N_1(w-v)+N_1(w+v)+2\pi f(T-w))\, dw \qquad [A.6]$$

where

$$S_1(x,y) = S((T+x)/2 , (T-y)/2) \qquad [A.7]$$

$$N_1(x) = N((T-x)/2). \qquad [A.8]$$

Thus,

$$\int_0^T \int_v^T S(t,t-v) \cos (N(t)+N(t-v)+ 2\pi f(2t-v)) \, dt \, dv$$
$$= \alpha_1 \cos 2\pi fT + \alpha_2 \sin 2\pi fT$$
$$= \alpha \cos (2\pi fT - \varepsilon_1) \qquad [A.9]$$

where

$$\alpha_1 = 0.5 \int_0^T \int_{-T+v}^{T-v} S_1(v-w,v+w) \cos (2\pi fw-N_1(w-v)-N_1(w+v)) \, dw \, dv$$
$$= \alpha \cos \varepsilon_1 \qquad [A.10]$$

$$\alpha_2 = 0.5 \int_0^T \int_{-T+v}^{T-v} S_1(v-w,v+w) \sin (2\pi fw-N_1(w-v)-N_1(w+v)) \, dw \, dv$$
$$= \alpha \sin \varepsilon_1 \qquad [A.11]$$

Similarly,

$$\int_0^T \int_v^T S(t,t-v) \sin (N(t)+N(t-v)+ 2\pi f(2t-v)) \, dt \, dv$$
$$= \alpha_1 \sin 2\pi fT - \alpha_2 \cos 2\pi fT$$
$$= \alpha \sin (2\pi fT - \varepsilon_1) \qquad [A.12]$$

Thus,

$$\text{var } (B) = \sigma^2 (1 + A \cos \varepsilon) \qquad [A.13]$$

$$\text{var } (C) = \sigma^2 (1 - A \cos \varepsilon) \qquad [A.14]$$

$$\text{cov}(B,C) = \sigma^2 A \sin \varepsilon, \qquad [A.15]$$

where

$$\sigma^2 = \int_0^T \int_v^T S(t,t-v) \cos (N(t)-N(t-v)+2\pi fv) \, dt \, dv \qquad [A.16]$$

$$= 0.5 \int_0^T \int_{-T+v}^{T-v} S_1(v-w,v+w) \cos(2\pi fv + N_1(w-v) - N_1(w+v))\, dw\, dv \qquad [A.17]$$

$$A = \alpha/\sigma^2 \qquad [A.18]$$

$$\varepsilon = 2\pi fT - \varepsilon_1 \qquad [A.19]$$

The correlation coefficient between B and C is

$$\rho = \frac{A \sin \varepsilon}{(1 - A^2 \cos^2 \varepsilon)^{0.5}} \qquad [A.20]$$

and the joint probability density function for B and C is

$$f(B,C) = \frac{1}{2\pi(1-A^2)^{0.5}\sigma^2} \exp\left(-\frac{B^2 + C^2 - A((B^2-C^2)\cos\varepsilon + 2BC \sin\varepsilon)}{2\sigma^2(1-A^2)}\right). \qquad [A.21]$$

On transforming to polar co-ordinates

$$r = (B^2 + C^2)^{0.5} \qquad [A.22]$$

$$\theta = \arctan(C/B) \qquad [A.23]$$

the joint probability density function of r and θ becomes

$$f(r,\theta) = \frac{r}{2\pi(1-A^2)^{0.5}\sigma^2} \exp\left(-\frac{r^2(1 - A\cos(2\theta-\varepsilon))}{2\sigma^2(1-A^2)}\right). \qquad [A.24]$$

On integration with respect to θ, the probability density function for r becomes

$$f(r) = \frac{r}{\sigma^2(1-A^2)^{0.5}} \exp\left(-\frac{r^2}{2\sigma^2(1-A^2)}\right) I_0\left(\frac{A r^2}{2\sigma^2(1-A^2)}\right). \qquad [A.25]$$

where $I_0(\,)$ is the modified Bessel function of order zero, defined for example in reference [3].

If $|A| = 1$, the above analysis breaks down. In this case, the correlation coefficient between B and C is 1 or -1 depending on the sign of sin ε and

$$\text{var}(B) = 2\sigma^2 \cos^2(\varepsilon/2) \qquad [A.26]$$

$$\text{var}(C) = 2\sigma^2 \sin^2(\varepsilon/2). \qquad [A.27]$$

Thus

$$C = B \tan(\varepsilon/2) \qquad [A.28]$$

$$r = (B^2 + C^2)^{0.5} = \frac{|B|}{|\cos(\varepsilon/2)|} = \frac{|C|}{|\sin(\varepsilon/2)|} \qquad [A.29]$$

and the probability density function for r is

$$f(r) = \frac{1}{\sqrt{(2\pi)}\,\sigma} \exp\left(-\frac{r^2}{4\sigma^2}\right). \qquad [A.30]$$

In any case, if R is the threshold described at the end of the first paragraph in section 2, the probability of false alarm,

$$p_{fa} = \int_R^\infty f(r)\,dr. \qquad [A.31]$$

If $A = 0$ (which is approximately true in most cases considered in subsequent sections), the probability density function is

$$f(r) = \frac{r}{\sigma^2} \exp\left(-\frac{r^2}{2\sigma^2}\right) \qquad [A.32]$$

and the probability of false alarm is

$$p_{fa} = \exp\left(-\frac{R^2}{2\sigma^2}\right). \qquad [A.33]$$

Now suppose that a target echo of the form given in equation [2.7] is present. The variances of B and C and the covariance of B and C will be the same as in the interference only case as given by equations [A.4] to [A.6]. The expected values of B and C will no longer be zero, but

$$E[B] = (2P)^{0.5} \int_D^E W(t-D) \cos (M(t-D) + 2\pi f_1 t + \theta_1) H(t) \cos (N(t)+2\pi ft)\, dt \qquad [A.34]$$

$$= (P/2)^{0.5} \int_D^E W(t-D) H(t) \{ \cos (M(t-D)-N(t)+2\pi(f_1-f)t+\theta_1) + \cos (M(t-D)+N(t)+2\pi(f_1+f)t+\theta_1) \}\, dt \qquad [A.35]$$

$$= (P/2)^{0.5} \{ Q_1 \cos (\theta_1 + \alpha) + Q_2 \cos(\theta_1 + \beta) \} \qquad [A.36]$$

where

$$Q_1 \cos \alpha = \int_D^E W(t-D) H(t) \cos (M(t-D) - N(t) + 2\pi(f_1-f)t)\, dt \qquad [A.37]$$

$$Q_1 \sin \alpha = \int_D^E W(t-D) H(t) \sin (M(t-D) - N(t) + 2\pi(f_1-f)t)\, dt \qquad [A.38]$$

$$Q_2 \cos \alpha = \int_D^E W(t-D) H(t) \cos (M(t-D) + N(t) + 2\pi(f_1+f)t)\, dt \qquad [A.39]$$

$$Q_2 \sin \alpha = \int_D^E W(t-D) H(t) \sin (M(t-D) + N(t) + 2\pi(f_1+f)t)\, dt. \qquad [A.40]$$

Similarly,

$$E[C] = (P/2)^{0.5} \{ -Q_1 \sin (\theta_1 + \alpha) + Q_2 \sin (\theta_1 + \beta) \} \qquad [A.41]$$

The joint probability density function of B and C with signal present is obtained by substituting (B-B) and (C-C) for B abnd C in the right hand side of equation [A.21] (where B and C denote E[B] and E[C] respectively):

$$f(B,C) = \frac{\exp \left(- \frac{(B-B)^2+(C-C)^2-A(((B-B)^2-(C-C)^2)\cos \varepsilon +2(B-B)(C-C)\sin \varepsilon)}{2\sigma^2 (1 - A^2)} \right)}{2\pi \sigma^2 (1 - A^2)^{0.5}} \qquad [A.42]$$

On transforming to polar co-ordinates using equations [A.22] and [A.23], the various terms in the above equation may be written

$$(B-B)^2 + (C-C)^2 = r^2 - (2\mathbb{P})^{0.5} r\,(Q_1 \cos(\theta+\theta_1+\alpha) + Q_2 \cos(\theta-\theta_1-\beta)) + (\mathbb{P}/2)\,(Q_1^2 + 2\,Q_1Q_2 \cos(2\theta_1+\alpha+\beta) + Q_2^2) \quad [A.43]$$

$$(B-B)^2 - (C-C)^2 = r^2 \cos 2\theta - (2\mathbb{P})^{0.5} r\,(Q_1 \cos(\theta-\theta_1-\alpha) + Q_2 \cos(\theta+\theta_1+\beta)) + (\mathbb{P}/2)\,(Q_1^2 \cos(2\theta_1+2\alpha) + 2\,Q_1Q_2 \cos(\alpha-\beta) + Q_2^2 \cos(2\theta_1+2\beta)) \quad [A.44]$$

$$2\,(B-B)\,(C-C) = r^2 \sin 2\theta - (2\mathbb{P})^{0.5} r\,(Q_1 \sin(\theta-\theta_1-\alpha) + Q_2 \sin(\theta+\theta_1+\beta)) + (\mathbb{P}/2)\,(-Q_1^2 \sin(2\theta_1+2\alpha) - 2\,Q_1Q_2 \sin(\alpha-\beta) + Q_2^2 \sin(2\theta_1+2\beta)) \quad [A.45]$$

and the joint probability density function for r and θ is

$$f(r,\theta) = \frac{r \exp\left(-\frac{XX}{2\sigma^2(1-A^2)}\right)}{2\pi\sigma^2(1-A^2)^{0.5}} \quad [A.46]$$

where

$$XX = r^2(1-A\cos(2\theta-\varepsilon)) - (2\mathbb{P})^{0.5} r\,(Q_1 \cos(\theta+\theta_1+\alpha) + Q_2 \cos(\theta-\theta_1-\beta)) + A\,(2\mathbb{P})^{0.5} r\,(Q_1 \cos(\theta-\theta_1-\alpha-\varepsilon) + Q_2 \cos(\theta+\theta_1+\beta-\varepsilon)) + (\mathbb{P}/2)\,(Q_1^2 + 2\,Q_1Q_2 \cos(2\theta_1+\alpha+\beta) + Q_2^2) - A\,(\mathbb{P}/2)\,(Q_1^2 \cos(2\theta_1+2\alpha+\varepsilon) + 2Q_1Q_2 \cos(\alpha-\beta+\varepsilon) + Q_2^2 \cos(2\theta_1+2\beta-\varepsilon)) \quad [A.47]$$

On substituting

$$\theta' = \theta + \theta_1 + \alpha \quad [A.48]$$

$$\delta = 2\theta_1 + 2\alpha + \varepsilon \quad [A.49]$$

$$\phi = \alpha - \beta + \varepsilon \quad [A.50]$$

the expression XX in the joint probability density function for r and θ' becomes

$$XX = r^2 (1-A \cos (2\theta'-\delta))$$
$$- (2\mathbb{P})^{0.5} r (Q_1 \cos \theta' + Q_2 \cos (\theta'-\delta+\phi)-A Q_1 \cos (\theta'-\delta) -A Q_2 \cos (\theta'-\phi))$$
$$+(\mathbb{P}/2) (Q_1^2(1-A \cos \delta) + 2 Q_1 Q_2 (\cos (\delta-\phi)-A \cos \phi) + Q_2^2 (1-A \cos (\delta-2\phi)))$$

[A.51]

Now the signal phase θ_1 is essentially random and so to obtain the probability density function of r and θ', averaged over all possible signal phases, $f(r,\theta')$ is integrated with respect to δ to obtain

$$f(r,\theta') = \frac{r \exp\left(-\frac{XX}{2\sigma^2(1-A^2)}\right) I_0(x/2\sigma^2(1-A^2))}{2\pi\sigma^2(1-A^2)^{0.5}}$$

[A.52]

where here

$$XX=r^2 - (2\mathbb{P})^{0.5} r (Q_1 \cos \theta' -A Q_2 \cos (\theta'-\phi))+(\mathbb{P}/2) (Q_1^2 + 2AQ_1Q_2 \cos \phi + Q_2^2)$$

[A.53]

$$x^2= A^2 r^4 + 2 A r^3 (2\mathbb{P})^{0.5} \{Q_2 \cos (\theta'-\phi)-AQ_1 \cos \theta'\}$$
$$+r^2 \mathbb{P} \{Q_2^2(2+A^2\cos 2(\theta'-\phi)+A^2Q_1^2(2+\cos 2\theta')-2AQ_1Q_2(2\cos \phi -\cos (2\theta'-\phi)\}$$
$$-r(2\mathbb{P}^3)^{0.5} \{A^2Q_1^3 \cos \theta'-AQ_1^2Q_2(\cos (\theta'+\phi)+2\cos (\theta'-\phi))+$$
$$Q_1Q_2^2(2 \cos \theta'+A^2\cos (\theta'-2\phi))-A Q_2^3 \cos (\theta'-\phi)\}$$
$$+(\mathbb{P}^2/4) \{A^2Q_1^4-4AQ_1^3Q_2\cos \phi +2 Q_1^2Q_2^2 (2+A^2\cos 2\phi)-4AQ_1Q_2^3\cos \phi +A^2Q_2^4\}$$

[A.54]

If $Q_2 = 0$ (which is approximately true in all cases studied),

$$f(r,\theta') = \frac{r \exp\left(\frac{r^2 - r (2\mathbb{P})^{0.5} Q_1 \cos \theta' + (\mathbb{P}/2) Q_1^2}{2\sigma^2 (1 - A^2)}\right) I_0(x /2\sigma^2(1-A^2))}{2\pi\sigma^2(1-A^2)^{0.5}}$$

[A.55]

where

$$x^2 = A^2r^4 - 2A^2 r^3 (2\mathbb{P})^{0.5} Q_1 \cos \theta' + A r^2 \mathbb{P} Q_1^2 (2+\cos 2\theta')$$
$$- A^2 r (2\mathbb{P}^3)^{0.5} Q_1^3 \cos \theta' + A^2 (\mathbb{P}/2)^2 Q_1^4$$

[A.56]

If A = 0 (which is again approximately true in the cases considered),

$$f(r,\theta') = \frac{r \exp\left(-\frac{r^2 - r(2\mathbb{P})^{0.5} Q_1 \cos\theta' + (\mathbb{P}/2) Q_1^2}{2\sigma^2}\right)}{2\pi\sigma^2} \qquad [A.57]$$

In any case the probability of detection

$$p_d = \int_R^\infty \int_0^{2\pi} f(r,\theta')\, d\theta'\, dr. \qquad [A.58]$$

In the case where $Q_2 = A = 0$,

$$p_d = \int_R^\infty \exp(-(2r^2 + \mathbb{P} Q_1^2)/(4\sigma^2))\, I_0(r(2\mathbb{P})^{0.5} Q_1/(2\sigma^2))\, dr \qquad [A.59]$$

$$= \int_{-\ln(p_{fa})}^\infty e^{-(u+P)} I_0(2\sqrt{(uP)})\, du \qquad [A.60]$$

on making the substitutions

$$P = \mathbb{P} Q_1^2/(4\sigma^2) \qquad [A.61]$$

$$u = r^2/(2\sigma^2) \qquad [A.62]$$

and using equation [A.33].

ANNEX B

ASSUMPTIONS MADE IN CALCULATING PROBABILITIES

In deriving equation [2.8] for the probability detection as a function of probability of false alarm and the quantity P (defined by equation [2.9]), the following assumptions were made:

(1) The quantities B and C (see equations [2.4] and [2.5]) are normally distributed.

(2) With interference alone, B and C have zero mean.

(3) The quantity A (see equation [A.18]) is zero.

(4) The quantity Q_2 (see equations [A.39] and [A.40]) is zero.

(5) The signal is coherent ie var(B) and var(C) are the same whether the signal is present or not.

Some of the effects of relaxing these assumptions will be considered in the remainder of this Annex.

B.1 The Distribution of B and C

Suppose that B and C are not normally distributed. Instead suppose that they are independent (assume A=0 so they have zero covariance), they have zero mean and they are identically distributed with probability density function $f_1(\cdot)$ which depends only on the variance σ^2 and not on any higher order moments. The probability density function may then be written

$$f_1(z) = f(z/\sigma)/\sigma \qquad [B.1]$$

where z represents either B or C and the function $f(\cdot)$ does not depend on any parameters. The probability of false alarm may be derived as in Annex A to be

$$p_{fa} = \int_R^\infty \int_0^{2\pi} r\, f_1(r\cos\theta)\, f_1(r\sin\theta)\, d\theta\, dr \qquad [B.2]$$

$$= \int_{R/\sigma}^\infty \int_0^{2\pi} u\, f(u\cos\theta)\, f(u\sin\theta)\, d\theta\, du \qquad [B.3]$$

where R is the threshold. Thus p_{fa} is a monotonic decreasing function of R/σ which has an inverse which will be denoted by $g(p_{fa}) = R/\sigma$.

Similarly, the probability of detection

$$p_d = \int_R^\infty \int_0^{2\pi} r\, f_1(r\cos\theta - B)\, f_1(r\sin\theta - C)\, d\theta\, dr \qquad [B.4]$$

$$= \int_{R/\sigma}^\infty \int_0^{2\pi} u\, f(u\cos\theta - B/\sigma)\, f(u\sin\theta - C/\sigma)\, d\theta\, du \qquad [B.5]$$

$$= \int_{g(pfa)}^\infty \int_0^{2\pi} u\, f(u\cos\theta - B/\sigma)\, f(u\sin\theta - C/\sigma)\, d\theta\, du \qquad [B.6]$$

where B and C are the mean values of B and C respectively. If f(x) is an even function with a single maximum at x=0, p_d will be an increasing function of $|B|/\sigma$ or $|C|/\sigma$. For a fixed ratio $|B/C|$, p_d is therefore an

increasing function of P (defined by equation [2.9]) if Q_2 is approximately zero. Hence P is still a sensible measure of detection performance, but , as in the case of the normal distribution with A≠0, the probability of detection may depend on $|B/C|$, which in turn depends on the signal phase.A measure of probability of detection independent of phase may be obtained (as in Annex A) by integrating equation [B.6] with respect to phase. Figures 23 and 24 show the variation of this integrated p_d with P for p_{fa} between 10^{-7} and 10^{-2} and

$$f(x) = 0.5 \exp(-|x|) \qquad \text{(figure 23)} \qquad [B.7]$$

$$f(x) = (4\pi)^{-0.5} \{ (.8)^{-0.5} \exp(-1.25\, x^2) + (3.2)^{-0.5} \exp(-.3125\, x^2) \} \qquad \text{(figure 24)} \qquad [B.8]$$

The latter function is the sum of two normal distribution functions. Comparison with figure 1 shows that the value of P required to obtain a particular probability of detection is higher using [B.7] or [B.8] than using the gaussian assumption. The difference for a 50% probability of detection is 5 to 10 dB using equation [B.7] or 1 to 2 dB using equation [B.8]. The difference is due to the increased height of the "tail" in equations [B.7] and [B.8] (ie increased values of f(x) for large x) and the consequent necessity of using a larger threshold to achieve the same false alarm rate.

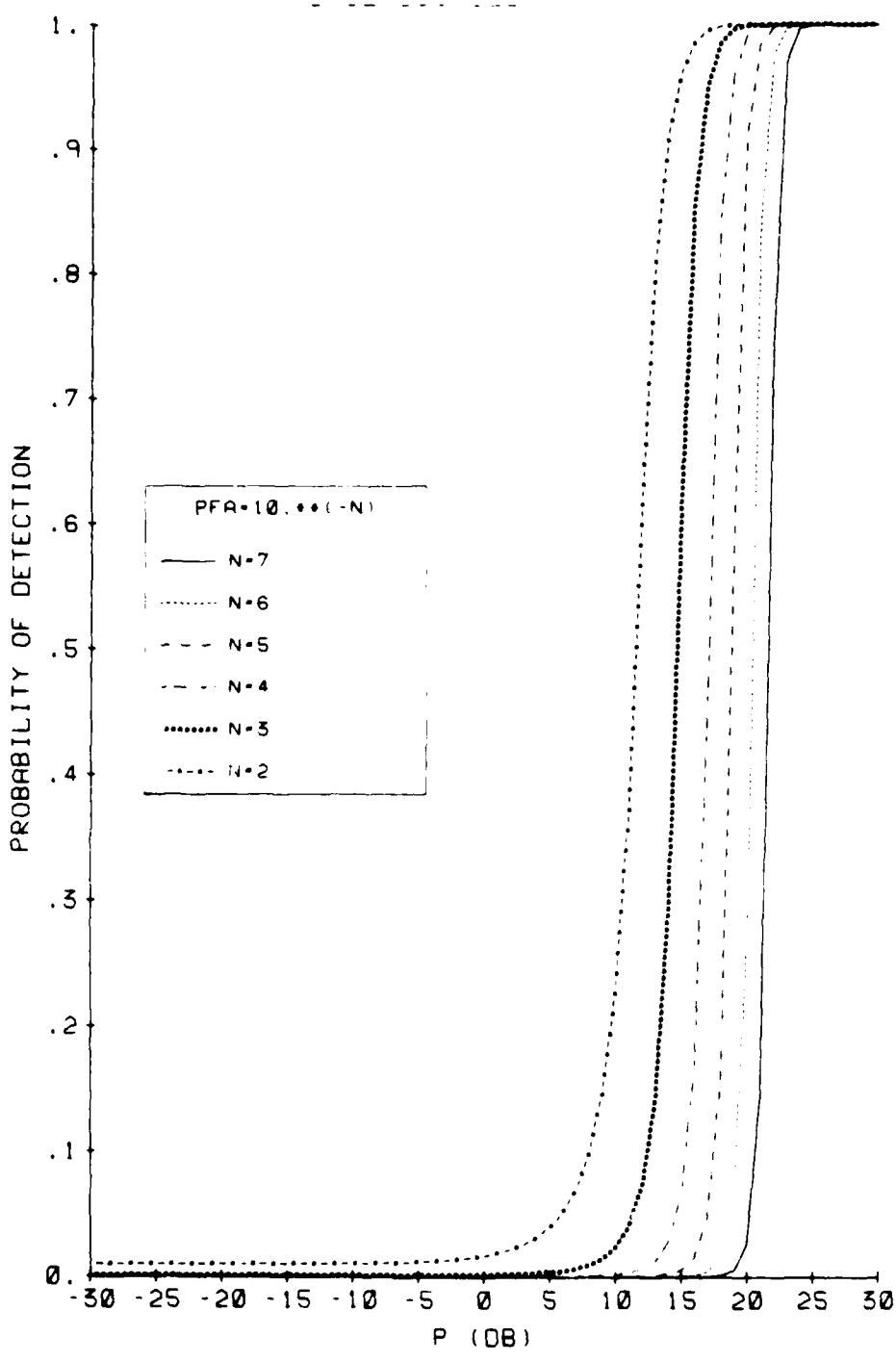

Figure 23(U) Transition Curves Exponential Probability Distribution

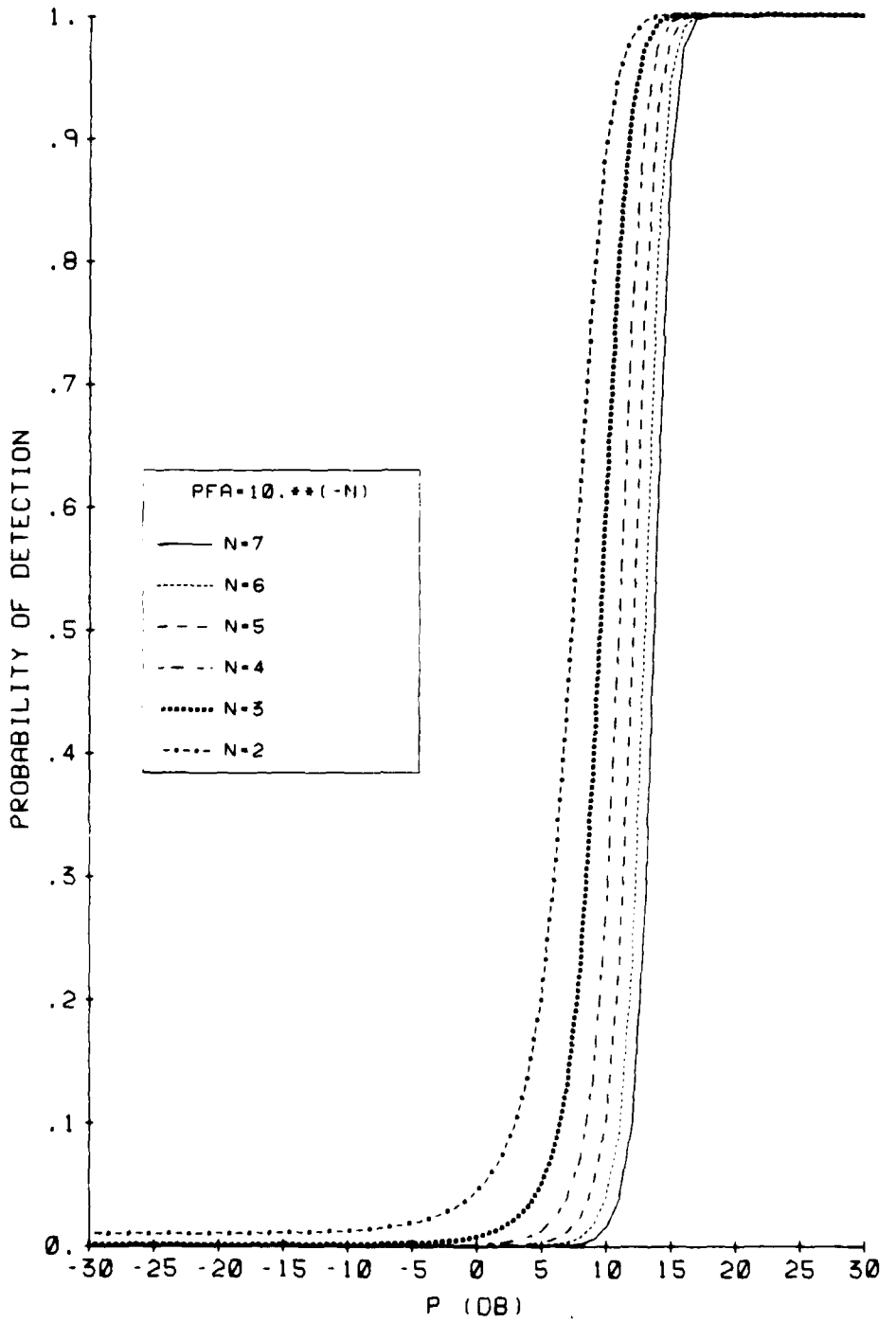

Figure 24(U) Transition Curves
Sum of Normal Probability
Distribution

B.2 The Mean of B and C

If B or C have non-zero mean (caused (say) by some dominant scatterer which is not the target), then by direct analogy with the calculations for p_d in Annex A, p_{fa} may be written

$$p_{fa} = \int_{R/\sigma}^{\infty} e^{-(u+Z)} I_0(2\sqrt{(uZ)})\, du \qquad [B.9]$$

where R is the threshhold and

$$Z = (B^2 + C^2)/(2\sigma^2) \qquad [B.10]$$

with B and C being here the mean values of B and C with interference alone. For a given probability of false alarm, the threshhold R and hence the probability of detection are increasing functions of Z. Figure 25 shows the variation of p_d with P for various values of Z and $p_{fa} = 10^{-5}$. The effect of increasing Z is to increase the value of P required for a given probability of detection. Even for Z=5 (which would increase the output interference power by a factor of 6) the increase in the value of P required for a 50% probability of detection is only about 4 dB.

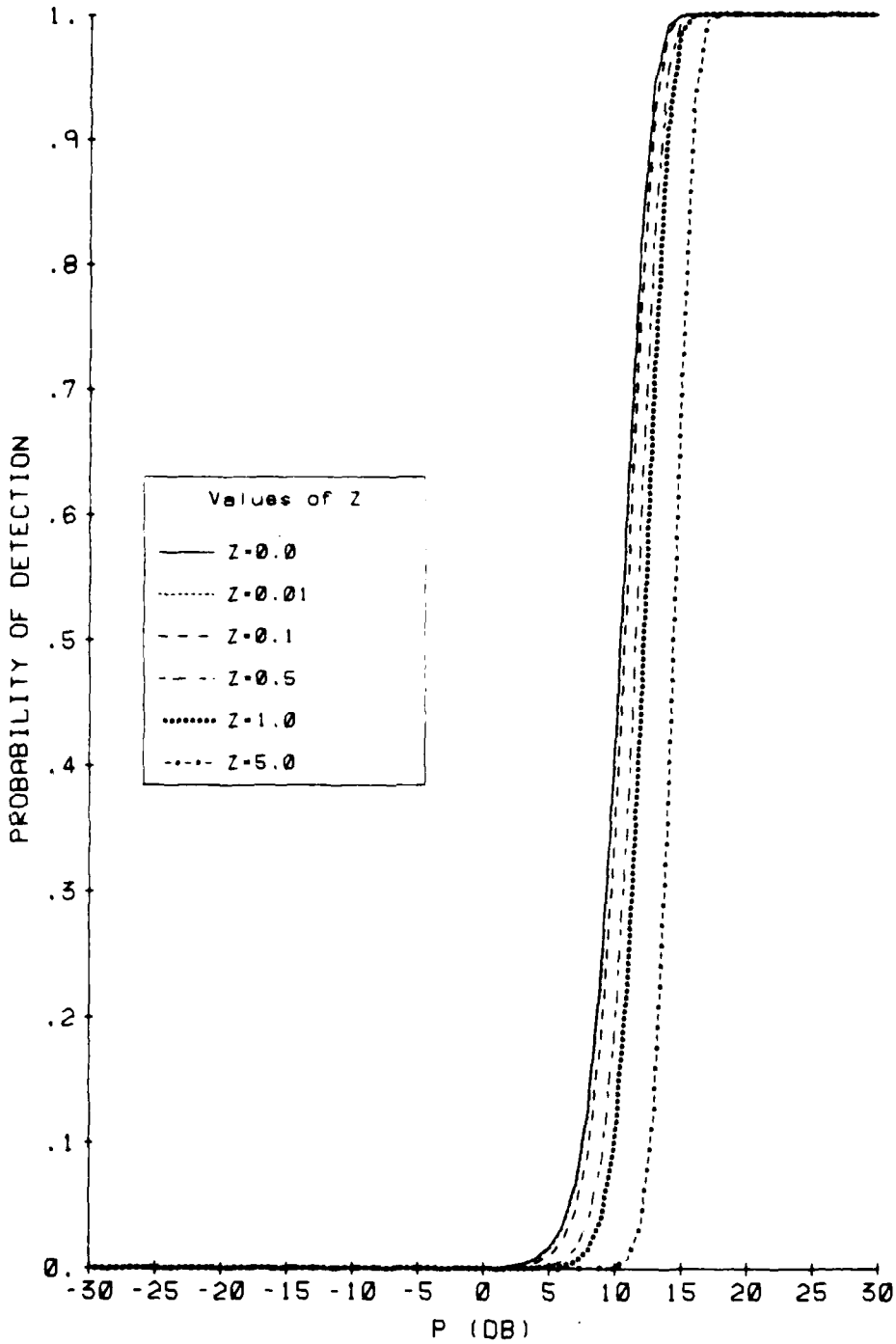

Figure 25(U) Transition Curves
for Selected Values of Z
PFA is 10**(-5)

B.3 The Quantity A

In figure 1, it is assumed that A (defined by equation [A.18]) is zero. If A is non-zero, equation [A.25] must be used for f(r) in equation [A.31] to calculate the probability of false alarm. Further equation [A.55] must be used for $f(r,\theta')$ in equation [A.58] to calculate the probability of detection. For $p_{fa} = 10^{-5}$, figure 26 shows the variation of probability of detection with P for various values of A. From the figure, it may be noted that increasing A increases the value of P required for a given probability of detection, but this increase is less than 3 dB for the largest possible value of A (=1) for a 50% probability of detection.

In the cases considered in section 4.1 and 4.2, where it is assumed that the carrier frequency - pulse length product is about 15000 (which is fairly typical), A is always small (about 10^{-2}) and its effect is insignificant.

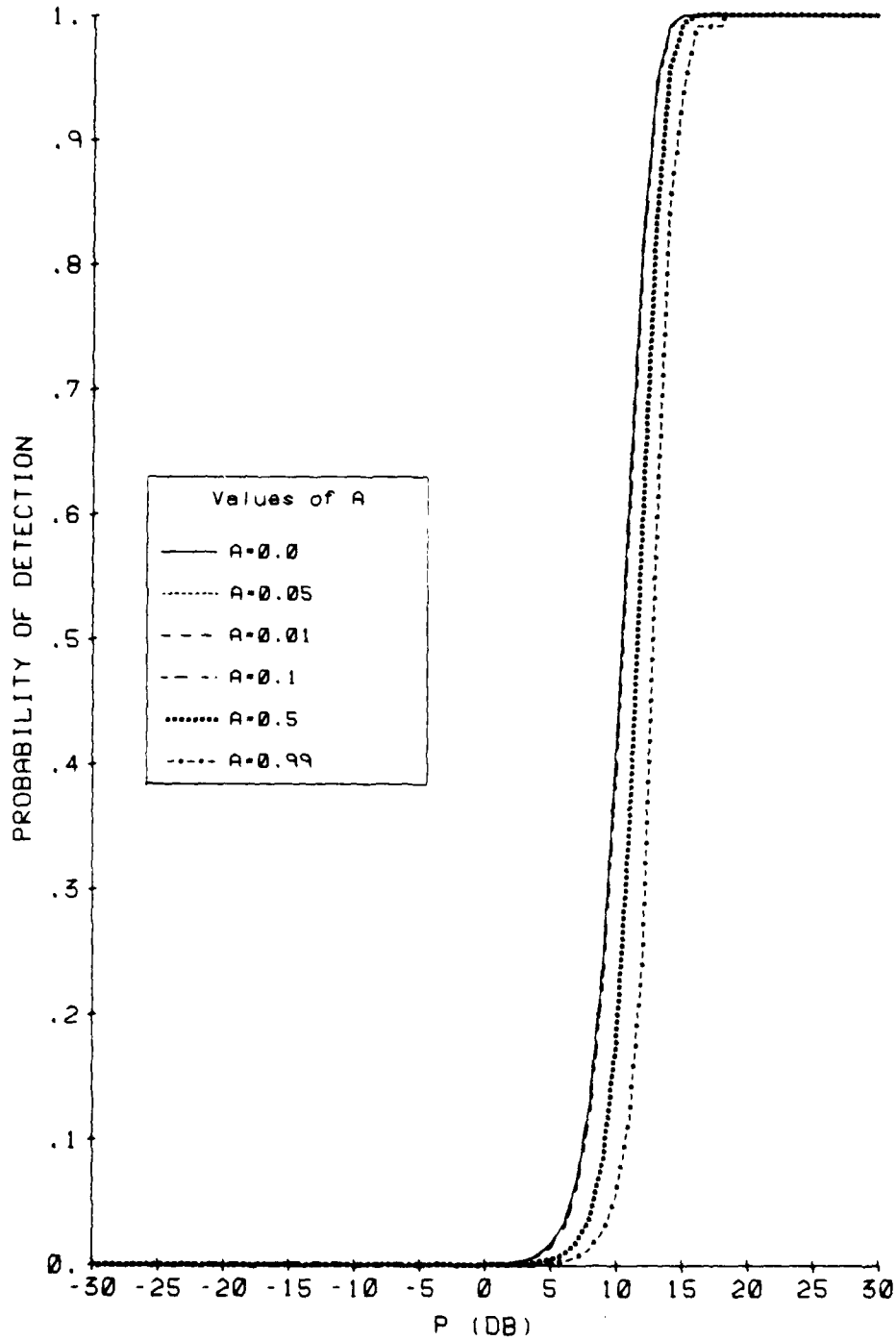

Figure 26(U) Transition Curves
for Selected Values of A
PFA is 10**(-5)

B.4 The Quantity Q_2

In figure 1, it is assumed that Q_2 (defined by equations [A.39] and [A.40]) is zero. If Q_2 is non-zero, equations [A.46] and [A.51] may be used in equation [A.58] to calculate the probability of detection. If A=0,

$$XX = r^2-(2\mathcal{P})^{0.5}r(Q_1\cos\theta'+Q_2\cos(\theta'-\delta+\phi)) + (\mathcal{P}/2)(Q_1^2+2Q_1Q_2\cos(\delta-\phi)+Q_2^2) \quad [B.11]$$

in equation [A.46], so that on integrating equation [A.58] with respect to θ', p_d may be expressed as in equation [A.59], but with Q_1^2 replaced by $Q_1^2+2Q_1Q_2\cos(\delta-\phi)+Q_2^2$. Hence

$$p_d = \int_{-\ln(p_{fa})}^{\infty} e^{-(u+P')} I_0(2\sqrt{(uP')})\, du \quad [B.12]$$

where

$$P' = P(1 + 2\kappa\cos(\delta-\phi) + \kappa^2) \quad [B.13]$$

$$\kappa = Q_2/Q_1. \quad [B.14]$$

For $p_{fa} = 10^{-5}$, figure 27 shows the variation of probability of detection with P for various values of Q_2 averaged over the arbitary phase angle $(\delta-\phi)$ (with A=0). From the figure it may be noted that the effect of Q_2 is minimal unless Q_2 is quite large (more than 0.1). Increasing Q_2 reduces the value of P required for a 50% probability of detection but increases the value required for a high (eg 90%) probability of detection.

In the cases considered in section 4.1 and 4.2, where it is assumed that the carrier frequency - pulse length product is about 15000 (which is fairly typical), Q_2/Q_1 is always small (about 10^{-5}) and its effect is insignificant.

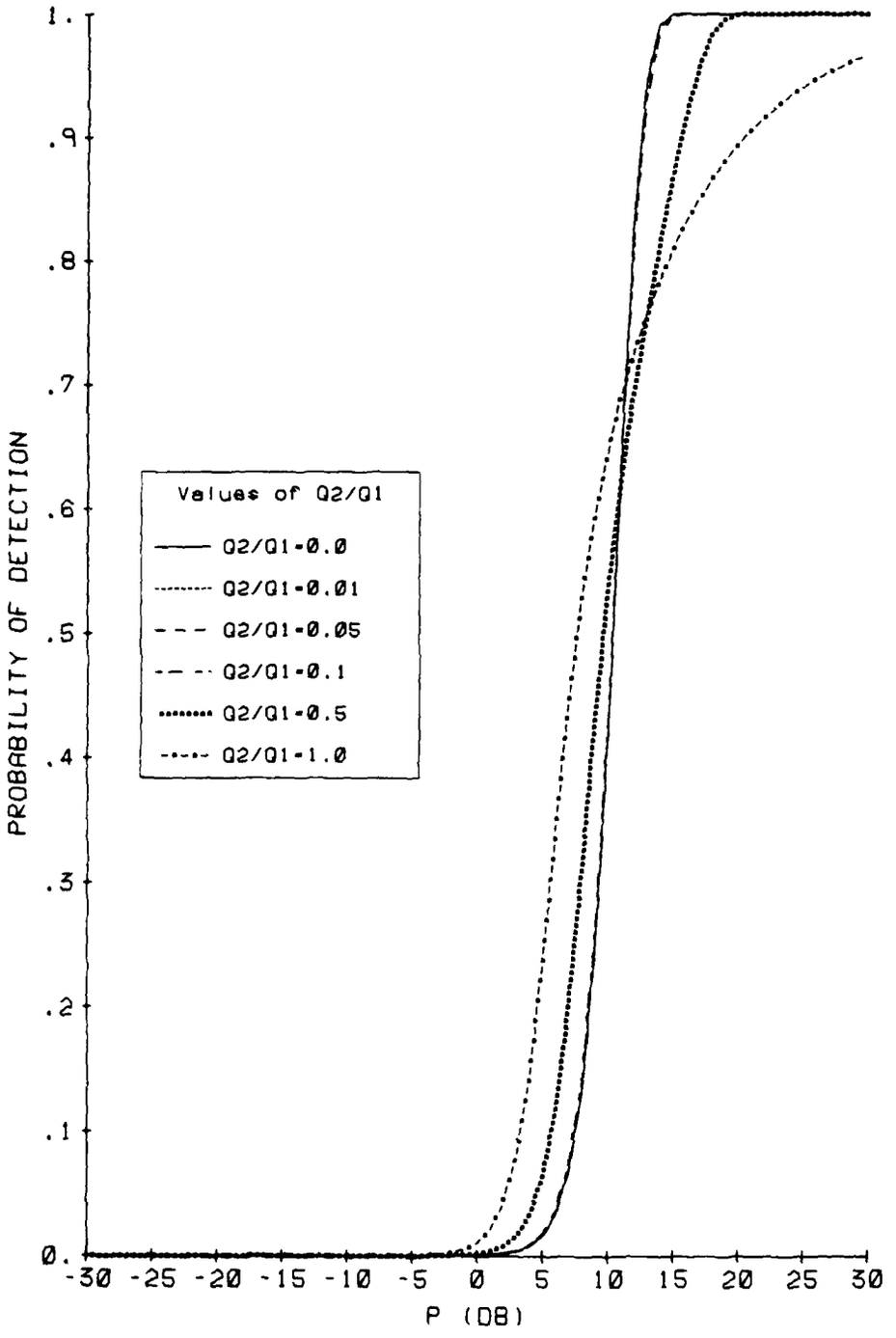

Figure 27(U) Transition Curves for Selected Values of Q2/Q1 PFA is 10**(-5)

B.5 Signal Coherence

Suppose that, due to multipath or other effects, the signal has a component which has the same characteristics as interference ie the contributions to B and C from this component have zero mean and non-zero variance. If k is the proportion of coherent power in the signal, then E[B] and E[C] are reduced by the proportion k. The increase in the variance of B and C depends on the exact nature of the interference-like component. If this component consists of a large number of "signals" with random phase, then it is of the form

$$x(t) = \int_0^{\pi} g(\theta') \, W(t) \cos (M(t) + 2\pi f t + \theta') \, d\theta' \qquad [B.15]$$

where

$$E[g(\theta')] = 0 \qquad [B.16]$$

$$E[g(\theta')g(\theta'')] = 2(1-k) \, \mathbb{P} \, \delta(\theta'-\theta'')/\pi. \qquad [B.17]$$

The expected value of x(t)x(u) is then

$$E[\, x(t)x(u) \,] = (1-k) \, \mathbb{P} \, W(t) \, W(u) \cos (M(t)-M(u)+2\pi f(t-u)) \qquad [B.18]$$

and the additional variance in B or C due to the presence of this extra interference is (using equation [A.1])

$$s^2 = (1-k) \, \mathbb{P} \int_0^T \int_0^T W(t) \, W(u) \, H(t) \, H(u) \cos (M(t)-M(u)+2\pi f(t-u)). \cos (N(t)-N(u)+2\pi f(t-u)) \, dt \, du \qquad [B.19]$$

$$= 0.5 \, (1-k) \, \mathbb{P} \int_0^T \int_0^T W(t) \, W(u) \, H(t) \, H(u) \cos (M(t)-M(u)-N(t)+N(u)) \, dt \, du \qquad [B.20]$$

$$= (1-k) \, \mathbb{P} \, Q_1^{\,2} / 2 \qquad [B.21]$$

$$= 2 \, (1-k) \, \mathbb{P} \, \sigma^2 \qquad [B.22]$$

Now the probability of false alarm may be calculated using equation [A.33]

in its present form, but the probability of detection is calculated from equation [A.59] with σ^2 replaced by ($\sigma^2 + s^2$). Hence

$$p_d = \int_{-\sigma^2 \ln(p_{fa})/(\sigma^2+s^2)}^{\infty} e^{-(u+Z)} I_0(2\sqrt{(uZ)})\, du \qquad [B.23]$$

where

$$P(k) = k \mathbb{P} Q_1^2 / 4(\sigma^2 + s^2) \qquad [B.24]$$

$$= k P(0) / (1 + 2(1-k)P(0)) \qquad [B.25]$$

and $P(0) = \mathbb{P} Q_1^2 / 4\sigma^2$ is the value of P (defined by equation [2.9]) if k were zero. For $p_{fa} = 10^{-5}$, figure 28 shows the variation of probability of detection as a function of P(0) for various values of k. It may be noted from the figure that decreasing k will decrease (slightly) the value of P required for a 50% probability of detection, but will increase (by up to 6 dB) the value of P required for a 90% probability of detection.

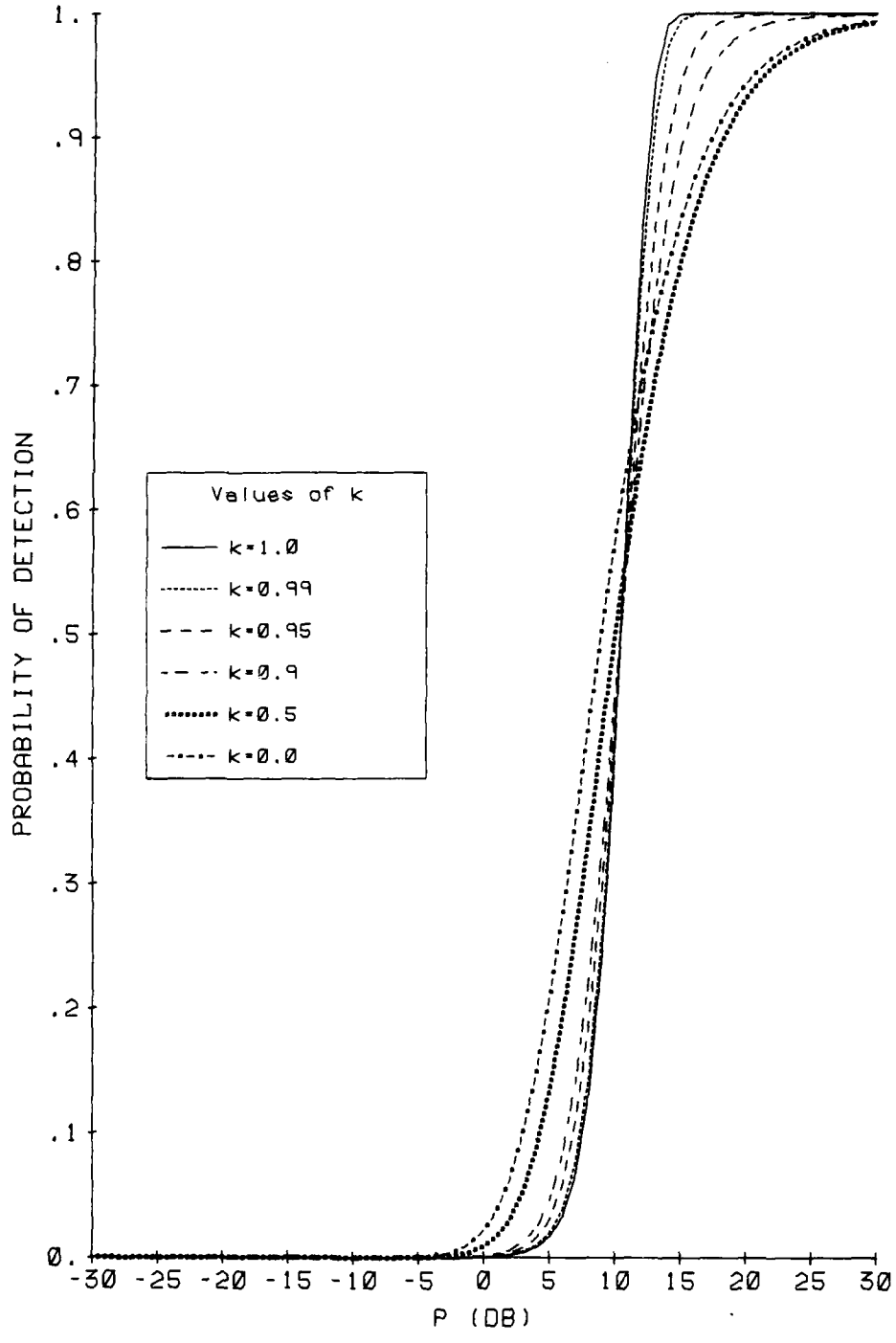

Figure 28(U) Transition Curves for Selected Values of k PFA is 10**(-5)

ANNEX C

ASSUMPTIONS MADE IN CALCULATING GAINS

In this Annex, generalised versions of equations [4.12] and [4.14] will be derived (from which these equations follow as a special case). These equations and the results of Annex A will be used to examine the effect of modifying some of the assumptions made in sections 4 and 5. These assumptions are listed at the end of this part and the remaining parts discuss the modification of each assumption in turn.

Suppose that the covariance of g (see section 4 for a definition of g) is of the form:

$$E[\, g(t,\zeta',f',\theta')\, g(u,\zeta'',f'',\theta'')\,] = 2\,\mathbb{R}\, V(t-u)\, L(f')\, \delta(f'-f'')\, X(\zeta'-\zeta'')\, \delta(\theta'-\theta'')/(\pi K) \qquad [C.1]$$

where the amplitudes g are independent for different phases and centre frequencies, L(f') gives the frequency distribution of the reverberation power, X gives the correlation with different path lengths (a delta function in section 4), V gives the correlation at different times (constant in section 4) and the functions are scaled so that the average reverberation power over the the analysis period is $\mathbb{R}$. The functions V and X are even. The expected value of x(t)x(u) may be written

$$E[\, x(t)x(u)\,] = (\mathbb{R}/K)\, V(t-u) \int_{t-K}^{t} \int_{u-K}^{u} \int_{-\infty}^{\infty} L(f')\, X(\zeta'-\zeta'')\, W(t-\zeta')\, W(u-\zeta'').$$

$$\int_0^{\pi} \cos(M(t-\zeta')+2\pi f t+\theta')\, \cos\,(M(u-\zeta'')+2\pi f' u+\theta')\, d\theta'\, df'\, d\zeta''\, d\zeta' \qquad [C.2]$$

$$= (\mathbb{R}/K)\, V(t-u) \int_{t-K}^{t} \int_{u-K}^{u} \int_{-\infty}^{\infty} L(f')\, X(\zeta'-\zeta'')\, W(t-\zeta')\, W(u-\zeta'').$$

$$\cos\,(M(t-\zeta')-M(u-\zeta'')+2\pi f'(t-u))\, df'\, d\zeta''\, d\zeta' \qquad [C.3]$$

$$= (\mathbb{R}/K)\, V(t-u)\, \{ \int_{-\infty}^{\infty} L(f') \cos 2\pi f'(t-u)\, df' \cdot$$

$$\int_{t-K}^{t} \int_{u-K}^{u} X(\zeta'-\zeta'')\, W(t-\zeta')\, W(u-\zeta'') \cos (M(t-\zeta')-M(u-\zeta''))\, d\zeta''\, d\zeta'$$

$$- \int_{-\infty}^{\infty} L(f') \sin 2\pi f'(t-u)\, df' \cdot$$

$$\int_{t-K}^{t} \int_{u-K}^{u} X(\zeta'-\zeta'')\, W(t-\zeta')\, W(u-\zeta'') \sin (M(t-\zeta')-M(u-\zeta''))\, d\zeta''\, d\zeta' \qquad [C.4]$$

Now, on letting $x = u-\zeta''$ and $y = t-\zeta'$ and $v=t-u$,

$$\int_{t-K}^{t} \int_{u-K}^{u} X(\zeta'-\zeta'')\, W(t-\zeta')\, W(u-\zeta'') \cos (M(t-\zeta')-M(u-\zeta''))\, d\zeta''\, d\zeta'$$

$$= \int_0^K \int_0^K X(v+x-y)\, W(y)\, W(x) \cos (M(y)-M(x))\, dy\, dx \qquad [C.5]$$

$$= \mathbb{W}(v) \quad \text{(say)}. \qquad [C.6]$$

$\mathbb{W}(v)$ is an even function of v (as may be seen by interchanging the order of integration and noting that X is even). An alternative expression for $\mathbb{W}(v)$ may be obtained by splitting the inner integral into two parts: from 0 to x and from x to K. On changing the order of integration in the first part and combining it with the second part,

$$\mathbb{W}(v) = \int_0^K \int_x^K (X(v+x-y)+X(v-x+y))\, W(y)\, W(x) \cos (M(y)-M(x))\, dy\, dx \qquad [C.7]$$

$$= \int_0^K \int_0^{K-x} (X(v+u)+X(v-u))\, W(u+x)\, W(x) \cos (M(u+x)-M(x))\, du\, dx \qquad [C.8]$$

$$= \int_0^K \int_0^{K-u} (X(v+u)+X(v-u))\, W(u+x)\, W(x) \cos (M(u+x)-M(x))\, dx\, du \qquad [C.9]$$

on letting $u = x-y$ and changing the order of integration. On making a further substitution $w = K-2x-v$ in the inner integral,

$$\mathbb{W}(v) = 0.5 \int_0^K \int_{-K+u}^{K-u} (X(v+u)+X(v-u))\, W_1(x-u)\, W_1(u+x) \cos(M_1(x-u)-M_1(u+x))\, dx\, du$$

where [C.10]

$$W_1(x) = W((K-x)/2) \qquad [C.11]$$

$$M_1(x) = M((iK-x)/2). \quad [C.12]$$

Expressions for the second double integral in equation [C.4] in which sin replaces cos may be derived in a similar way to obtain

$$W_1(v) = \int_{t-K}^{t}\int_{u-K}^{u} X(\zeta'-\zeta'') W(t-\zeta') W(u-\zeta'') \sin (M(t-\zeta')-M(u-\zeta'')) d\zeta'' d\zeta' \quad [C.13]$$

$$= \int_0^K\int_0^{K-u} (X(v+u)-X(v-u)) W(u+x) W(x) \sin (M(u+x)-M(x)) dx du \quad [C.14]$$

$$= 0.5\int_0^K\int_{-K+u}^{K-u} (X(v+u)-X(v-u)) W_1(x-u) W_1(u+x) \sin(M_1(x-u)-M_1(u+x)) dx du \quad [C.15]$$

where W_1 is an odd function.

If W and M are symmetric about K/2 (which is true for the CW and FM chirp pulses and the common shading functions), W_1 and M_1 are even functions and

$$W(v) = \int_0^K\int_0^{K-u} (X(v+u)+X(v-u)) W_1(u-x) W_1(u+x) \cos (M_1(u-x)-M_1(u+x)) dx du \quad [C.16]$$

$$W_1(v) = 0. \quad [C.17]$$

Additionally, if X is the Kroneker delta function, as in sections 4 and 5,

$$W(v) = \int_0^{K-v} W(v+x) W(x) \cos (M(v+x)-M(x)) dx \quad [C.18]$$

$$= \int_0^{K-v} W_1(v-x) W_1(v+x) \cos (M_1(v-x)-M_1(v+x)) dx. \quad [C.19]$$

Now consider the other integrals in equation [C.4]. If L(f') has a main peak at f'=μ, define

$$L(v) = V(v) \int_{-\infty}^{\infty} L(x+\mu) \cos 2\pi fxv \, dx \quad [C.20]$$

$$L_1(v) = V(v) \int_{-\infty}^{\infty} L(x+\mu) \sin 2\pi xv \, dx. \qquad [C.21]$$

The integrals in equation [C.4] may then be written

$$V(t-u) \int_{-\infty}^{\infty} L(f') \cos 2\pi f'(t-u) \, df' = L(t-u)\cos 2\pi\mu(t-u) - L_1(t-u)\sin 2\pi\mu(t-u) \qquad [C.22]$$

$$V(t-u) \int_{-\infty}^{\infty} L(f') \sin 2\pi f'(t-u) \, df' = L(t-u)\sin 2\pi\mu(t-u) + L_1(t-u)\cos 2\pi\mu(t-u) \qquad [C.23]$$

If $L(f')$ is symmetric about $f'=\mu$, as occurs with the functions considered in sections 4 and 5,

$$L(v) = 2\, V(v) \int_{0}^{\infty} L(x+\mu) \cos 2\pi xv \, dx \qquad [C.24]$$

$$L_1(v) = 0. \qquad [C.25]$$

In any case,

$$E[\, x(t)x(u) \,] = \mathbb{R} \{ (L(t-u)\, W(t-u) - L_1(t-u)\, W_1(t-u)) \cos 2\pi\mu(t-u) - (L_1(t-u)\, W(t-u) + L(t-u)\, W_1(t-u)) \sin 2\pi\mu(t-u) \}. \qquad [C.26]$$

which is an even function of (t-u) only and will be denoted $Z(t-u)$. The average reverberation power over the analysis period is $\mathbb{R}$ if

$$L(0)\, W(0) = K. \qquad [C.27]$$

The function W is scaled by equation [2.2] so that equation [C.27] scales the product of V and L.

In the cases considered in section 4 and 5, equation [C.26] becomes

$$E[\, x(t)x(u) \,] = (\mathbb{R}/K)\, L(t-u)\, W(t-u) \cos 2\pi\mu(t-u) \qquad [C.28]$$

where L and W are given by equations [C.24] and [C.18] with $V(v)=1$. From equations [2.2] and [C.18], $W(0)=K$ so that equation [C.27] implies

$$L(0)=1. \qquad [C.29]$$

Substituting Z(t-u) for E[x(t)x(u)] in equation [2.11] gives

$$\sigma^2 = \int_0^T Z(v) \int_v^T H(t)\, H(t-v) \cos\left(N(t)-N(t-v)+2\pi f v\right) dt\, dv \qquad [C.30]$$

$$= 0.5 \int_0^T Z(v) \int_{-T+v}^{T-v} H_1(w-v)\, H_1(w+v) \cos\left(N_1(w-v)-N_1(w+v)+2\pi f v\right) dt\, dv \qquad [C.31]$$

where

$$H_1(x) = H\left((T-x)/2\right) \qquad [C.32]$$

$$N_1(x) = N\left((T-x)/2\right). \qquad [C.33]$$

Define

$$H(v) = \int_v^T H(t)\, H(t-v) \cos\left(N(t)-N(t-v)\right) dt \qquad [C.34]$$

$$= 0.5 \int_{-T+v}^{T-v} H_1(w-v)\, H_1(w+v) \cos\left(N_1(w-v)-N_1(w+v)\right) dw \qquad [C.35]$$

$$H_1(v) = \int_v^T H(t)\, H(t-v) \sin\left(N(t)-N(t-v)\right) dt \qquad [C.36]$$

$$= 0.5 \int_{-T+v}^{T-v} H_1(w-v)\, H_1(w+v) \sin\left(N_1(w-v)-N_1(w+v)\right) dt \qquad [C.37]$$

which are directly analogous to the definitions of W and W_1. Equation [C.31] then becomes

$$\begin{aligned}\sigma^2 = (R/K) \int_0^T \{ & \left(L(v)\, W(v) - L_1(v)\, W_1(v) \right) H(v) \cos 2\pi\mu v \cos 2\pi f v \\ & - \left(L_1(v)\, W(v) + L(v)\, W_1(v) \right) H(v) \sin 2\pi\mu v \cos 2\pi f v \\ & - \left(L(v)\, W(v) - L_1(v)\, W_1(v) \right) H_1(v) \cos 2\pi\mu v \sin 2\pi f v \\ & + \left(L_1(v)\, W(v) + L(v)\, W_1(v) \right) H_1(v) \sin 2\pi\mu v \sin 2\pi f v \}\, dv.\end{aligned} \qquad [C.38]$$

Each of the products of sin or cos may be written as the sum of two sin or

cos terms with argument $2\pi(f-\mu)v$ and $2\pi(f+\mu)v$. The integrals containing the second of these arguments will be small compared with those containing the first if $(f-\mu)T << (f+\mu)T$, as in practical situations. Thus in the cases considered in section 4 and 5 where H and N are symmetric about T/2,

$$\sigma^2 = R/_{2K} \int_0^T L(v)\, W(v)\, H(v) \cos 2\pi(f-\mu)v \, dv \qquad [C.39]$$

$$H(v) = \int_0^{T-v} H_1(w-v)\, H_1(w+v) \cos (N_1(w-v)-N_1(w+v)) \, dw \qquad [C.40]$$

$$H_1(v) = 0. \qquad [C.41]$$

The additional assumptions made in sections 4 and 5 are listed below. Some effects of varying these assumptions are described in the following sections.

(1) The start of the signal coincides with the start of the analysis period ie D=0 in equation [2.7].

(2) The analysis and signal frequencies coincide ie $f_1=f$.

(3) The duration of the signal equals the duration of the analysis period ie T=K

(4) The scatterers have constant properties for times equal to the length of the analysis period ie V(v)=1.

(5) The scatterers are independent for different path lengths ie $X(v)=\delta(v)$.

C.1 The Start of the Signal and Analysis Period Coincide

The condition D=0 (ie the start of the signal and analysis periods coincide) is required for equations [4.20] or [4.27] to be valid for Q_1. However if D>0 (but all the other assumptions are unchanged), the values of σ^2 are unchanged but Q_1 is given by

$$Q_1^2 = \left(\int_D^T W(t-D)\, H(t) \cos\left(M(t-D) - N(t) \right) dt\right)^2 + \left(\int_D^T W(t-D)\, H(t) \sin\left(M(t-D) - N(t) \right) dt\right)^2 \qquad [C.42]$$

If D<0 a similar expression for Q_1^2 may be written with different integration limits. The lower limit becomes zero and the upper limit T+D=T-|D|. On letting t'=t-D, an equation equivalent to [C.42] may be derived in which H and W are interchanged, M and N are interchanged and D is replaced by |D|. In the following D>0 only will be considered, as D<0 gives identical results by interchanging shaping and shading.

For CW pulses and each of the combinations of H(t) and W(t) used in section 4, the degradation in P is presented in figure 29 for values of D/T between 0 and 1. This is the same as figure 2 except that here the degradation is taken relative to its value when D=0, not necessarily relative to its optimal value.If there is no overlapping of analysis periods, the maximum degradation will occur if the signal starts at time T/2 (if it starts at a later time during the period, the next period will contain the signal for a longer time and it should be considered with D<0, giving identical results to those in the figure) and corresponds to D/T=0.5. If the analysis periods overlap, the maximum will correspond to a lower value of D/T, but more processing will be required and the false alarm rate may be increased due to the increase in the number of analysis periods per unit of time. Of course the overlapping periods will not be independent so that this increase may not be significant.

For FM pulses with M(t)=N(t),

$$Q_1^2 = \left(\int_D^T W(t-D)\, H(t) \cos\left(M(t-D) - M(t) \right) dt\right)^2 + \left(\int_D^T W(t-D)\, H(t) \sin\left(M(t-D) - M(t) \right) dt\right)^2 \qquad [C.43]$$

For a chirp pulse where M(t) is given by equation [4.23],

$$Q_1^2 = \left(\int_D^T W(t-D)\, H(t) \cos 2\pi\beta \{ 2D(t-T/2) - D^2 \}\, dt\right)^2 +$$
$$\left(\int_D^T W(t-D)\, H(t) \sin 2\pi\beta \{ 2D(t-T/2) - D^2 \}\, dt\right)^2.$$
$$= T^2\left(\int_{D/T}^1 W((u-D/T)T)\, H(uT) \cos (2\pi Du/S)du\right)^2 +$$
$$T^2\left(\int_{D/T}^1 W((u-D/T)T)\, H(uT) \sin (2\pi\, Du/S)du\right)^2 \qquad [C.44]$$

where $S=(2\beta T)^{-1}$ is the inverse of the FM bandwidth. When using FM pulses, the analysis periods overlap and the start of successive intervals differ by a time ΔT which should be set less than or equal to S. Figure 30 shows the degradation in the gain for values of D/S between 0 and 5 (assuming that $S/T << 1$ ie the bandwidth- pulse length product is large so that the lower limits of integration in equation [C.44] may be set equal to zero). If the starting times of the analysis periods are separated by $\Delta T=S$, the maximum degradation will occur when D/S = 0.5 and is about 4 dB with no shading or shaping, but is rather less (at most 1.5 dB) otherwise. For small values of D/S (less than 1), the degradation is greatest when there is no shading or shaping, indicating that a plot of processor output as a function of analysis period start time would have a sharper peak corresponding to the signal in this case. However, for larger values of D/S (at least 3) the situation is reversed and the degradation is greater when the shading or shaping schemes are used. Thus the "side lobes" in the plot will be lower. This lowering of side lobes has important implications if there is another unwanted signal. The use of shading and shaping may reduce its interference effect, even if it is quite large.

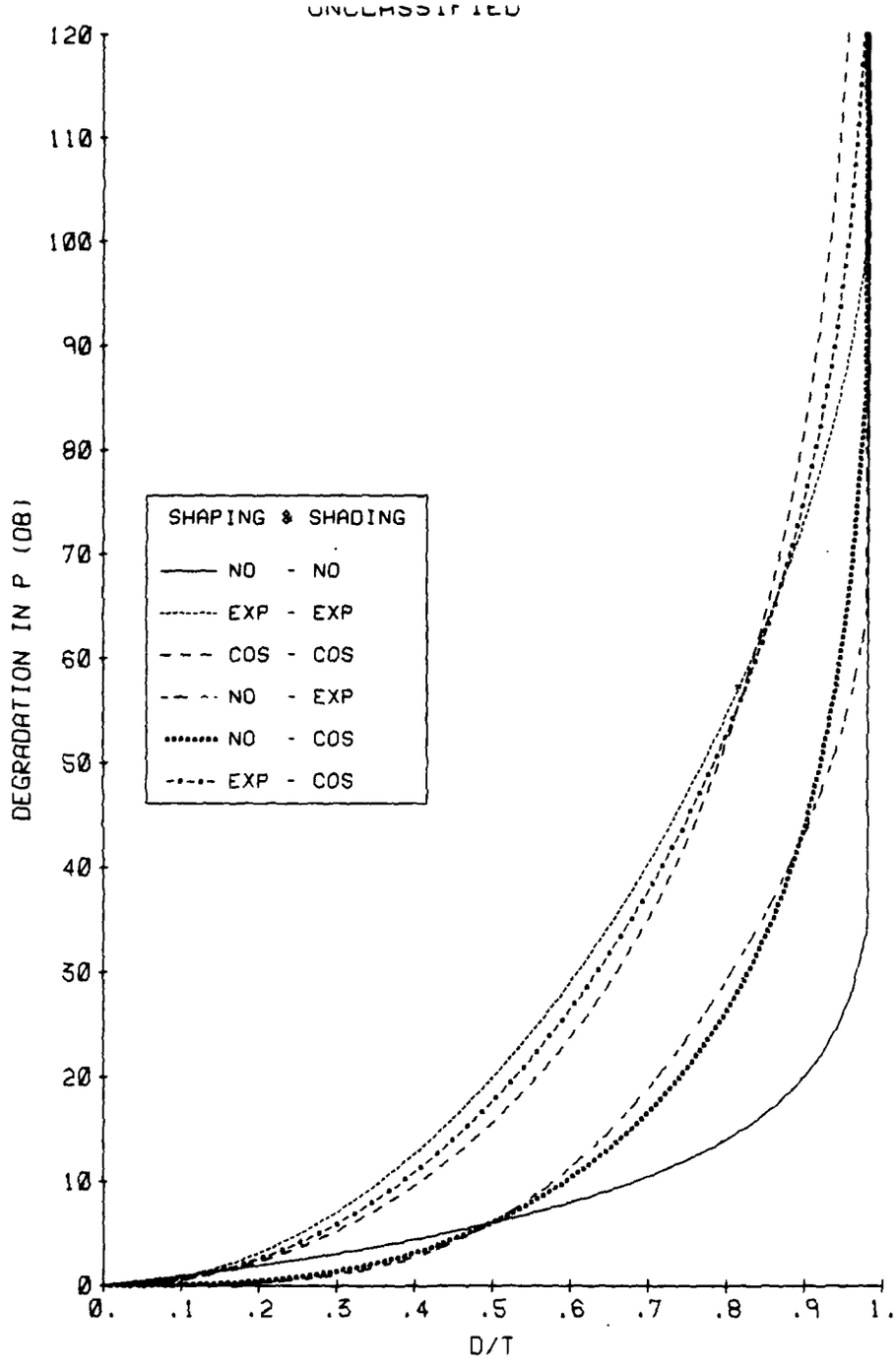

Figure 29(U) Degradation in Gain as Function of D/T for CW Pulse

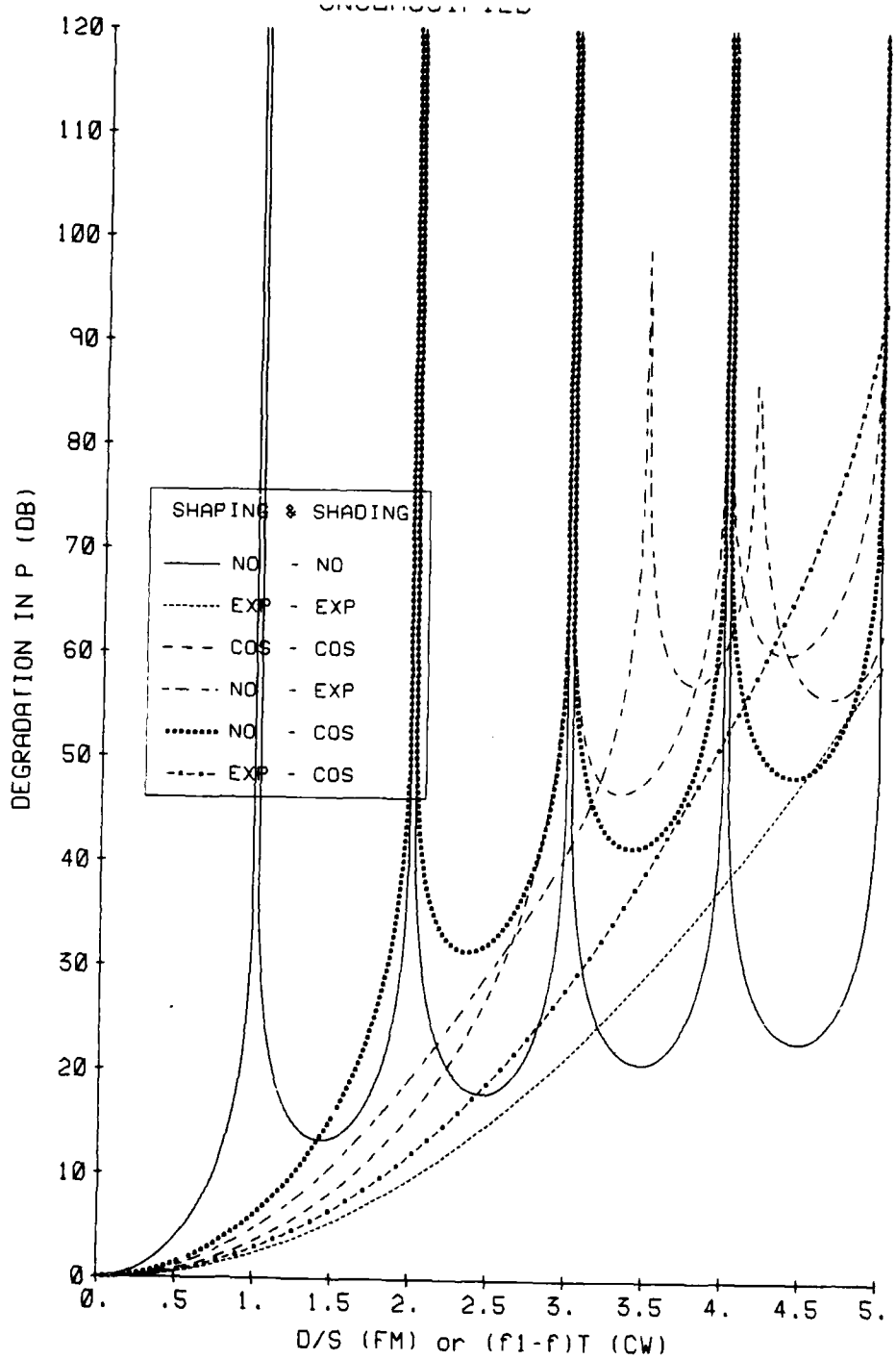

Figure 30(U) Degradation in Gain as Function of D/S for FM Pulse or (f-f1)T for CW Pulse

C.2 The Analysis and Signal Frequencies Coincide

The condition $f=f_1$ (*ie the centre analysis frequency is the same as* the centre signal frequency) is required for equations [4.20] or [4.27] to be valid. However, if $f\neq f_1$ (and all other assumptions are unchanged except that possibly D>0), the values of σ^2 are unchanged but Q_1 is given by

$$Q_1^2 = \left(\int_D^T W(t-D)\, H(t) \cos\left(M(t-D) - N(t) + 2\pi(f- f_1)t \right)dt\right)^2 + \left(\int_D^T W(t-D)\, H(t) \sin\left(M(t-D) - N(t) + 2\pi(f- f_1)t \right)dt\right)^2 \qquad [C.45]$$

For a CW pulse,

$$Q_1^2 = T^2\left(\int_{D/T}^1 W((u-D/T)T)\, H(uT) \cos\left(2\pi|f- f_1|Tu \right)du\right)^2 + T^2\left(\int_{D/T}^1 W((u-D/T)T)\, H(uT) \sin\left(2\pi|f- f_1|Tu \right)du\right)^2 \qquad [C.46]$$

which is exactly the same as equation [C.44] with D/S replaced by $(f-f_1)T$, so that figure 30 also shows the degradation in P due to the frequency mismatch for values of $|f-f_1|T$ between 0 and 5 if D=0. As it would be expected that the frequency bins would be separated by at most $\Delta f=T^{-1}$, the maximum loss due to frequency mismatch would correspond to $|f-f_1|T=0.5$ or 4 dB with no shading or shaping. As for the FM case, the signal spectral peak is broader using shading or shaping, but the side lobes are lower, improving the rejection of a strong unwanted signal at another frequency.

The combined effect of having $D\neq 0$ and $f\neq f_1$ is illustrated in figure 31, where the degradation in P is plotted as a function of $(f-f_1)T$ for selected values of D/T and no shading or shaping. Notice that the worst case of $D/T=0.5$ and $(f-f_1)T=0.5$ gives a degradation of about 6 dB.

For an FM chirp pulse,

$$Q_1^2 = T^2\left(\int_{D/T}^{1} W((u-D/T)T)\, H(uT) \cos\left(2\pi(D/S+(f-f_1)T)u\right)du\right)^2 + T^2\left(\int_{D/T}^{1} W((u-D/T)T)\, H(uT) \sin\left(2\pi(D/S+(f-f_1)T)u\right)du\right)^2 \quad [C.47]$$

In this case, the detection algorithm is performed at one centre frequency only (so that f=F, the transmitted pulse centre frequency). Hence, even if D=0, $|f-f_1|T$ can be quite large if there is significant doppler shift in the signal return. If $|f-f_1|T>0.5$, a different analysis period would give the largest processor output so the estimated range to the target would be in error - the largest output may be estimated by adding an integer multiple of S to D such that $q=|D/S+(f-f_1)T|\leq 0.5$. Figure 30 shows the degradation in P as a function of q in the case where $|D|/T$ is zero or close enough to zero to be ignored. The degradation for values of q>0.5 correspond to the reduction in echo in range cells neighbouring the one with maximum response. If the frequency shift is such that $|D|/T$ may not be ignored, figure 31 shows the degradation in P as a function of q and selected values of $|D|/T$ in the case of no shading or shaping.

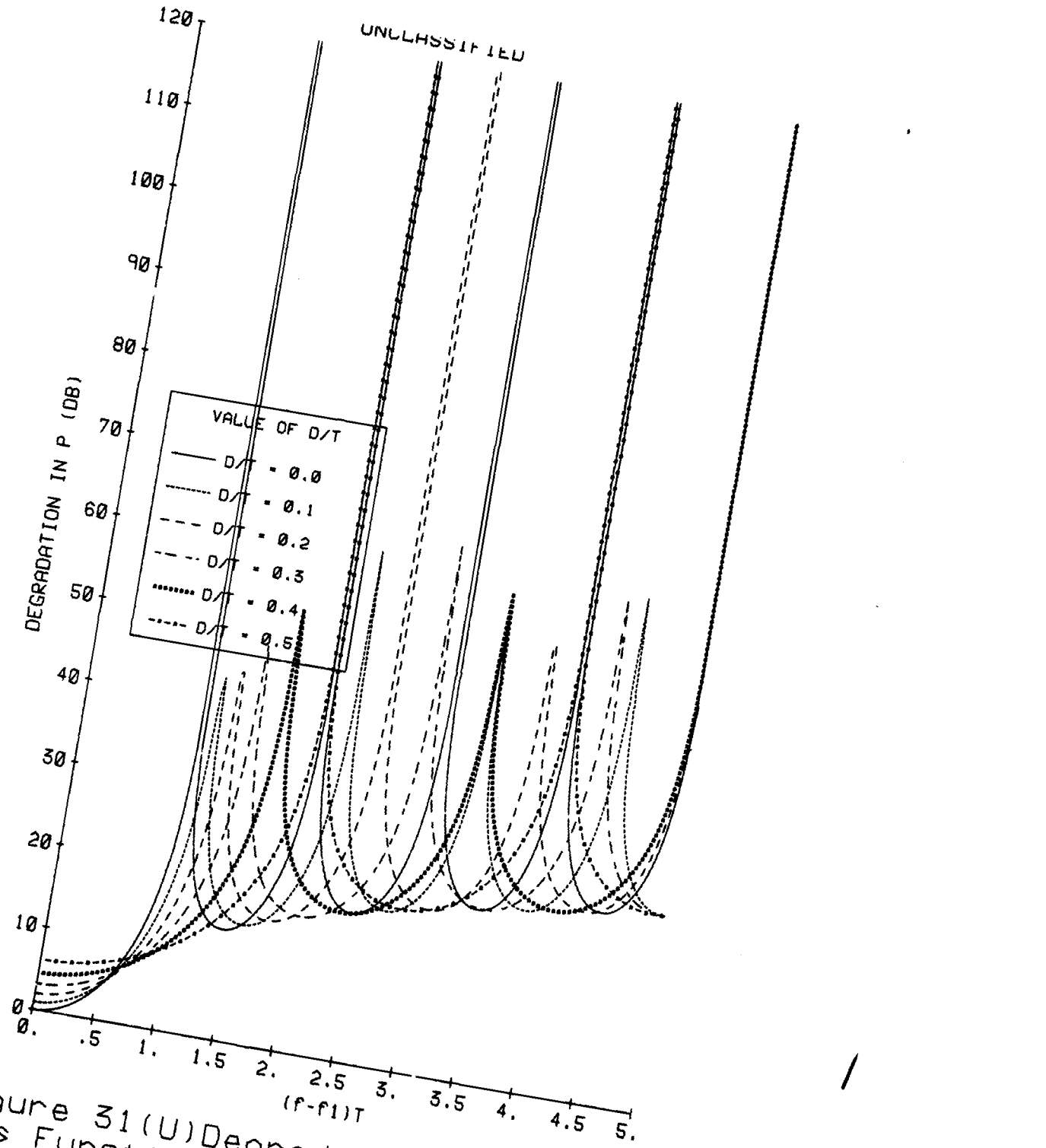

Figure 31(U)Degradation in Gain as Function of (f-f1)T for CW Pulse for Selected D/T

C.3 The Pulse and the Analysis Period Have Equal Length

Equality in the length of the pulse K and the length of the analysis period T is necessary for the equation [4.20] or [4.27] for Q_1^2 to be valid. If $T \neq K$, these equations should be replaced by

$$Q_1^2 = \left(\int_{\max[0,(T-K)/2]}^{\min[T,(T+K)/2]} W(t-(T-K)/2)\, H(t)\, dt\right)^2 \qquad [C.48]$$

if it is assumed that the signal pulse and analysis period are aligned so that their centres coincide (ie the frequency modulation of the signal and the analysis replica are the same throughout the integration period). This alignment gives the gretest value of Q_1^2. The values of σ^2 are also changed in this case. Since $W(v)=0$ unless $0 \leq v \leq K$,

$$\sigma^2 = \mathbb{R}/_{2K} \int_0^{\min[T,K]} L(v)\, W(v)\, H(v) \cos 2\pi(f-\mu)v \, dv \qquad [C.49]$$

$$= \mathbb{R}/_{2} \int_0^{\psi} L(Ku)\, W(Ku)\, H(Ku) \cos \omega u \, du \qquad [C.50]$$

where $u = v/K$, $\psi = \min[1, T/K]$ and $\omega = 2\pi(f-\mu)K$.

For CW pulses, the gain as a function of ω is shown in figures 32 to 40 in the case where $L(v)=1$ (case 1 from table 1) for T/K taking the values 0.1, 0.5, 0.9, 1.0, 1.1 and 2.0. The case $T/K = 10.$ is also included in figures 36, 38 and 40, but not in the others as the line is strongly oscillatory and tends to obscure the other lines. The figures show the 9 possible combinations of shading and shaping functions from tables 2 and 3. In this case, the quantity J from section 5.1 (the integral in equation [C.50]) may be written

$$J = \sum_{n=0}^{\infty} (-1)^n \left(\frac{S^{(2n)}(\psi) \sin \omega\psi}{\omega^{2n+1}} + \frac{S^{(2n+1)}(\psi) \cos \omega\psi - S^{(2n+1)}(0)}{\omega^{2n+2}} \right) \qquad [C.51]$$

where

$$S(u) = W(Ku)\, H(Ku).$$

Now $S(\psi)=0$ since $W(K)=0$ and $H(T)=0$, but in this case,

$$S'(\psi) = \begin{cases} K\,W(T)\,H'(T) & \text{if } T < K \\ K\,W'(K)\,H(K) & \text{if } T > K. \end{cases} \qquad [C.52]$$

For the shading and shaping functions from tables 2 and 3, $S'(\psi)$ is non-zero for $T<K$ unless cos shading is used and $S'(\psi)$ is non-zero for $T>K$ unless cos shaping is used. This is different from the results of section 5.1 and explains the oscillations in figures 32 and 33 and the lack of oscillations for some lines in figures 37, 38 and 40. Note also that

$$S'(0) = K\,(\,T\,W'(0) + K\,H'(0)\,) \qquad [C.53]$$

so that $S'(0)$ is non-zero unless both cos shading and shaping are used as in section 5.1. Hence the gain will increase with ω^2 (ie 6 dB per doubling of ω) except where cos shaping and shading are used. If both cos shaping and shading are used, $S'(0)=S'(\psi)=S''(\psi)=S'''(0)=S'''(\psi)=S^{(4)}(\psi)=0$ and

$$S^{(5)}(\psi) = \begin{cases} -K^5\,W(T)\,H''(0) & \text{if } T < K \\ -K^5\,W''(0)\,H(K) & \text{if } T > K. \end{cases} \qquad [C.54]$$

$$\begin{aligned} S^{(5)}(0) &= K^5\,(\,T\,W^{(5)}(0) + K\,H^{(5)}(0)\,) \\ &= -\,K^5\,(\,T\,\{W''(0)\}^2 + K\,\{H''(0)\}^2\,) \end{aligned} \qquad [C.55]$$

Hence the gain oscillates in this case also but is proportional to ω^6 as may be seen in figure 34. In figures 35 and 36, it would be expected that there would be oscillatory behaviour for both $T<K$ and $T>K$, since $S'(\psi)\neq 0$. However $S'(\psi)$ is very small if $T<K$ in figure 35 or if $T>K$ in figure 36 since $H(0)$ or $W(0)$ are very small in the respective cases. Thus the oscillations are present but not noticeable in these figures. In figure 39, it would be expected that there would be no oscillation if $T<K$ since $S'(\psi)=0$. However, $S'(0)$ is small and for the values of ω being considered, an oscillation from a higher order term in equation [C.51] gives the (reducing) oscillatory behaviour in this case. This effect also explains the small oscillations then $T/K=0.1$ in figure 37 and when $T/K=10$ in figure 40.

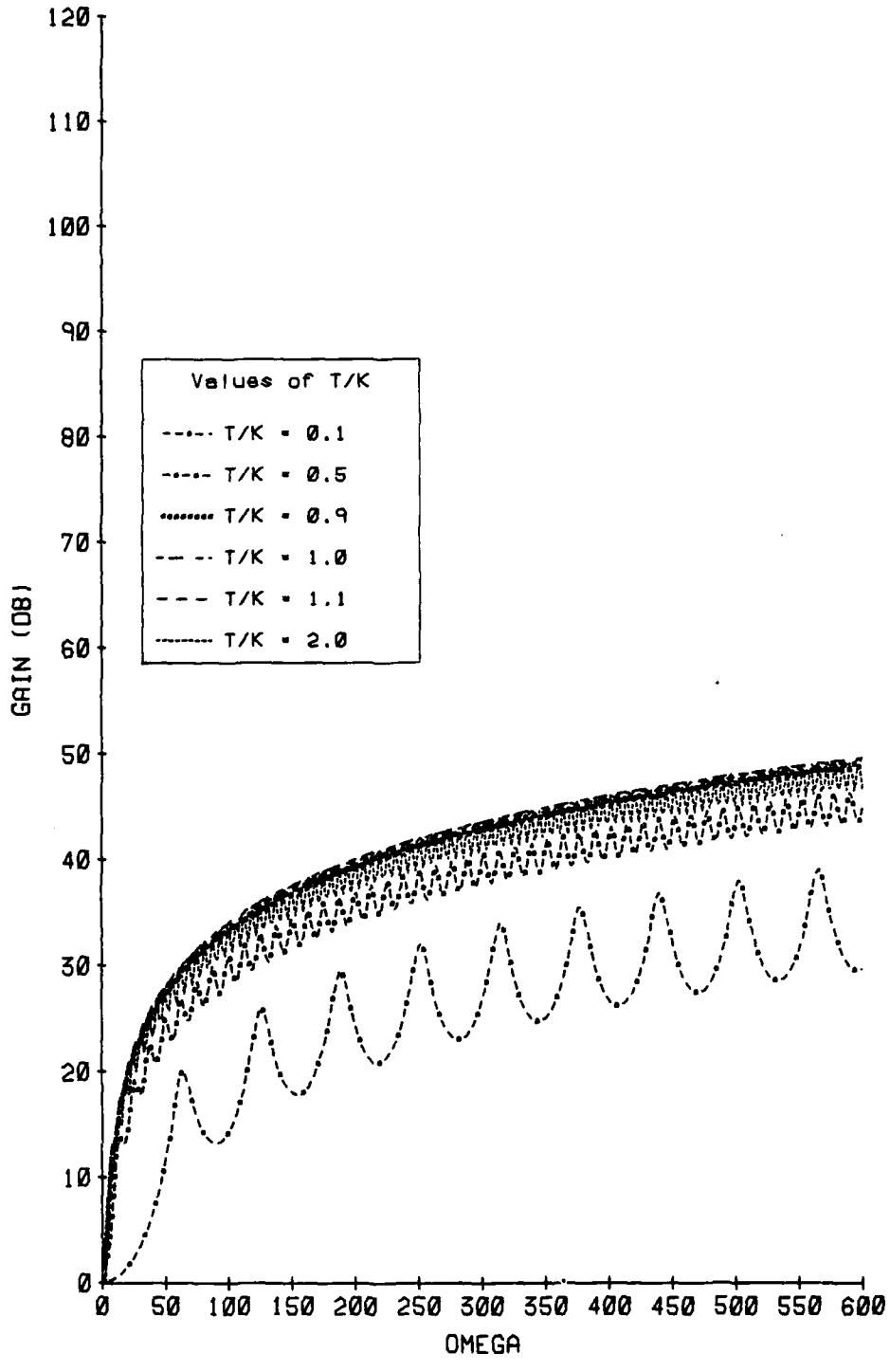

Figure 32(U) Gain for various T/K, No Shading and No Shaping, PFA = 10.**(-5)

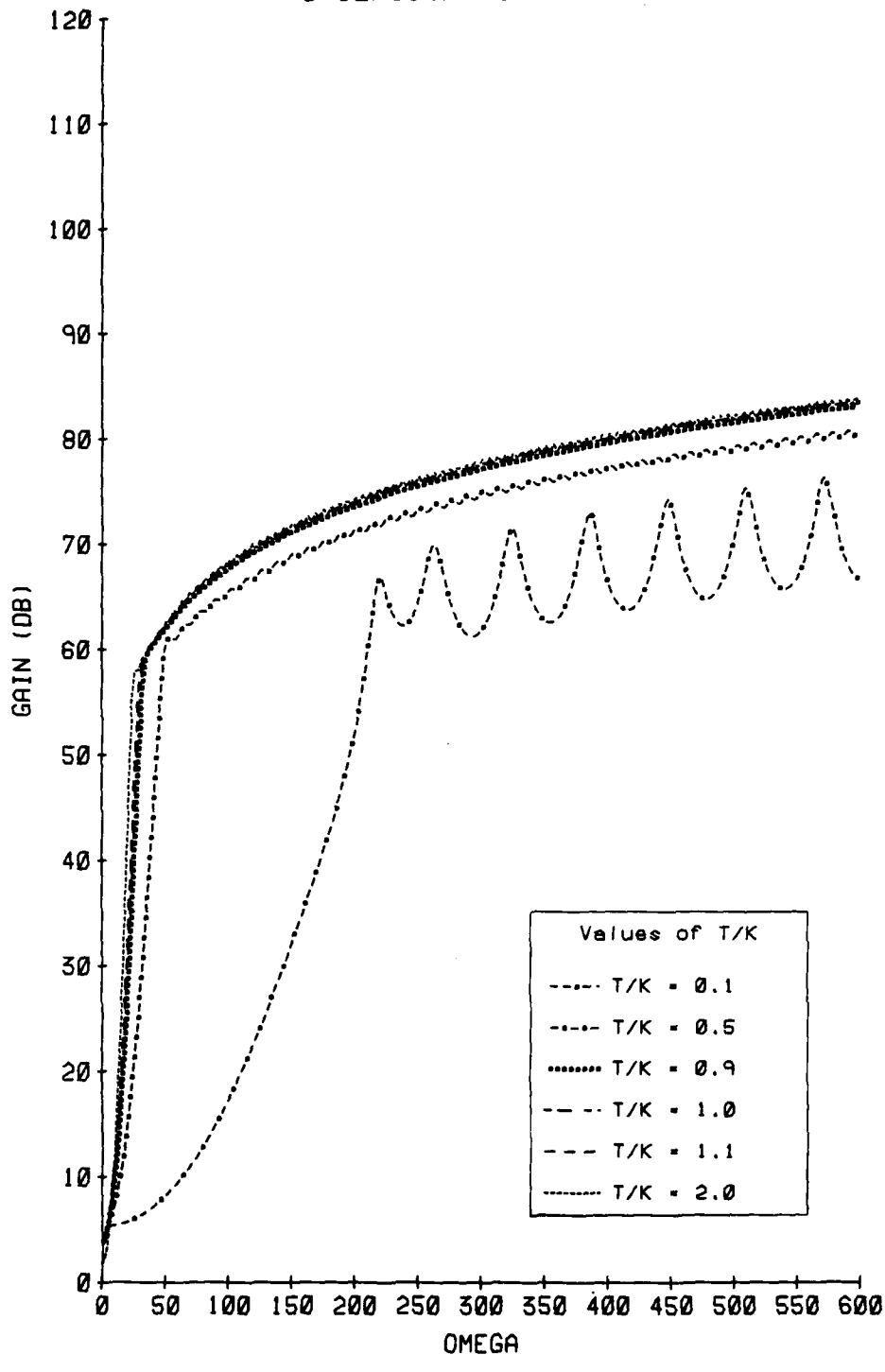

Figure 33(U) Gain for various T/K, Exp Shading and Exp Shaping, PFA = 10.**(-5)

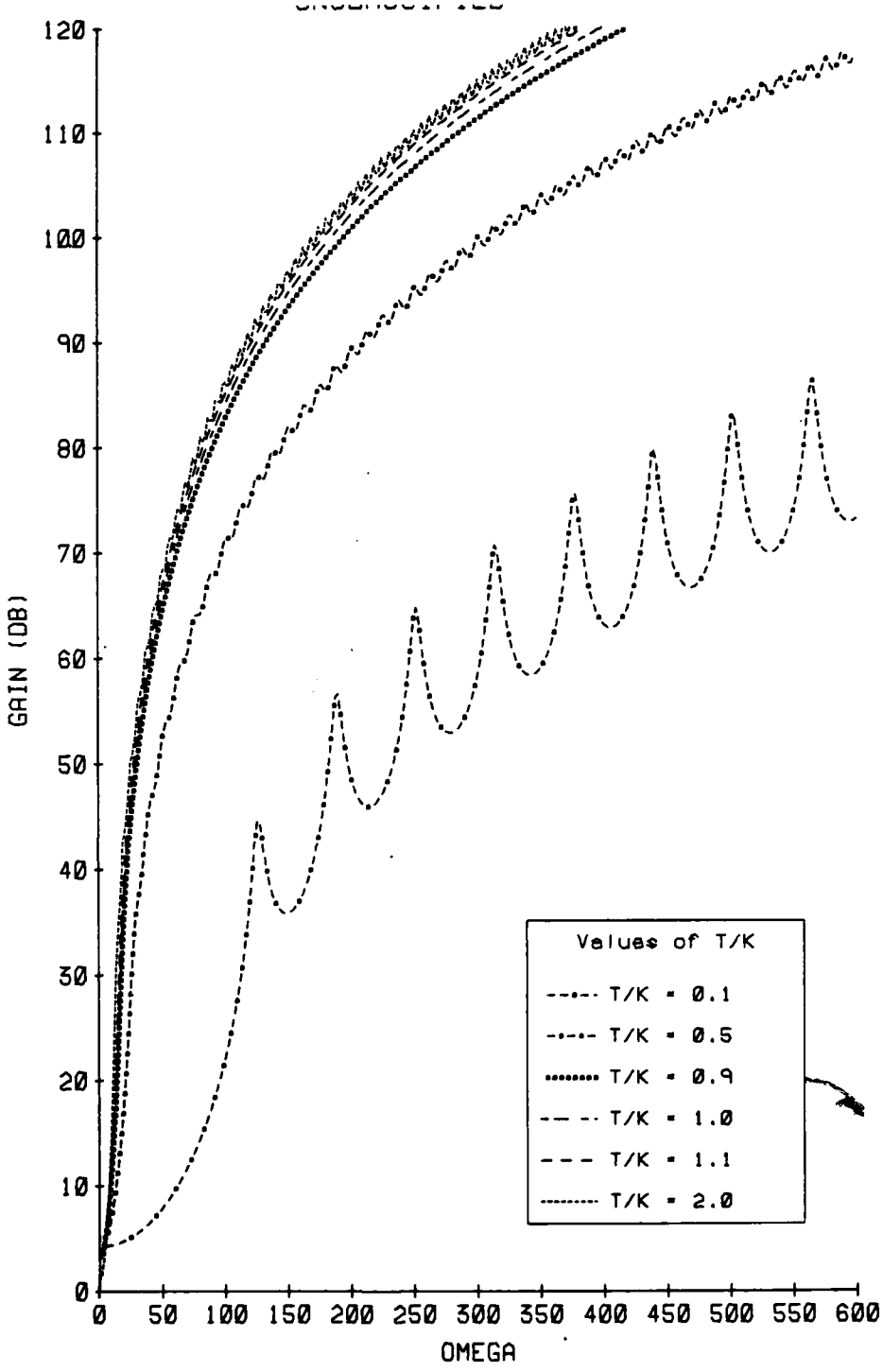

Figure 34(U) Gain for various T/K, Cos Shading and Cos Shaping, PFA = 10.**(-5)

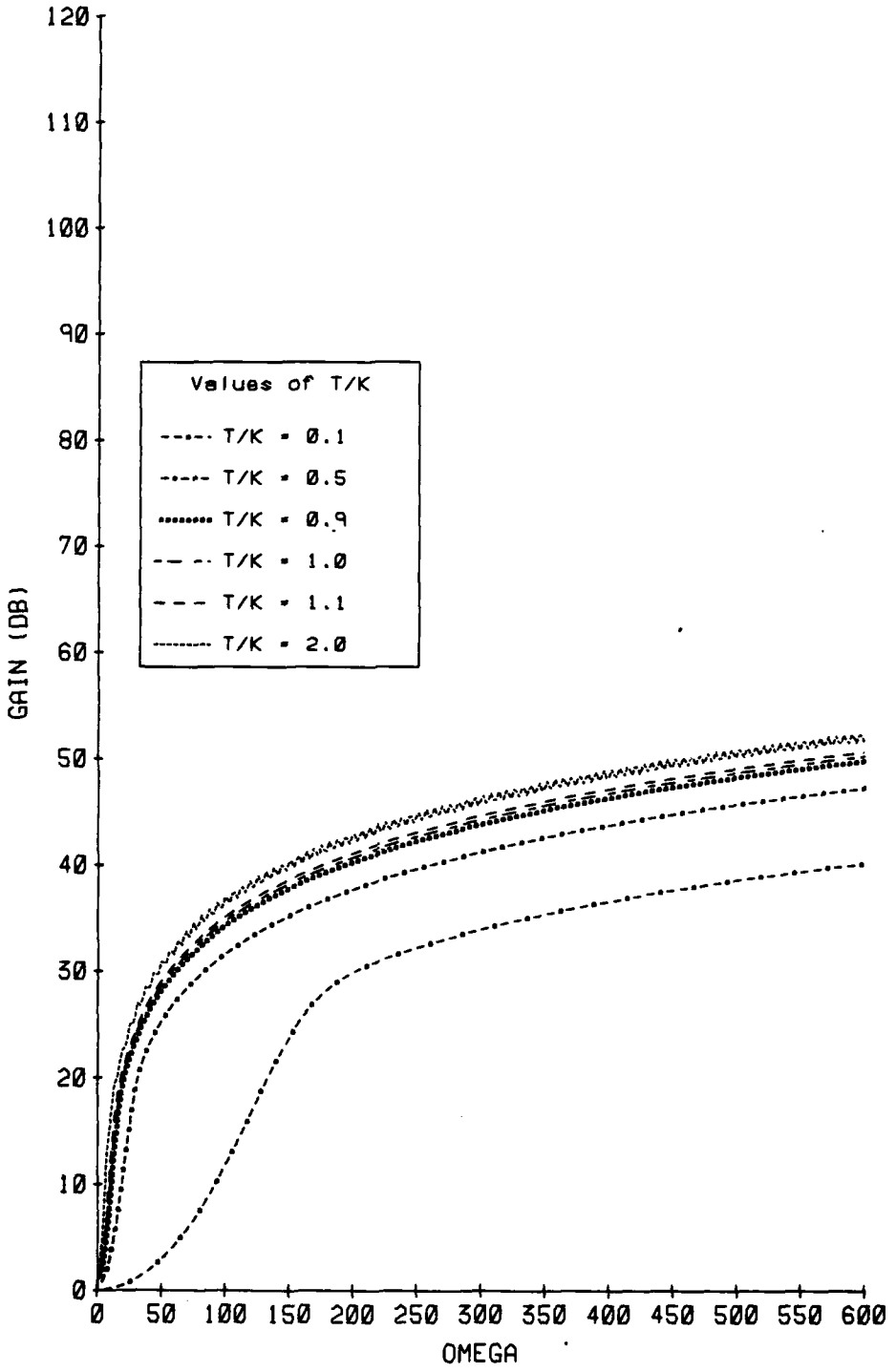

Figure 35(U) Gain for various T/K, Exp Shading and No Shaping, PFA = 10.**(-5)

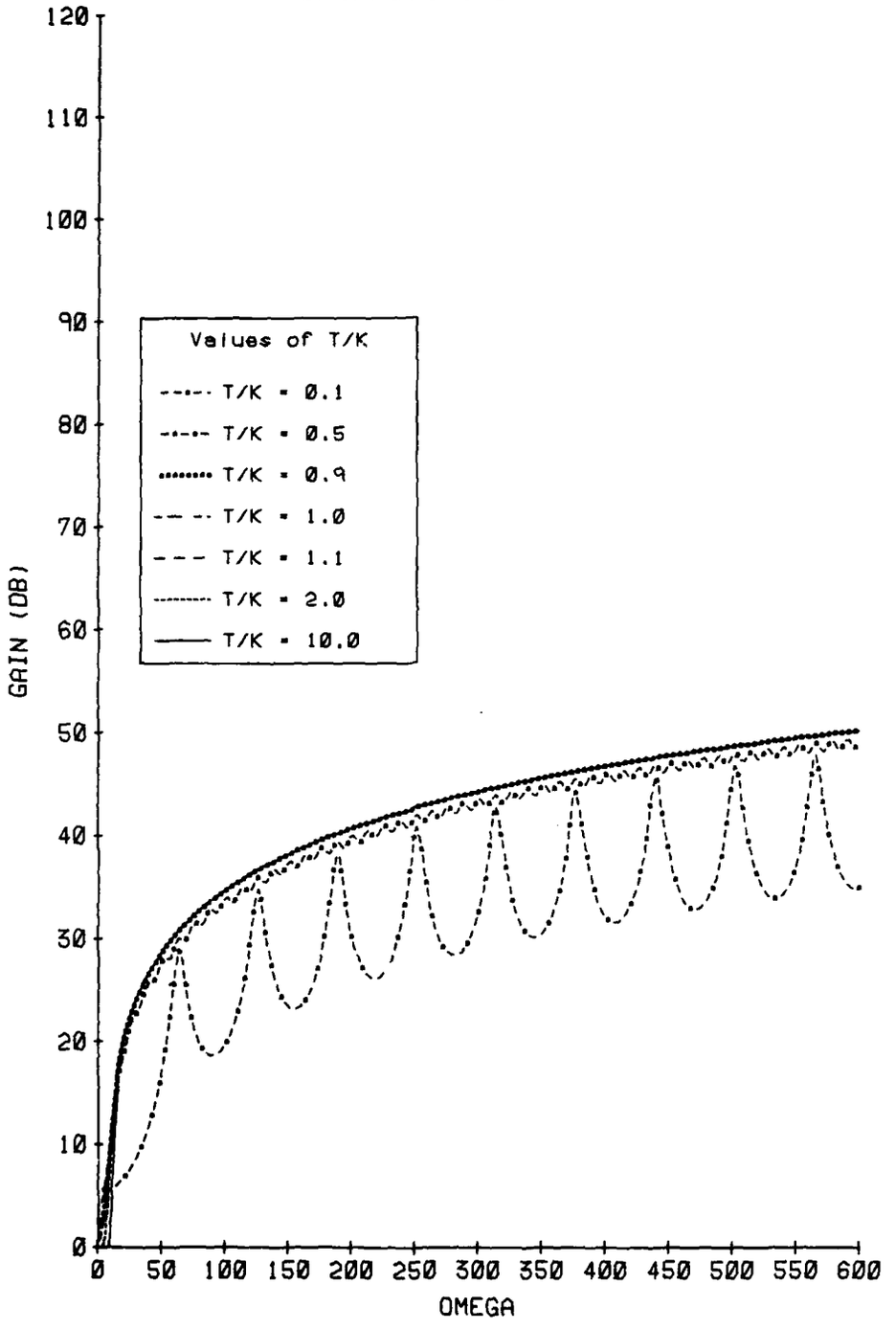

Figure 36(U) Gain for various T/K, No Shading and Exp Shaping PFA = 10.**(-5)

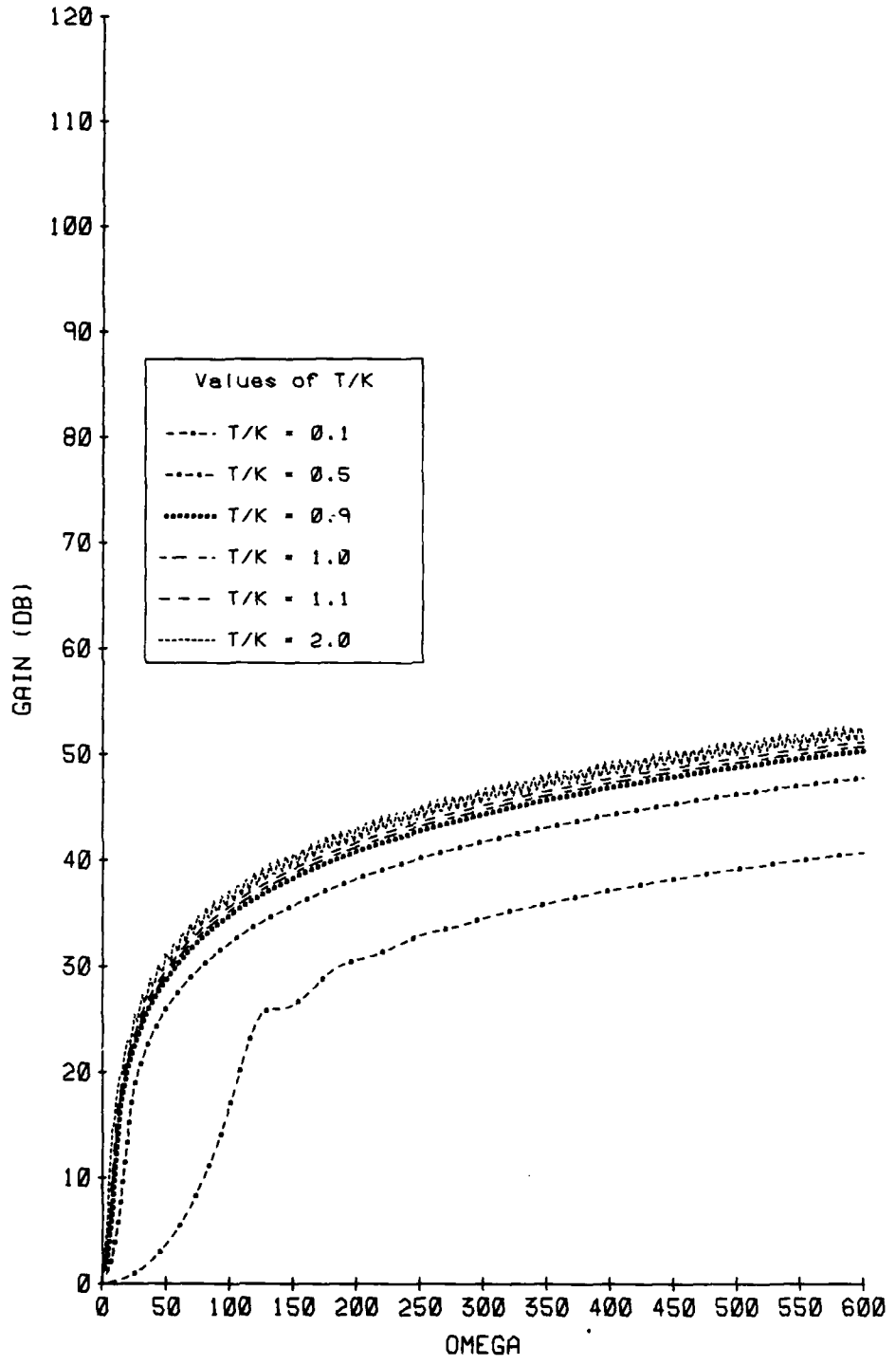

Figure 37(U) Gain for various T/K, Cos Shading and No Shaping, PFA = 10.**(-5)

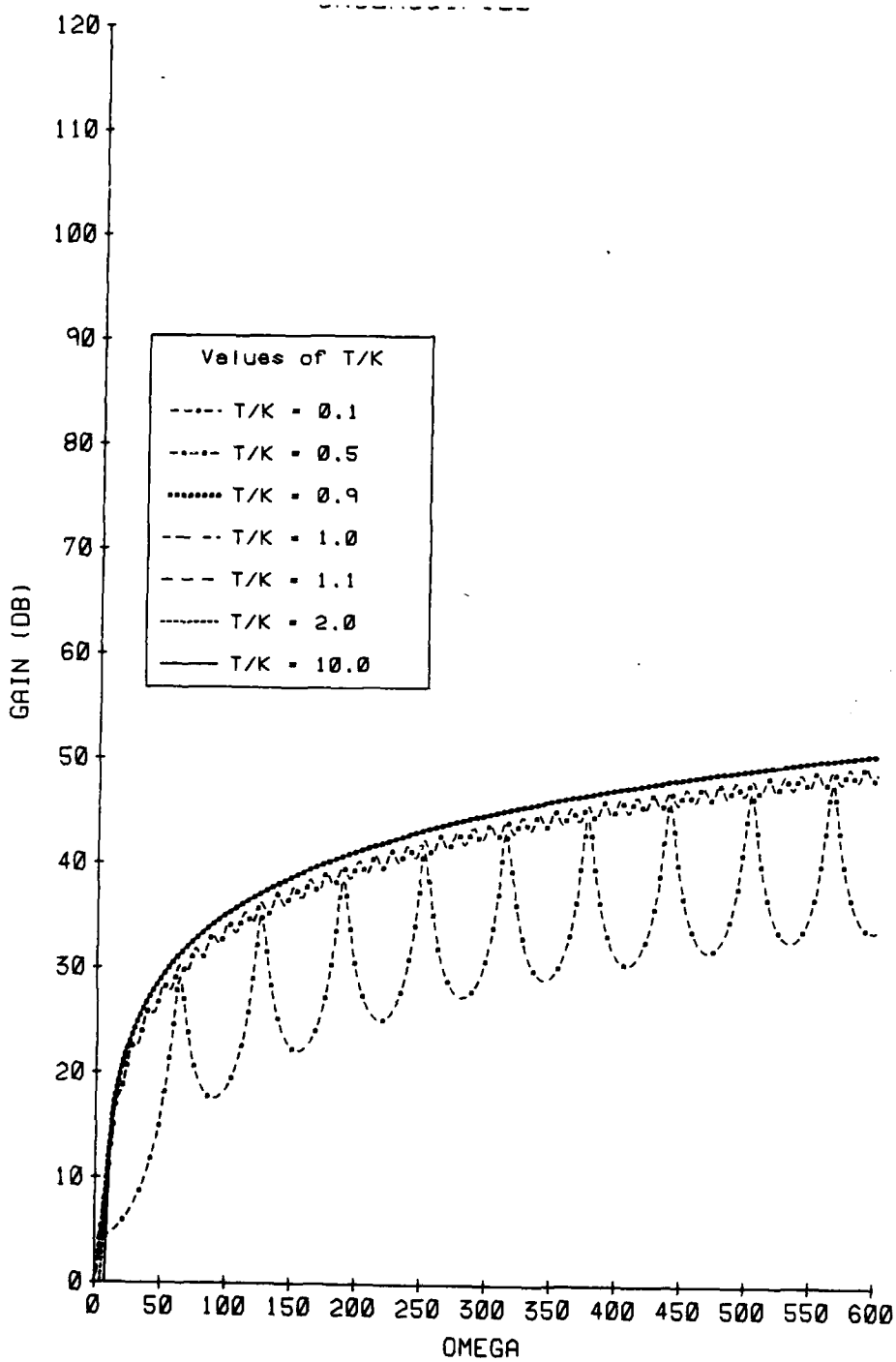

Figure 38(U) Gain for various T/K, No Shading and Cos Shaping PFA = 10.**(-5)

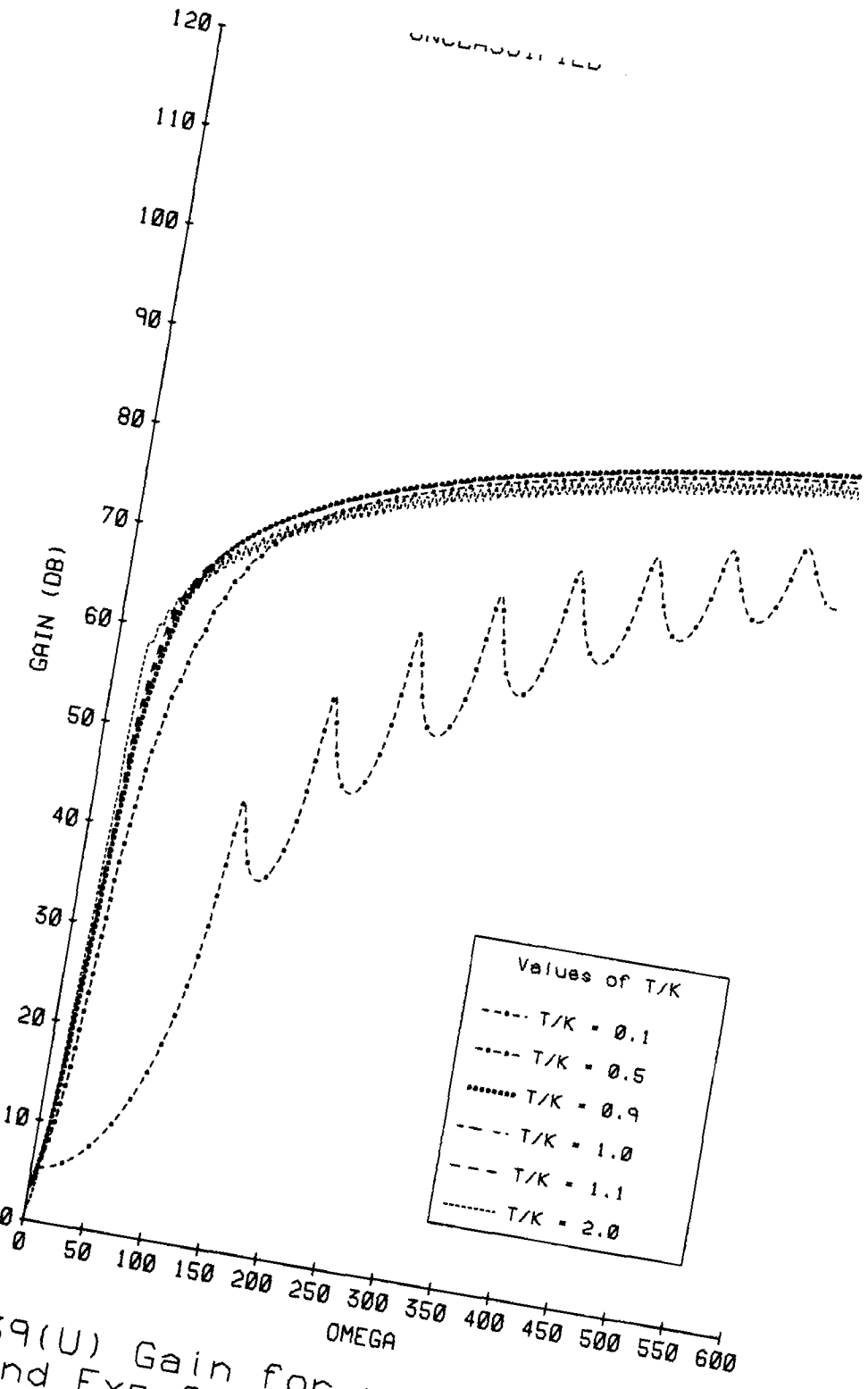

Figure 39(U) Gain for various T/K, Cos Shading and Exp Shaping, PFA = 10.**(-5)

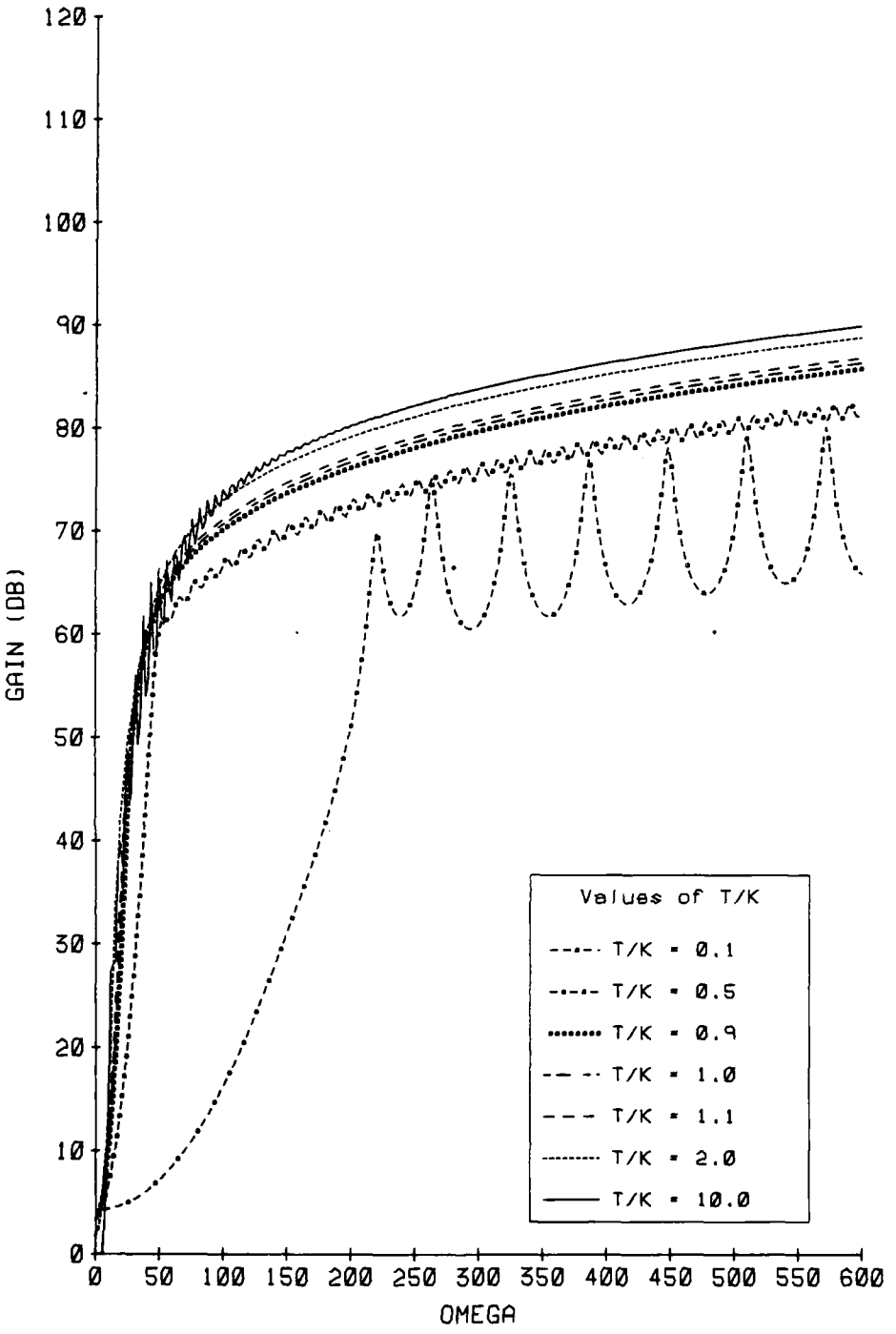

Figure 40(U) Gain for various T/K, Exp Shading and Cos Shaping PFA = 10.**(-5)

For an FM chirp pulse, the analysis of section 5.2 gives the result (similar to equation [5.25]) that when $\omega=0$

$$J = T^2\gamma^{-1} \int_0^{\gamma\psi} L(vK/\gamma)\, W(vK/\gamma)\, H(vK/\gamma)\, dv \qquad [C.56]$$

where

$$\gamma = 2\pi\beta K^2 \qquad [C.57]$$

$$\psi = \min [1, T/K]. \qquad [C.58]$$

Hence

$$J \sim \chi\, T^2/\gamma \qquad [C.59]$$

where

$$\chi = \lim_{\gamma\to\infty} \int_0^{\gamma} L(vK/\gamma)\, W(vK/\gamma)\, H(vK/\gamma)\, dv. \qquad [C.60]$$

$$= \int_0^{\infty} h_1(v)\, h_2(v)\, dv. \qquad [C.61]$$

where

$$h_1(v) = \int_0^1 W_1^2(Kw) \cos vw\, dw \qquad [C.62]$$

$$h_2(v) = \int_0^1 H_1^2(Kw) \cos vw\, dw \qquad [C.63]$$

Substituting equations [C.62] and [C.63] into equation [C.61] gives

$$\chi = \lim_{\lambda\to\infty} \chi(\lambda)$$

where

$$\chi(\lambda) = 0.5 \int_0^{T/K}\int_0^1 H_1^2(Kw)\, W_1^2(Kx) \int_0^{\lambda} (\cos(w-x)v+\cos(w+x)v)\, dv\, dx\, dw \qquad [C.64]$$

$$= 0.5 \int_0^{\psi}\int_0^{\psi} H_1^2(Kw)\, W_1^2(Kx) \sin(w-x)\lambda / (w-x)\, dx\, dw + QQ \qquad [C.65]$$

where the additional terms are grouped together into the term QQ. These terms QQ may all be expressed in the form

$$\int_a^b g(x) \sin \lambda x \, dx$$

where g(x) is integrable in the Riemann sense. Riemann's lemma(see, for example reference [4], page 40) states that integrals of this form approach zero as $\lambda \to \infty$, so that $QQ \to 0$ as $\lambda \to \infty$ and QQ . Ignoring QQ and letting u=(w-x) in equation [C.65],

$$\chi(\lambda) = \int_0^{\psi} f(u) \sin \lambda u / u \, du \qquad [C.66]$$

where

$$f(u) = \int_u^{\psi} H_1^2(Kw) \, W_1^2(K(w-u/\lambda)) \, dw. \qquad [C.67]$$

Provided that (f(u)-f(0))/u is integrable for $0 \le u \le \psi$ (which will be true for any sensible shaping or shading functions), Riemann's lemma implies

$$\int_0^{\psi} (f(u) - f(0)) \sin \lambda u / u \, du \to 0 \qquad [C.68]$$

as $\lambda \to \infty$. Hence

$$\chi = f(0) \lim_{\lambda \to \infty} \int_0^{\lambda\psi} \sin u / u \, du \qquad [C.69]$$

$$= (\pi/2) \int_0^{\psi} H_1^2(Kw) \, W_1^2(Kw) \, dw. \qquad [C.70]$$

This justifies equation [5.33] in the case where T=K.

By substituting the expression for J given by equations [C.59] and [C.70] into equation [5.1] and noting that equation [C.48] may be rewritten

$$Q_1^2 = K^2 \left(\int_0^{\psi} W_1(Ku) \, H_1(Ku) \, du\right)^2 \qquad [C.71]$$

the gain G may be written

$$G = \gamma \left(\int_0^{\Psi} W_1(Ku)\, H_1(Ku)\, du\right)^2 / \pi \int_0^{\Psi} W_1^2(Ku)\, H_1^2(Ku)\, du. \qquad [C.72]$$

This may be maximised by choosing shading and shaping functions such that $W_1(Ku)\, H_1(Ku) = 1$ eg no shading or shaping. The gain is independent of T/K for $T/K \geq 1$ if there is no shading, but if other shading functions are used, since H_1 depends on T, the gain does depend on T/K.

C.4 The Scatterers have Constant Properties

This condition is necessary in order that V(v)=1 and the functions L(v) in table 1 be valid. If the scatterers do not have constant properties (ie the target strength or speed or position of the scatterers changes during a time period equal in length to the pulse), then V(v) will be a non-increasing, non-negative function, scaled so that V(0)=1. The functions L(v) in table 1 should then be multiplied by V(v). If the new function L(v) is of the form of one of the functions in table 1, then the graphs in figures 4 to 21 may be used to deteremine the gain for a CW pulse. Alternatively, the analysis in section 5 shows that for large ω the gain depends only on L'(0) (or if this is zero, on the lowest derivative of L which is non-zero at the origin). The gain for an FM pulse is probably unaffected as previously noted in sections 4 and 5 for all but small values of γ.

C.5 The Scatterers are Independent

If the scatterers are independent for different path lengths, then X(v)=δ(v) in equation [C.1]. However, multiple paths to and from a single scatterer may have different lengths, and it is possible that there may be some small correlation between scattered pulses arriving at slightly different times, so that X(v) may be non-zero over a region of non-zero length. Alternatively, the scatterers may form a periodic structure (eg ocean waves) so that the amplitudes of scattered pulses arriving at times differing by a constant may be correlated. In this case, X(v) may be of the form

$$X(v) = a_0 \delta(v) + \sum_{i=1}^{N} a_i (\delta(v-v_i) + \delta(v+v_i)) \qquad [C.69]$$

Although the form of X(v) may not be known, the following gives an indication of the changes required to the analysis of section 5 if X(v)≠δ(v).

The function W (defined by equations [C.5] and [C.6]) may be written

$$W(v) = \int_0^K (X(v+u) + X(v-u)) W_0(u)\, du \qquad [C.70]$$

where $W_0(u)$ is the function W in the case where X(v) is equal to δ(v). The function X is scaled so that W(0) = K as before. The expressions for Q_1^2, L, H that are used in sections 4 and 5 remain unchanged.

For a CW pulse, the important difference of a more general X(v) on the analysis of section 5.1 is that, even for cos shaping, W(t) may not be zero. In this case, the gain will be oscillatory for large w, since $S^{(2n+1)}(1)$ will be non-zero for the smallest value of n for which $S^{(2n+1)}(0)$ is non-zero. For example, if L(v)=1 and H'(0)≠0, then

$$S'(0) = T^2(H'(0)+W'(0)) \neq 0 \qquad [C.71]$$

$$S'(1) = T\, H'(T)\, W(T) \neq 0 \qquad [C.72]$$

since H'(T) = H'(0). Thus,

$$J \sim T\,(\,H'(T)\,W(T)\cos\omega - T\,(\,H'(0)+W'(0)\,)\,)\,/\,\omega^2 \qquad [C.73]$$

and the gain is proportional to ω^2 and oscillatory. If X(v) may be written

$$X(v) = a\,\delta(v) + b\,X_1(v) \qquad [C.74]$$

where $X_1(v)$ is even, non-negative and is either bounded or consists of the sum of delta functions, none of which is centred at v=0 or v=±K, then the contribution to W'(0) from $X_1(v)$ is zero and

$$W'(0) = a\,W_0'(0). \qquad [C.75]$$

However,

$$W(T) = \int_0^T (\,X_1(T+u) + X_1(T-u)\,)\,W_0(u)\,du \qquad [C.76]$$

so that an increase in b, which probably gives a decrease in a in order that

$$W(0) = a\,K + 2\,b\int_0^T X_1(u)\,W_0(u)\,du = T, \qquad [C.77]$$

increases the oscillatory component of the gain but may decrease the non-oscillatory component. If W(T) = 0 (which would be fortuitous rather than planned if b≠0 due to the uncertain nature of the function X(v)), the oscillatory term is zero and the larger b is compared with a, the larger will be the gain. In fact if a=0 (as assumed incidently in the base case in section 4), W'(0)=0 even with a shaping function which is non-zero at the endpoints of the pulse. In this case, selecting the shading function such that H(0)=H(T)=0 so that H'(0)=0 is sufficient to ensure that the gain is proportional to ω^4 (or higher powers), still assuming that L(v)=1. The shaping function is then only relevant in determining the proportionality factor.